Carbon Nanotube−Inorganic Hybrids

Dominik Eder*

Department of Materials Science and Metallurgy, University of Cambridge, New Museums Site, Pembroke Street, Cambridge CB2 3QZ, United Kingdom

Received July 15, 2008

Contents

* E-mail: de235@cam.ac.uk.

1. Motivation and General Aspects

1.1. Introduction

The world of nanomaterials provides exciting challenges and opportunities for chemists, physicists, biologists, and material scientists. The use of nanomaterials as building blocks for devices not only helps downscale conventional technologies by at least an order of magnitude but also offers a cheaper and more environmentally friendly production route, due to a drastic reduction in the necessary amount of raw materials, thus mimicking nature's efficient ways of managing with less when it comes to chemical and physical processing.[1] Moreover, chemical and physical properties of substances can be considerably altered and fine-tuned when they exist on a nanoscopic scale, introducing the particle size as a powerful new parameter.[2] The quantum dot (QD), a nanosized cluster displaying atom-like behavior,[3] is a familiar example of this effect.

Scaling down the particle size to nanometer dimensions also increases the specific surface area of the material; thus, applications with reactions at the gas−solid or liquid−solid interface will also benefit from this "striving to the smaller". Typical applications include catalysis, energy conversion, electrochemistry, and environmental chemistry, where the use of nanomaterials increases response time, efficiency, and sensitivity.[4] One of the major challenges in nanoscale science is the synthesis of nanomaterials with monodisperse sizes, uniform morphologies, and functionalized surfaces. Regarding potential electronic applications, such as nanocapacitors or nanotransistors, addressing and assembling arrays of particles become necessary. For alignment and functionalization procedures, nanoparticles with an anisotropic morphology are advantageous because of their ability to shear align, form porous structures, and percolate at low concentrations.

Many conventional materials, such as metals, ceramics, and plastics, cannot fulfill all requirements for new technologies seeking to solve the world's most immediate problems related to energy and the environment. In many cases, however, the combination of two materials can show properties superior to those of their individual constituents. A well-known example is inorganic fiber-reinforced polymer composites, which in recent years have become ubiquitous in applications where lightweight, tough materials are required, including aerospace, high-end automotive, and sporting equipment. Decreasing the size of the inorganic units to the same level as the organic building blocks has led to more homogeneous materials, which allowed a further refinement of material properties on the molecular level. This has resulted in the introduction of organic−inorganic hybrids, such as metal organic frameworks. In contrast to nanocom-

10.1021/cr800433k
Published on Web 01/28/2010

Dominik Eder received his Ph.D. in Physical Chemistry in 2003 from the University of Innsbruck, Austria, working on the in situ characterization of metal oxide-supported noble metal catalysts with electrochemical impedance spectroscopy. For his thesis, he was awarded the Sosnovski Medal 2004 from the University of Innsbruck. After his civil service at the Red Cross in Innsbruck, he joined the Macromolecular Materials Laboratory (Prof. A. H. Windle) in the Department of Materials Science and Metallurgy at the University of Cambridge in 2005, where he worked as an Erwin Schroedinger Research Fellow on the synthesis of oxide nanotubes. In 2006, he was awarded an APART Advanced Research fellowship from the Austrian Academy of Science. He is currently associated with the Functional Inorganic and Hybrid Materials group (Prof. K. Cheetham) in the same Department and his research interests include the synthesis of functional oxide nanostructures and CNT−inorganic hybrids and their application in photocatalysis, environmental catalysis, and batteries.

posites, which simply combine the individual properties of the components, these hybrid materials merge the properties of the components in a way that creates new properties distinct from those of either building block.[5,6]

This review focuses on a new class of hybrid materials made from carbon nanotubes (CNTs) and inorganic glasses or ceramics, CNT−inorganic hybrids. The many advantages of CNTs in hybrid materials include their high aspect ratio (>1000) and tubular geometry, which provides ready gas access to a large specific surface area and percolation at very low volume fractions. Their excellent mechanical, electrical, and optical properties support CNTs as an ideal building block in hybrid materials. The high thermal conductivity of CNTs enable them to behave as a heat sink during calcination and activation treatments, thereby stabilizing small inorganic moieties that can decorate the sidewalls of the CNTs. This results in materials with higher specific surface areas that allow the use of less material, reducing cost and toxicity. Over the past few years, CNTs have been combined with a variety of inorganic compounds, including oxides, nitrides, carbides, chalcogenides, and ceramics. Out of these, the oxides are by far the most commonly explored species. Figure 1 shows the evolution of publications since the year 2000 that deal with either the synthesis or application of new CNT−oxide hybrids (Sources: ISI Web of Knowledge (Thomson Reuters) and Scopus (Elsevier)).

Although still in a very early stage of research, CNT−inorganic hybrids have shown exceptional performance in applications such as gas sensors (SnO_2) and photovoltaics (ZnO), exhibiting an enhanced ability to trap electrons and reduce the electron-hole recombination rate compared to the bulk materials. CNTs can also serve as additional photosensitizers in photocatalysts (TiO_2) or intrinsic capacitors in supercapacitors and batteries (MnO_2, RuO_2). These few examples prove the great potential of these hybrids and show that the next technological frontiers will be opened by

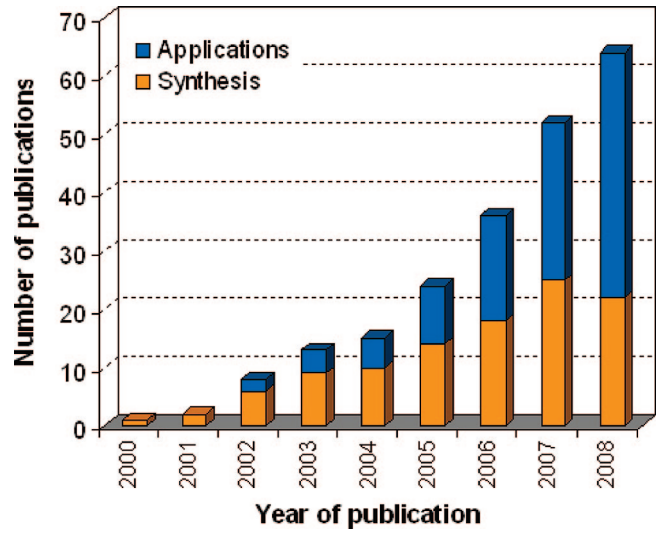

Figure 1. Number of publications dedicated to the synthesis and application of CNT−oxide hybrid materials since the year 2000.

understanding and optimizing material combinations and their synergistic functions, rather than through a better understanding and application of a particular material.

This review offers a comprehensive critical evaluation of CNT−inorganic hybrids and their potential applications and is structured in the following way. Starting with an attempt to distinguish between various hybrid materials, such as metal−organic frameworks and nanocomposites (section 1.2), I will then introduce CNTs as building blocks for hybrid materials (section 2.1) and discuss the challenges involved, including purification and functionalization issues (section 2.2). This will be followed by an overview of CNTs whose hollow central cavities have been filled with various metals and inorganic compounds (known as *meta*-CNTs), which can be seen as a first attempt to produce CNT−inorganic hybrid structures (section 2.3). The second part of the review provides a comprehensive summary of various chemical and physical synthesis techniques, which I categorize into ex situ (section 3.1) and in situ (section 3.2) routes. Finally, the last part of the review demonstrates the potential of CNT−inorganic hybrids for a wide range of applications (section 4) and discusses the remaining challenges and future prospects (section 5).

1.2. Hybrid Materials

The last two decades have seen the development of some new types of hybrid materials, such as nanocomposites and metal oxide frameworks, and their implementation in various applications that require, for example, light structural, bioactive, or smart materials.[5]

(1) *Nanocomposites* are multiphase materials, in which one phase (filler) is dispersed in a second phase (matrix), resulting in a combination of the individual properties of the component materials. Filler materials are typically inorganic building blocks in the nanosize regime and in the form of particles, whiskers, fibers, lamellae, or a mesh. The matrix can be either organic (e.g., polymer) or inorganic (e.g., ceramic or metal). The materials are typically synthesized ex situ by simple mixing techniques (e.g., ball milling or shear mixing), which often results in a heterogeneous distribution of the filler and consequently in nonuniform properties. As an example, the result of the incorporation of inorganic nanoparticles, nanorods, carbon fibers, CNTs and galleries of clay minerals into

Table 1. Definitions for Hybrid Various Materials

	nanocomposites	metal−organic frameworks	CNT−inorganic hybrids
composition	two phases: a filler is distributed within organic or inorganic matrix	single phase: inorganic units are linked by organic groups on the molecular scale	two phases: the CNTs are coaxially coated with inorganic second component
formation	both phases are discrete building blocks	often formed in situ by molecular precursors	inorganic phase can be formed either in situ (molecular precursor) or ex situ (building blocks)
properties	use of individual properties, known structure−property relationship	properties are combined to create multifunctional materials with yet unknown properties	synergistic effects similar to hybrid frameworks create new properties

an organic polymer or a ceramic matrix is considered to be a nanocomposite material. In contrast to some other hybrid materials, nanocomposites simply use the intrinsic properties of their individual components, whose discrete and controllable size, shape, and structure enable a good structure−property relationship. In this respect, the purpose of the filler is often to mechanically reinforce the matrix or to alter its thermal, electrical, or barrier properties, and as such, these nanomaterials have already had a considerable impact in applications such as lightweight structural materials in aerospace, electrically conducting plastics, and packaging materials with reduced gas permeability.

(2) Other hybrid materials, such as *metal−organic frameworks*, consist of a single phase containing both inorganic and organic building blocks and merge the properties of the components on the molecular scale in a way that creates novel properties distinct from those of either building block. For instance, the organic component can provide biocompatibility and chemical functionality and allows easy shaping and better processing of the materials. The inorganic components provide mechanical and thermal stability but also new functionalities, which depend on the chemical nature, the structure, the size, and the crystallinity of the inorganic phase. They can implement or improve electronic, magnetic, and redox properties, density, refraction index, etc. So in this case, the final materials are not merely the sum of the primary components, but rather completely new materials with new properties. A synergistic effect often occurs from the close proximity of the two phases through size domain effects and the nature of the interfaces. Considering these effects, the ultimate aim is to create so-called *smart materials* that can react to environmental changes or switchable systems, as these will pave the way to novel technologies, such as electroactive and electrochromic materials, chemical and biosensors, smart coatings, and biohybrid materials.[7]

(3) This review article focuses on a new type of hybrid materials, *CNT−inorganic hybrids*, which replace the organic compound with CNTs. In contrast to nanocomposites, the CNTs are coaxially coated with the inorganic compound. A significant synergistic effect in CNT-hybrids is expected through size domain effects and charge transfer processes through the CNT−inorganic interface, which will be discussed in section 4 in more detail. Consequently, this new class of functional materials combines the multiphase characteristics of nanocomposites with functions of hybrid frameworks (Table 1).

In general, hybrid materials can be further classified into *Class I* and *II* materials. This distinction is based on the strength of interaction between the two components, which also affect the hybrids' properties. The synthesis strategies and properties of Class I and II hybrids have been intensively described in several books[5,6,8] and reviews;[7,9,10] hence, this review will only provide a short summary.

• *Class I* hybrids typically show weak interactions between the two phases, such as van der Waals, hydrogen bonding, or weak electrostatic interactions. Examples of these hybrid materials include organic dyes or monomers that are attached to a sol−gel matrix or inorganic nanoparticles that are embedded in a polymer blend. Interpenetrating networks (IPNs) are another example of Class 1 hybrid materials and are formed when an inorganic and an organic compound form networks that interpenetrate each other without strong chemical interactions.

• *Class II* hybrids are formed via strong chemical interactions between the components, for example, when the discrete inorganic building blocks are covalently bonded to organic polymers, when inorganic sol−gel networks are modified with organic functional groups (e.g., ORCOMER), or when inorganic and organic polymers are covalently connected to each other by capping or linking agents. The building blocks can be produced in a variety of shapes, structures, and size distributions and with the desired material properties. Hence, this step-by-step approach generally enables a good structure−property prediction.

Both approaches can be combined in a powerful template-assisted synthesis process for designing novel complex materials. The template can be either the organic or the inorganic compound in the form of one-dimensional structures (e.g., CNTs, inorganic wires, polymer fibers, biomolecules, or DNA) or multidimensional networks (e.g., gyroid-phase block copolymers and polymer blends, zeolites, and membranes). With this technique, a new generation of crystalline microporous hybrid solids have recently been discovered by Cheetham and Rao,[11] Stein,[12,13] Ferey et al.,[14,15] Wiesner et al.,[16,17] Yang and Stucky,[18] and Yaghi et al.,[19,20] just to mention a few. Among other characteristics, these materials combine exciting magnetic and electronic properties with very high surface areas (from 1000 to 4500 m^2/g[21,22]).

An important advantage of hybrid materials is the diversity in suitable synthesis routes. In contrast with pure solid-state inorganic materials that often require a high-temperature treatment for their processing, hybrid materials may benefit from the convenience of traditional polymer-processing techniques (e.g., extrusion, compression, molding, etc.). This is either because of their large organic content or because of the formation of cross-linked inorganic networks from small molecular precursors, as in polymerization reactions. Hence, these materials can be produced at low temperatures (often using sol−gel and hydrothermal reactions) in various morphologies, such as 3D networks, thin films, or nanoparticles.

Table 2. Advantages and Disadvantages of Various CNT Synthesis Techniques

synthesis technique	description	product	advantages	disadvantages	improvements
DC arc discharge	1991: Iijima[381] 1992: Ebbesen and Ajayan[382]	MWCNTs and SWCNTs (with catalyst)	easy design, few structural defects	short tubes and low yield, low purity, random diameters	magnetic field, rotating electrode, liquid N_2
laser ablation	1995: Smalley[383]	primarily SWCNTs	few defects, good control over diameter	most costly method, poor scalability, requires Class 4 lasers	ultrafast electron laser
molten salt	1995: Terrones and Kroto[384]	primarily MWCNTs	simple process, used for filling CNTs	low yield and crystallinity; poor controllability	
chemical vapor deposition	1998: Endo[385]	both types	high yields, easy scalability, long tubes, alignment and pattern growth	some defects, medium purity	plasma enhanced, aerosol process, laser assisted, CoMoCat, HiPCo,

Table 3. Summary of Physical Properties of CNTs in Comparison with Graphite; Values Take from Ref 20

property	SWCNTs	MWCNTs	graphite
specific gravity	0.8 g/cm^3	<1.8 g/cm^3	2.26 g/cm^3
elastic modulus	∼1.4 TPa	∼0.3−1 TPa	1 TPa (in plane)
strength	50−500 GPa	10−60 GPa	
resistivity	5−50 $\mu\Omega$ cm		50 $\mu\Omega$ cm (in plane)
thermal conductivity	3000 W m^{-1} K^{-1}		3000 W m^{-1} K^{-1} (in plane) 6 W m^{-1} K^{-1} (c-axis)
magnetic susceptibility	22 × 10^6 EMU/g (perpendicular) 0.5 × 10^6 EMU/g (parallel)		0.5 × 10^6 EMU/g (parallel)
thermal expansion	negligible		−1 × 10^{-6} K^{-1} (in plane) 29 × 10^{-6} K^{-1} (c-axis)
thermal stability	600−800 °C in air 2800 °C in vacuum		450−650 °C in air

The choice of synthesis techniques for CNT−inorganic hybrids and the extent of their synergistic function depend on the type and purity of CNTs and the modification of their surface chemistry. Therefore, the next section will summarize the characteristics and properties of CNTs and their synthesis routes.

2. Carbon Nanotubes in Hybrid Materials

2.1. Why Carbon Nanotubes?

Carbon nanotubes and fullerenes have defined the research field of nanotechnology like no other type of material. With applications as diverse as integrated circuits and memory devices, sensors and filters, solar cells, and field emission displays,[23] as well as artificial muscles[24] and the space elevator,[25] CNTs have been popularized in science fiction novels and television documentaries throughout the world. A vast number of review articles and textbooks have been dedicated to the unique and fascinating properties of CNTs; hence, this review will only provide the very basics required for understanding their role in CNT−inorganic hybrids.

Many textbooks describe CNTs in simple terms as tubular structures made entirely of rolled-up layers of interconnected carbon atoms,[26,27] with diameters ranging from about one nanometer to tens of nanometers and lengths up to centimeters. CNTs can be open-ended or closed by a hemispherical fullerene-type cap, depending on their synthesis method.[28] Along with structures related to those of fullerenes,[29] CNTs are considered a third allotropic form of carbon, with the others being diamond and graphite. They are classified as either (a) "single-walled" tubes (SWCNTs, $0.7 < d < 2$ nm), which consist of a single layer of graphene sheet seamlessly rolled into a cylindrical tube, or (b) multiwalled CNTs (MWCNT, $1.4 < d < 150$ nm), which comprise multiple concentric tubes separated by about 0.34 nm.

CNTs are generally produced by four main techniques (arc discharge, laser ablation, molten salt intercalation, and chemical vapor deposition), which are frequently discussed in detail in several reviews.[23,30−32] Depending on the resulting purity, defect concentration, yield, and other parameters, each technique has several advantages and disadvantages, which are summarized in Table 2.

In general, CNTs possess large specific surface areas due to their hollow geometry, while their structural integrity and chemical inertness support relatively high oxidation stability. Other advantages include their exceptional physical properties, which have been extensively discussed in several books[28,33,34] and reviews[32,35,36] and are summarized in Table 3 (taken from refs 28 and 36) in comparison with graphite.

• Electrical properties: The electrical resistivity of CNTs is determined by the unique structure of graphite and the quantum mechanical properties associated with their 1D character and small size, which results in the near-total elimination of electron collisions (scattering). Hence, CNTs are ballistic conductors, whose resistance is independent of the nanotube length. Furthermore, they can carry the highest current density of any known material, with reported measurements as high as 10^9 A/cm^2. For comparison, copper wires burn out at 10^6 A/cm^2.[37] Depending on their helicity and diameter, CNTs can be either metallic or semiconducting. This is of importance as semiconducting SWCNTs may perform better in applications that involve charge transfer processes, including sensors, field emission devices, and photocatalytic applications, while metallic CNTs are preferred as interconnects in electronic devices or as conductive filler in CNT-composites. Consequently, this requires standardization of synthesis and improvement in separation and purification techniques, which will be discussed in the next section.

Table 4. Summary of Typical Purification Techniques for CNTs

	metals[a]	carbon[b]	functional[c]	comments
heating in air/O_2		X	X	opens tips
heating in wet O_2		X		
HCl_{conc}	X[d]			assisted with microwave or magnetic field
HNO_3/H_2SO_4	X	X	X	open tips, shortens CNTs
microwave		X[e]		aided by acids (e.g., HCl)
Ar @ 2000 °C	X	X		anneals crystal structure

[a] Treatment can remove metal catalyst residues. [b] Carbon residues (e.g., amorphous or organic aromatic debris). [c] Purification introduces covalently bonded functional groups. [d] Only if not covered with carbon or encapsulated within CNT. [e] Only amorphous carbon around metal particles.

• Mechanical properties: The mechanical properties of CNTs originate from the strong C═C double bonds, which yield a very large Young's modulus in their axial direction (1.4 TPa for single-walled CNTs).[38] CNTs have an expected elongation-to-failure of 20−30%, which, combined with their stiffness, projects to a tensile strength well above 100 GPa (e.g., steel: 1−2 GPa)—by far the highest known.[39] However, both Young modulus and tensile strength are strongly reduced by the presence of defects in the graphitic walls of CNTs, such as Stone-Wales defects. Hence, experimental values tend to be considerably smaller than theoretical predictions.[40] Because of their high aspect ratio, CNTs are also very flexible and thus potentially suitable for applications in composite materials that require anisotropic properties.[41]

• Thermal properties: Theoretical works predicted room-temperature thermal conductivities of individual single-walled CNTs of up to 6600 W/(m K).[42] CNTs would therefore transmit nearly twice as much heat as isotopically pure diamond. Experimental studies give somewhat lower values, with Hone et al. reporting room-temperature thermal conductivities of 300 W/(m K) for bulk single-walled CNTs and of 3000 W/(m K) for individual multiwalled CNTs.[43]

In summary, due to their remarkable mechanical, electrical, biological, optical, and thermal properties, CNTs promise enormous potential for various technological areas in the energy, information, aerospace, medicine, and chemical industries, where they can be used as gas adsorbents, templates, actuators, composite reinforcements, catalyst supports, or chemical sensors, among other things. For the same reasons, they are promising building blocks for hybrid materials. The next section describes some requirements for CNTs to be successfully implemented in hybrid materials.

2.2. Preparation of CNTs for Use in Hybrid Materials

In this section, we will consider the purification, the separation, and the functionalization of CNTs as preparation for their use in hybrid materials. As-produced CNTs contain a variety of impurities such as fragments of wrapped-up graphene sheets, amorphous carbon, fullerenes, and metal catalyst particles.[44] As these impurities interfere with most of the desired properties as well as with the biocompatibility of the CNTs, it is desirable to remove them, preferably without affecting the performance of the CNTs themselves (section 2.2.1).

Furthermore, many applications require uniform and stable dispersions of CNTs. However, pristine single-walled CNTs are insoluble in most organic solvents and aqueous solutions and tend to aggregate as a result of van der Waals interactions between individual tubes. It is also desirable to select CNTs by structure and size and to separate semiconducting from metallic CNTs, as the electronic properties of SWCNTs depend on their chirality and diameter (section 2.2.2). Finally, the CNT surface can be functionalized in order to improve the chemical reactivity, to recognize specific target molecules, or to enhance the interactions with other compounds in hybrid materials (section 2.2.3).

2.2.1. Purification of CNTs

Purification of CNTs has been a matter of intensive study.[45−49] Table 4 shows the advantages and disadvantages of various common purification techniques. The efficiency and yield of the purification procedure depends on a variety of factors, such as metal content, oxidation time, environment, oxidizing agent, and temperature.[46]

For instance, oxidative treatment of CNTs is a simple way to remove carbonaceous impurities. A variety of oxidizing atmospheres have been tested, including air,[50] a mixture of H_2S and O_2,[51] and steam.[52] However, oxidation often damages the CNTs' surface, especially when combined with ultrasonication or high-temperature treatment. Generally, the suitable oxidation temperature should remain well below that for CNT combustion, which can range from 550 to 850 °C, depending on the number of structural defects. Additionally, the metal residues can act as an oxidation catalyst, decreasing the oxidation temperature even further. Oxidation with strong acids, such as HNO_3/H_2SO_4,[53] also creates structural defects and the formation of various organic groups, hence altering the surface chemistry of the CNTs.

To remove metal residues without affecting the carbonaceous species, the CNTs are typically treated in strong nonoxidizing acids such as HCl. Assisted by a magnetic field, these acids predominantly dissolve the metal particles that are not covered by amorphous carbon or encapsulated within CNTs. In contrast, microwave-assisted purification heats up the metal and thus primarily removes the amorphous carbon attached to it.[47]

Annealing at high temperatures in vacuum or inert gas is a powerful alternative to the oxidizing techniques above.[54,55] With this technique, amorphous and graphitic defects can be removed selectively simply by adjusting the temperature (600−2000 °C). The metal residues are typically removed at temperatures close to the melting point of the nanosized metal particles (e.g., above 1600 °C for Fe). Finally, at very high temperatures (1900−2000 °C) the carbon atoms in the CNT walls rearrange, thus decreasing the number of structural defects and so enhancing the degree of graphitization.

2.2.2. Separation of Metallic and Semiconducting CNTs

In contrast to the purely metallic MWCNTs, SWCNTs can be either metallic or semiconducting, depending on their diameter and chirality. For many applications, including nanoscale electronic, optoelectronic, and sensing devices, it is desirable to use SWCNTs that are either purely metallic or purely semiconducting. For instance,

metallic SWCNTs find application as leads in a nanoscale circuit, whereas nanoscale Schottky-type field-effect transistors would require semiconducting SWCNTs. As the synthesis of electronically pure monochiral nanotubes has yet to be accomplished, the current strategy is to separate the two CNT types. Much progress was achieved in 2003, with the introduction of four separation routes—three chemical and one physical.

The chemical approach utilizes the stronger interactions of various chemical molecules with one type of SWCNT over the other. For instance, surfactants, such as octadecylamine,[56] have a strong affinity toward semiconducting CNTs, while diazonium reagents,[57] biomolecules, and DNA[58,59] favor the metallic type. Once attached to the CNTs, they form larger aggregates, which can be separated easily by standard separation techniques such as ion-exchange chromatography or microfiltration. In a similar way, CNTs have been separated according to their length,[60] diameter,[59] and chirality.[61]

The physical method of Krupke et al. extracts metallic SWCNTs based on AC dielectrophoresis.[62,63] When exposed to an alternating electric field (10 MHz), the SWCNTs develop an induced dipole moment, which causes the two types of CNTs to migrate along the electric field gradient in opposite directions. The metallic SWCNTs deposit onto the electrodes, while the semiconducting SWCNTs remain in suspension. This process is limited by the tendency of SWCNTs to agglomerate into mixed bundles, causing a coadsorption of both CNT types. These separation techniques can be improved by using better dispersions (e.g., with surfactants).[64] However, much improvement is still required, particularly in scaling-up the separated CNT amounts.

2.2.3. Functionalization

Functionalization of CNTs remains one of the most studied areas in the CNT research field, and many review articles have been dedicated to this topic.[65−70] In general, CNTs can be functionalized by (a) covalent attachment of chemical groups through bonding to the π-conjugated skeleton of the CNT or (b) noncovalent adsorption or wrapping of various functional molecules.

The most common covalent functionalization involves the addition of carbonyl and carboxyl groups via an aggressive treatment with a mixture of HNO_3/H_2SO_4 or by plasma etching.[69] The latter technique can also be used to introduce basic functionalities when applied in a nitrogen atmosphere. Carboxyl groups may then be acylated with thionyl chloride to make a basis for various amine compounds[71] or to attach to various proteins and DNA.[72−74] Other commonly used chemical reactions to attach organic groups include cycloadditions (e.g., Bingel, Diels−Alder), electrophilic and nucleophilic additions, ozonolysis, halogenation, or radical reactions (oxidative and reductive).[65,68,70]

Covalent functionalization of CNTs has been shown to be an efficient method for increasing their solubility and chemical reactivity.[75,76] However, it also introduces additional structural defects and disrupts the delocalized electron system in the CNT sidewalls, and consequently alters the electronic and mechanical properties to a degree that would significantly affect the performance in hybrid materials.[44]

In contrast, noncovalent functionalization utilizes van der Waals interactions and hydrogen bonding. Various surfactants and polymers have been applied to enhance the CNTs' solubility in hydrophilic solvents and to increase their dispersion in polymer or ceramic matrices.[41] Currently, there is much interest in functionalizing CNTs with biomolecules such as peptides or DNA.[66,77,78] Another approach uses the well-known $\pi-\pi$ interactions between aromatic compound (e.g., porphyrins, pyrens) and the delocalized electron system in CNTs.[79,80]

The CNT reactivity is directly related to the π-orbital mismatch caused by an increased curvature. Therefore, a distinction must be made between the sidewall and the endcaps of a nanotube. The sidewalls can be considered as curved graphite, while the tips are reminiscent of the structure of a fullerene hemisphere and are thus relatively reactive. Hence, most reactions will occur first at the tips and then on the surface, especially where structural defects are present. The difference in reactivity can be used to selectively open and functionalize (covalently) the tips of CNTs, while the sidewalls remain inert.[65] This route has frequently been used to fill CNTs with inorganic compounds (section 2.3) and to attach metal particles onto the tips of CNTs (nanoplug[81]). In contrast, by using nonconvalent interactions, surfactants, aromatic compounds, and biomolecules, the inorganic nanoparticles can be attached equally on both tips and sidewalls. Thus, this route is ideal for the deposition of uniform and complete inorganic coatings.

2.3. Filling CNTs

The earliest attempt toward CNT−inorganic hybrids (in 1993) was the filling of MWCNTs with metal oxides (PbO[82] and Bi_2O_5[83]), carbides (Y_3C and TiC[84]), and metals (Ni[85]). Because of their larger inner diameter (5−50 nm) compared with SWCNTs (1−1.5 nm), most efforts had been spent on filling MWCNTs, and it was not until five years later that Sloan et al. reported the filling of SWCNTs with $RuCl_3$.[86] Since then, many atoms, molecules, and compounds have been incorporated into both MWCNTs and SWCNT,[87] including such fascinating molecules as fullerenes (C_{60}@CNT, "peapods"[88]).

Initially, the motivation arose mainly from the prospect of forming encapsulated or (upon oxidation) freestanding inorganic nanowires. Soon, the possibility was considered of using the CNTs as nanocapsules, to protect the encapsulated material from reaction/oxidation due to contact with the atmosphere, and even as nanoreactors, whose confined reaction volume was expected to yield nanomaterials with new crystal structures and chemical compositions and with novel properties.

There have been various methods of filling, mainly depending on the cavity diameter to be filled and on physical properties of the material being inserted (e.g., viscosity, surface tension). The inserted material can be solid, liquid, or vapor; hence many physical properties have to be considered, including solubility, melting point, surface tension, boiling point, viscosity, and decomposition temperature.[87] Furthermore, the inner diameter of the CNTs will determine the maximum size of the inserted molecules or compounds and, hence, the filling efficiency.[89]

CNTs can be filled in situ during the synthesis process (either arc-discharge[90] or CVD[91]), with the advantages that the CNT integrity remains intact and the encapsulated material is completely protected from the postsynthesis atmosphere. Furthermore, this allows filling with compounds with surface tensions too high for other processes. However, the choice of materials is restricted to those that can be used as catalysts for the CNT growth (Fe, Co, Ni, etc). In contrast,

Table 5. Comprehensive List of Inorganic Compounds Used in CNT Hybrid Materials Including Applied Synthesis Techniques and Tested and Potential Applications

inorganic compound	synthesis routes	applications	Nr
Al_2O_3	ex situ - noncovalent[149,386,387] in situ - hydrothermal[233] in situ - sol−gel[218] chemical vapor deposition[259,388] physical vapor deposition[247,248]	field emission oxidation resistance[389]	>5
$BaSrO_3$	physical vapor deposition[245]	field emission[351,390]	1−2
CeO_2	in situ - sol−gel[200] in-situ - hydrothermal[199,233,391]	heterogeneous catalysis gas sensors	1−2
Co_3O_4	in situ - sol−gel[210] chemical vapor deposition[253]	magnetics batteries[392]	3−5
Cu_2O	in situ - hydrothermal[229,230,393,394]	photocatalysis	1−2
Eu_2O_3	ex situ -non covalent[135] in situ - hydrothermal[232]	diodes, lasers	2
Fe_xO_y	ex situ - covalent[395] in situ - hydrothermal[226,231,396]	magnetics biosensors[324] heterogeneous catalysis[397]	3−5
HfO_2	physical vapor deposition[247,248]	oxidation resistance	1
MgO	physical vapor deposition[242]	field emission[242,342,350,353,398] electrocatalysis[111]	3−5
MnO_2	in situ - electrochemical[167−169] in situ - electrodeposition[179,334] in situ - hydrolysis[399] chemical vapor deposition[400]	electrocatalysis[399] heterogeneous catalysis supercapacitors[110,167,179,188,332,333,400,335] oxidation resistance[168]	3−5
MoO_2	in situ - hydrolysis[292]	electrocatalysis[292]	1
NiO	in situ - sol−gel[209,253] chemical vapor deposition[253]	supercapacitors[181,209,330,331]	1
RuO_2	in situ - electrodeposition[182,183] in situ - sol−gel[207,208,216] in situ - hydrothermal[237] physical vapor deposition[158,246] chemical vapor deposition[183,251,261]	supercapacitors[182,207,208,237,246,251,338] biosensors heterogeneous catalysis[216,294,298]	>5
SiO_2	ex situ - covalent[114,401] in situ - sol−gel[118,215,218,219,402] physical vapor deposition[243,247,248,403,404]	field emission[346] oxidation resistance[215,405]	>5
SnO_2	in situ - sol−gel[194,198,199,201,202,406] in situ - hydrothermal[199,234,235,407,408] chemical vapor deposition[250,409]	gas sensors[201,203,210,319,321,410−413] electrocatalyis[302] nanofluids[414] batteries[202,408,415]	>5
TiO_2	ex situ - covalent[114] ex situ - noncovalent[149] in situ - electrodeposition[180,416] in situ - microemulsion[177] in situ - sol−gel[55,191−193,195,204,218,417−419] in situ - hydrothermal[224,225] chemical vapor deposition[259,420]	photocatalysis[196,205,206,224,278,280,282,421,422,281] optoelectronics[112,423] biosensors electrocatalysis[197,293,424] supercapacitors[180,415] batteries[177,425] oxidation resistance[195]	>5
VO_2, V_2O_5	in situ - electrochemical[170]	batteries[336,337,426] heterogeneous catalysis[170]	2
WO_3	in situ - electrochemical[300]	gas sensors[314,427] heterogeneous catalysis[300]	2
ZnO	in situ - electrochemical[428] in situ - microemulsion[178] in situ - sol−gel[220,221,429] in situ - hydrothermal[224,227] physical vapor deposition[244,247,248,254,348] chemical vapor deposition[256−258,430]	photocatalysis[221,224] optoelectronics[220,255] diodes, lasers[244] field emission[240,348]	>5
ZrO_2	ex situ - noncovalent[318] in situ - hydrothermal[431,432] physical vapor deposition[247,248] chemical vapor deposition[260]	oxidation resistance dielectric devices[260] heterogeneous catalysis chemical sensors[318]	3−5
carbides (Fe, W, Ta, Ti)	in situ - electrochemical[175] in situ - sol−gel[214] chemical vapor deposition[213,433]	heterogeneous catalysis electrochemistry[211] field emission[213,434]	3−5
chalcogenides (Zn, Cd, Hg; X = S, Se, Te)	ex situ - covalent[134,435] ex situ - noncovalent[166,436] in situ - electrochemical[164−166] in situ - hydrothermal[228] in situ - sol−gel[217]	optoelectronics[165]	>15
nitrides (Ti,Fe)	in situ - sol−gel[212] physical vapor deposition[211] chemical vapor deposition[252]	field emission[252]	2−3

ex situ filling enables the use of a variety of compounds but typically requires a multistep process including preoxidation to open the CNT tips (heating in air or treatment in oxidizing acids)[83,92] and post-treatment to remove any excess material

via washing or vacuum annealing.[93] The filling is either carried out from the gas phase (sublimation or capillary condensation)[94,95] or from the liquid phase (capillary wetting from suspension, solution, or melt).[96,97] The filling strategies with their various advantages and problems were summarized and discussed recently by Monthioux et al.,[87] as well as in earlier reviews.[98,99]

Although both MWCNTs and SWCNTs have been filled with a vast number of compounds, little is known about their properties and potential in applications. This has been frequently blamed on high impurity levels in the synthesized hybrids, the lack of bulk quantities, and the need for specifically designed measurement devices.[87] In general, the distinction should be made between the intrinsic properties of the filler, the altered properties of the encapsulated material due to the confined space, and novel properties arising from interactions between the filler and CNTs (a requirement for CNT−inorganic hybrids). For example, theoretical calculations predict a change from semimetallic to semiconducting properties of a HgTe crystal upon its encapsulation in SWCNTs.[100] Although this system had shown early promise of demonstrating the modification of electronic properties in filled CNTs due to the geometric constraints, experimental results have so far been rather disappointing. To date, there has been no evidence for charge transfer between the filler and the CNTs, band gap modulation, or any change in thermal or electric properties.

3. Synthesis of CNT−Inorganic Hybrids

Instead of filling CNTs (see previous section), the inorganic component can be attached to the outer surface of CNTs to produce novel hybrid materials. The various synthesis strategies for CNT−inorganic hybrids can be categorized as ex situ and in situ techniques. The ex situ (building block) approach first produces the inorganic component in the desired dimensions and morphology (typically spherical nanoparticles), then modifies and attaches this component to the surface of CNTs via covalent, noncovalent, or electrostatic interactions. In contrast, the in situ approach carries out the synthesis of the inorganic component in the presence of pristine or functionalized CNTs, onto which the inorganic material grows as particles, nanowires, or thin films.

As the ex situ process has been discussed in recent reviews,[101,102] this review summarizes this approach with a few significant examples and then focuses on the in situ approach for the formation of oxides, nitrides, and carbides. Table 5 summarizes the inorganic materials hitherto used in CNT−inorganic hybrids, along with their synthesis technique and potential applications. The references in the application column represent initial studies on CNT−inorganic hybrids tested for the desired application and will be discussed in section 4.

3.1. Ex Situ Approach: Attaching Nanoparticles to CNTs

In this ex situ or building block approach, nanoparticles (mostly metals or semiconductor QDs) are attached to the CNTs via linking agents that utilize covalent, noncovalent, or electrostatic interactions. In this approach, either the inorganic nanoparticles or the CNTs (or both) require modification with functional groups. The type of functionalization and, thus, the strength of interaction determine the distribution and concentration of the inorganic nanoparticles on the CNT surface.

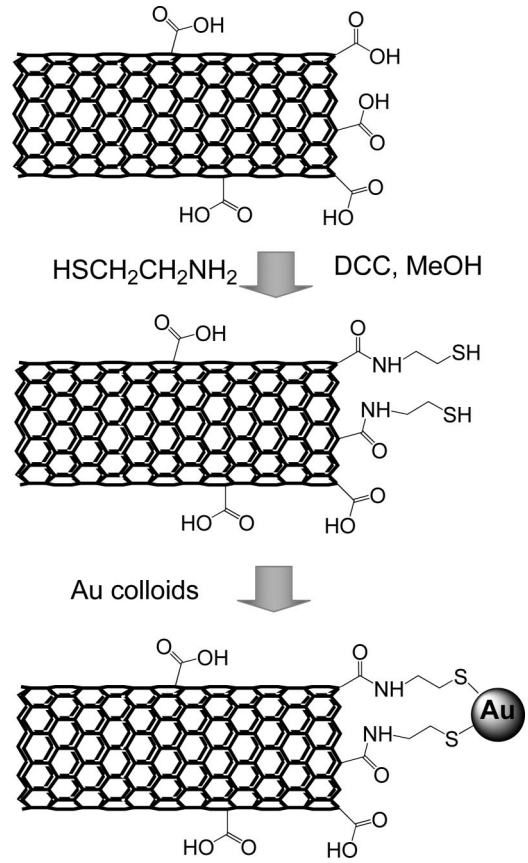

Figure 2. Common ex situ process for the covalent attachment of Au nanoparticles to amino- or mercapto-terminated CNTs. Redrawn from ref 103.

3.1.1. Covalent Interactions

Carboxyl groups on the surface of acid-treated CNTs (see section 2.2.3) are often used to attach amine-terminated or mercapto-terminated inorganic nanoparticles via amide bonds.[103] This can be achieved either by directly linking amine-terminated or mercapto-terminated nanoparticles with the carboxyl groups or by modifying these carboxyl groups into thiol groups, which then anchor to colloidal nanoparticles (Figure 2). In a similar way, QDs have been linked by first stabilizing them with a mixed monolayer of trioctylphosphine oxide (TOPO) and 2-aminoethanethiol.[104] The resulting amino-functionalized QDs then reacted with the carboxylic groups of the acid-treated CNTs to form amide bonds.

Banerjee et al. used a multistep procedure to attach modified CdSe QDs to functionalized CNTs[105] (Figure 3): (1) SWCNTs were first oxidized in a H_2SO_4/KMnO4 solution, and the resulting carboxylic groups were reacted with ethylenediamine to form amine-terminated amide groups. (2) CdSe nanoparticles were stabilized with TOPO, which was substituted by a thiol ligand, using *p*-mercaptobenzoic acid, to form acid-terminated CdSe nanocrystals. (3) The modified CdSe nanoparticles were linked to the functionalized CNTs in the presence of 1-ethyl-3-(3-dimethylaminopropyl) carbodiimide hydrochloride (EDC). In a similar way, thiol-stabilized ZnS-capped CdSe QDs were protected with 2-aminoethanethiol and linked to the acid-terminated CNTs in the presence of EDC.[106]

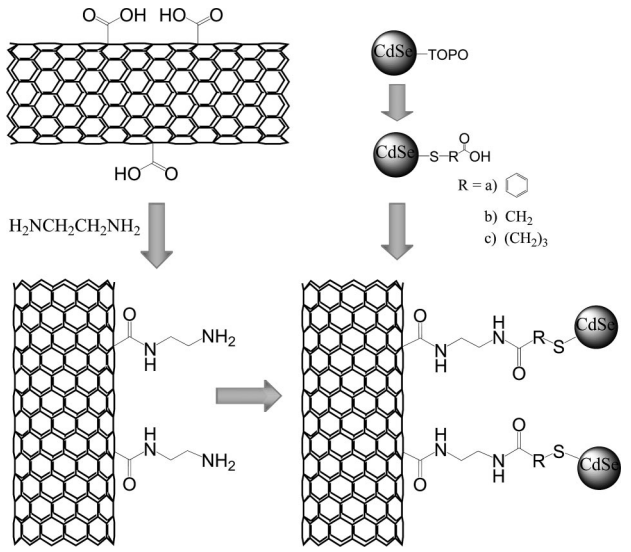

Figure 3. Multistep process for linking modified CdSe QDs to CNTs via amide bonds, involving (1) the oxidation of CNTs in $KMnO_4$ and functionalization with ethylenediamine and (2) the thiolization of CdSe and termination with acid groups. Redrawn from ref 105.

Among the various metal nanoparticles, gold has been used most frequently due to its excellent potential in biosensing and other medical applications.[107] The Au nanoparticles have been linked to the acid-terminated CNTs using aminothiols, bifunctional thiols, or thioether bonds.[108,109]

In contrast, metal oxides can be attached to the carboxyl groups without any linking agent due to their hydrophilic nature, as recently demonstrated for MnO_2,[110] MgO,[111] TiO_2,[112] and $Zr(SO_4)_2$.[113] However, the authors observed only weak interactions between the oxides and the acid-terminated CNTs, resulting in rather nonuniform distributions of the nanoparticles. Better adhesion was observed when capping agents were used. For instance, Sainsbury and Fitzmaurice produced capped TiO_2 and SiO_2 nanoparticles ($d \approx 4-5$ nm) via a standard sol−gel process using titanium tetraisopropoxide (TTIP) and tetraethyl orthosilicate (TEOS) as precursors with cetyltrimethyl ammoniumbromide (CTAB) as the capping agent.[114] MWCNTs were modified with 2-aminoethylphosphoric acid and then mixed with the oxide nanoparticles. The authors showed that the phosphonic acid groups on the CNTs were well-distributed and provided an excellent driving force for the attachment of TiO_2 nanoparticles (Figure 4).

3.1.2. Noncovalent Interactions

Alternatively, the nanoparticles can be attached to pristine CNTs via van der Waals interactions, hydrogen bonding, $\pi-\pi$ stacking, or electrostatic interactions. For instance, surfactants such as sodium dodecylsulfate (SDS) were used to decorate MWCNTs with nanoparticles of pure Pt,[115] EuF_3, and TbF_3[116] particles. Similarly, Whitsitt et al. evaluated various surfactants for their ability to facilitate the deposition of SiO_2 NPs onto SWCNTs.[117,118] In the presence of SDS, the SiO_2 nanoparticles were deposited around bundles of SWCNTs, while dodecyl dimethyl ammoniumbromide (DTAB) enabled a significantly better dispersion and debundling of the SWCNTs so that individual nanotubes were coated.

The functionalization of the inorganic nanoparticles with hydrophobic capping agents provides another route. As an

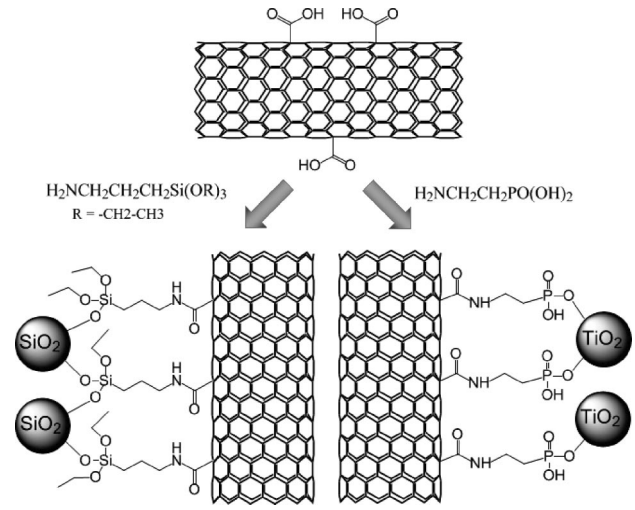

Figure 4. Example of an ex situ attachment of SiO_2 and TiO_2 nanoparticles to functionalized CNTs via silane and phosphonic acid bonds, respectively. Redrawn from ref 114.

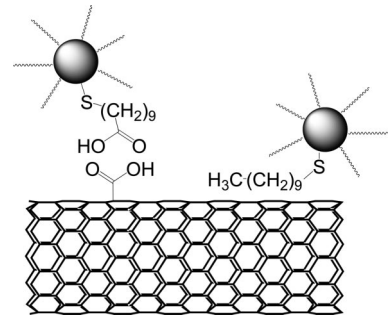

Figure 5. Mixed nonconvalent attachment of modified Au nanoparticles to CNTs via hydrogen bonds and hydrophobic interactions. Redrawn from ref 121.

example, Au clusters were first modified with a monolayer of octanethiols[119] or dodecanethiols[120,121] and then simply dispersed in a suspension of pristine SWCNTs in dichloromethane. The advantage of this approach is that both coverage and morphology of the hybrid materials can be controlled by modifying the length and functionality of the chains in the capping agents.[122]

Han et al. used both hydrophobic and hydrogen-bond interactions in their work.[121] The authors modified Au nanoparticles (2−5 nm) with a mixed monolayer of decanethiol and mercaptoundecanoic acid, providing mixed chemical functionality, and immersed them in a suspension of acid-treated CNTs. The alkyl chains of decanethiol offered hydrophobic interactions with the unmodified part of the CNT surface, while the acid-modified nanoparticles formed strong hydrogen bonds with the carboxylic groups of CNTs that could not even be dissembled upon heat treatment at 300 °C (Figure 5). Furthermore, as the acid groups are typically concentrated around the tip of the CNTs (especially when using weak oxidizing conditions), this approach has the potential for selective immobilization of one type of nanoparticle at the tips of the CNTs via H-bonds, while adsorbing another type hydrophobically on the sidewalls.

3.1.3. $\pi-\pi$ Stacking

Similar to noncovalent attachment, this approach uses the moderately strong interactions between delocalized π-electrons of CNTs and those in aromatic organic compounds, such as derivatives of pyrene,[123−125] porphyrins,[126−128] ph-

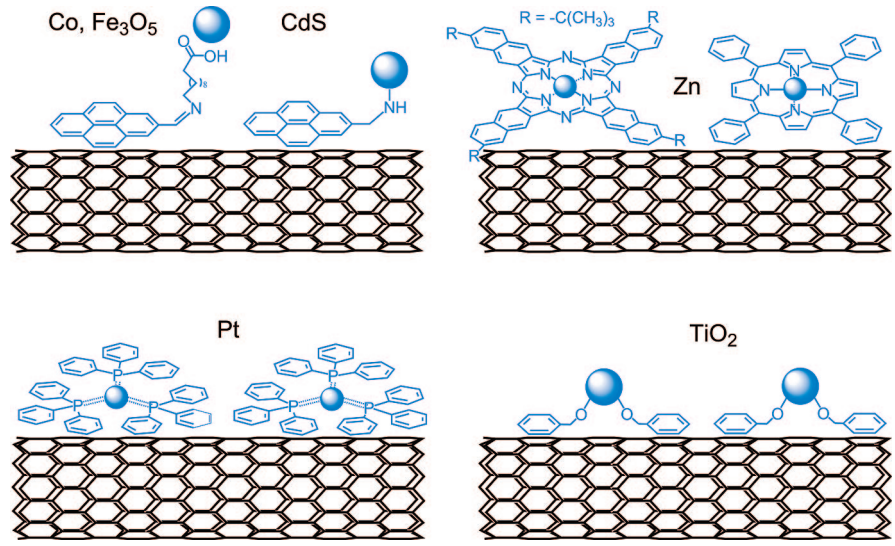

Figure 6. Examples of linking agents and ligands used to attach inorganic nanoparticles to pristine CNTs via $\pi-\pi$ interactions: (a) pyrene derivatives, (b) porphyrins and phthalocyanines, (c) triphenyl phosphines, and (d) benzyl alcohol.

thalocyanines,[129] or combinations thereof,[130] as well as benzyl alcohol[55] or triphenylphosphine (Figure 6).[131] These molecules are often modified with long alkyl chains that are terminated with thiol, amine, or acid groups, which can then connect to the inorganic nanoparticles and enable their attachment to pristine CNTs via $\pi-\pi$ stacking.

For example, Au nanoparticles have been anchored with thiol-terminated[132] or amine-terminated[133] pyrene molecules. Li et al. used 1-aminopyrene to immobilize CdS nanoparticles as large as 20 nm,[134] while pyrene derivatives with a carboxylic termination were used to anchor magnetic nanoparticles such as Co or Fe_3O_4.[135] In contrast with pyrene derivatives, compounds with phenyl groups typically support weaker $\pi-\pi$ interactions but are smaller in size and thus can attract more nanoparticles. For instance, very dense layers of metal nanoparticles close to the surface of CNTs have been achieved for Pt nanoparticles using triphenylphosphine (PPh3) as a linking agent.[131]

One of the major advantages of this approach is that the pyrene compounds remain strongly adsorbed on the CNT surface after workup steps (e.g., washing, filtration) and thus provide enhanced solubility and allow continuous redispersing of the modified CNTs in various aqueous and organic solvents. Furthermore, spectroscopic experiments on CNT−Pt[136] and CNT−porphyrin hybrids[126,137] revealed an enhanced charge transfer from the inorganic nanoparticles to the CNTs, mediated by the aromatic compound. This was also observed for attached Co and Fe_3O_4 nanoparticles,[135] whose magnetic and electronic properties were altered due to a strong electron transfer. Moreover, this effect is tunable by the length of the chain.

3.1.4. Electrostatic Interactions

The fourth approach utilizes electrostatic interactions between modified CNTs and inorganic nanoparticles. Among the known examples, the deposition of ionic polyelectrolytes to attract charged nanoparticles is the most common route.[138−142]

The choice of polyelectrolyte determines whether the CNTs are positively or negatively charged. For instance, oxidized CNTs have been coated with a thin film of poly(diallyldimethylammonium chloride) (PDDA), a cationic polyelectrolyte, which served as the real template for negatively charged Au nanoparticles.[141] Alternatively, by depositing a second layer of a negatively charged polymer, such as poly(sodium 4-styrenesulfonate) (PSS), on top of the PDDA layer, the surface of the CNT could be negatively charged and would then accept positively charged nanoparticles such as SiO_2.[142,143] The order of polymer deposition can also be inverted as shown by the group of Liz-Marzan, who first adsorbed PSS to provide a stable dispersion of negatively charged CNTs.[142,144,145] After the deposition of a thin layer of SiO_2 via hydrolysis of TEOS, a second layer of the positive charged PDDA was added, which provided an excellent anchor for CdTe nanoparticles (Figure 7). The SiO_2 spacer in this rather complex hybrid material minimized the photoluminescence quenching by the CNTs and preserved the quantum confinement effects.[144]

These polyelectrolytes typically bond covalently to the functional groups on the CNT, in contrast to polyethyleneimine (PEI), which interacts with CNTs via physisorption.[146] Another example is the use of Nafion to make the surface of CNTs negatively charged.[147] Nafion is a biocompatible perfluorosulfonated polymer with a polar side chain and with unique ion-exchange properties. Luong et al. immobilized Pt nanoparticles on the modified CNT surface by strong electrostatic interactions and tested this hybrid material for use in fuel cells.[147] Continuous metal coatings were obtained in a similar way, as shown for Au.[148] The metal nanoparticles were stabilized with tetraoctylammonium cations and dispersed in chloroform, into which the CNTs were immersed. Subsequent heating caused the nanoparticles to melt and amalgamate to form a metal nanowire with the CNTs as the cores. Sun et al. deposited Al_2O_3, ZrO_2, and TiO_2 nanoparticles on charged CNTs in a slightly modified way.[149] CNTs were pretreated in NH_3 at 600 °C to induce a positive surface charge. The addition of PEI increased the positive charges even further and enabled a better dispersion. Commercially available α-Al_2O_3 and 3Y-TZP were then dispersed in poly(acrylic acid) (PAA), which provided a negative surface potential over a wide range of pH values. Upon mixing, the Al_2O_3 and ZrO_2 nanoparticles formed strong electrostatic attractive interactions and covered the CNT surface completely.

Sun et al. attached nanocrystals of TiO_2 to acid-treated SWCNTs, also using PEI as a modifier (Figure 8).[150] In the

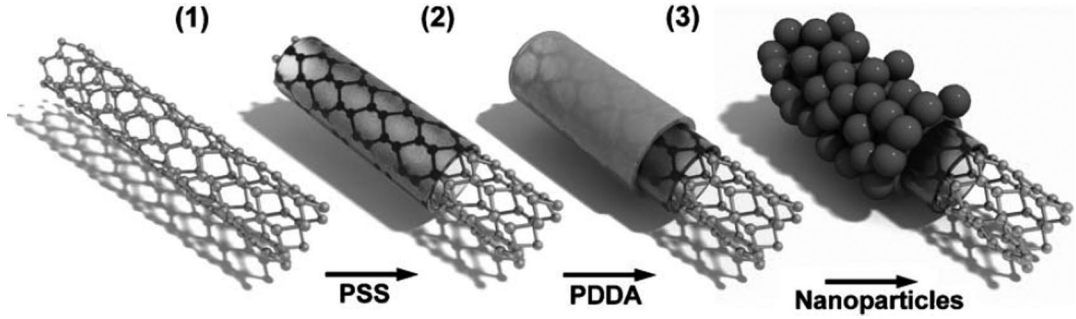

Figure 7. Example of the deposition of inorganic nanoparticles on CNTs via electrostatic interactions using polyelectrolytes: (1) polymer wrapping around a CNT using PSS, (2) self-assembly of PDDA on top of PSS, and (3) dense layer of inorganic nanoparticles around the modified CNT. Reprinted with permission from ref 145. Copyright 2006 Royal Society of Chemistry.

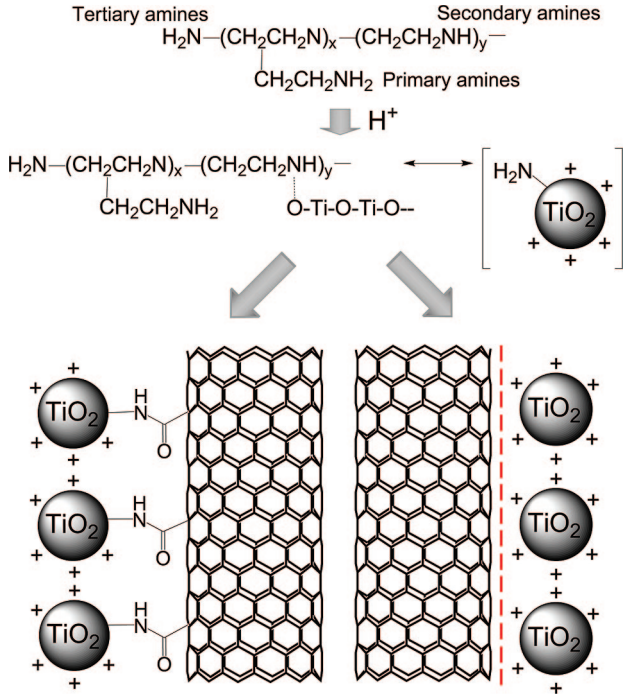

Figure 8. Two-step process for the attachment of TiO_2 nanoparticles to CNTs: (1) modification of the nanoparticles with positively charged PEI, containing primary, secondary, and tertiary amines, and (2) attachment via amide linkage or electrostatic interactions. Redrawn from ref 150.

first step, $TiCl_4$ was mixed with PEI, whose charged amino groups (25% primary, 50% secondary, and 25% tertiary amine) were protonated at a pH of 8. The positively charged amino groups of PEI accelerated the hydrolysis of $TiCl_4$ into TiO_2-nanoparticles and stabilized them electrosterically. These amine-terminated TiO_2-nanoparticles with positive charge then attached to acid-treated SWCNTs, either via amide linkage (Ieft-hand side) or through electrostatic interaction (right-hand side). Another route has been suggested by Jerome et al.,[151] who grafted MWCNTs with poly-2-vinylpyridine (P2 VP) to form carboxylate terminated alkyl chains, onto which positively charged magnetic Fe_3O_4 nanoparticles were anchored. The main advantage of the polymer route is that the polymers provide a very dense, uniform distribution of either negative or positive charges over the entire CNT surface, which enables very dense assemblies of inorganic nanoparticles.

In summary, these few examples demonstrate the simplicity and feasibility of the ex situ approach, which remains the method of choice for the deposition of metal nanoparticles and quantum dots. The main advantage is the possibility of using prepared nanoparticles with controlled morphology, structure, shape, and size, and, therefore, a good structure−property relationship. The downside of this route, however, is the need to chemically modify either the CNTs or the inorganic component. This process is often work-intensive, and functionalization alters both the surface chemistry of the CNTs and also, particularly for SWCNTs, their physical properties. Furthermore, the use of predefined building blocks restricts the synthesis of novel hybrid materials and, thus, the development of new physical properties.

3.2. In Situ Synthesis Directly on the CNT Surface

The inorganic compound can also be formed directly on the surface of pristine or modified CNTs. The main advantage of this route is that the inorganic compound can be deposited as a continuous amorphous or single-crystalline film with controlled thickness, or as discrete units in the form of nanoparticles, nanorods, or nanobeads. Furthermore, the CNTs may act as a support to stabilize uncommon or even novel crystal phases or prevent crystal growth during crystallization and phase-transformation processes. Finally, a variety of chemical and physical synthesis techniques can be applied. The deposition can be carried out either in solution via electrochemical reduction of metal salts, electro- or electroless deposition, sol−gel processing, and hydrothermal treatment with supercritical solvents, or from the gas phase using chemical deposition (CVD or ALD) or physical deposition (laser ablation, electron beam deposition, thermal evaporation, or sputtering).

3.2.1. Electrochemical Techniques

Electrochemistry is a powerful technique for the deposition of various nanoparticles (especially metal particles), as it enables effective control over nucleation and growth.[152,153] Most research has been conducted on the deposition of noble metals and alloys such as Pd,[152,154] Pt,[153−155] Au,[154] Ag,[153] and bimetallic Pt−Ru,[156] as they are the metals of choice for applications like heterogeneous catalysis and electrocatalysis,[157] supercapacitors,[158] gas sensors,[159] and biosensors.[160]

In general, metal nanoparticles are obtained via reduction of metal complexes, such as $H[AuCl_4]$, $K_2[PtCl_4]$, and $(NH_4)_2[PdCl_4]$, by chemical agents (chemical reduction), or by electrons (electrodeposition). The size of the metal nanoparticles and their coverage on the sidewalls of CNTs can be controlled by the concentration of the metal salt and various electrochemical deposition parameters, including nucleation potential and deposition time.[152,153,161]

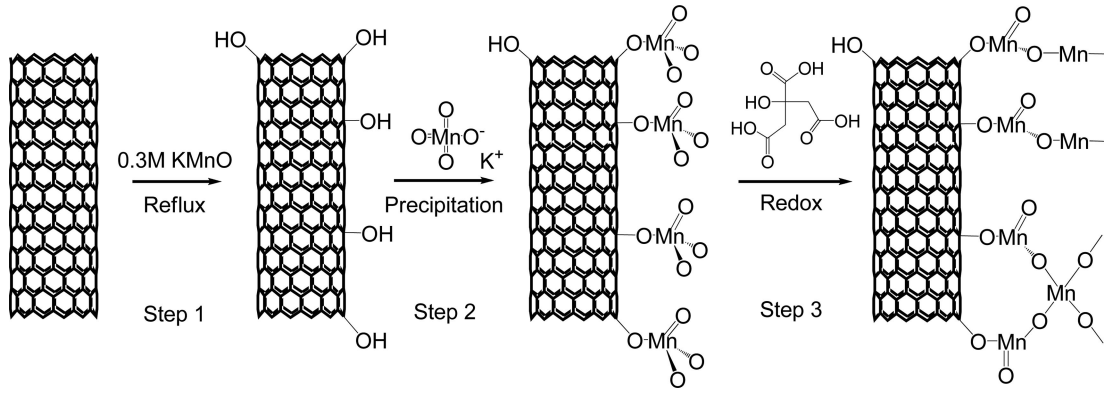

Figure 9. Example of the deposition of MnO_2 on CNTs via chemical reduction. The multistep process involves (1) the oxidation of MWCNTs with $KMnO_4$ to form hydroxyl groups, (2) the precipitation of permanganate ions, and (3) their reduction with citric acid to MnO_2. Reprinted with permission from ref 168. Copyright 2007 Elsevier Publishing.

3.2.1.1. Chemical Reduction and Oxidation. These techniques involve reactions, in which the reduction of the precursor is carried out with liquid or gaseous reducing agents with the aid of heat, light, ultrasound, microwave, or supercritical CO_2.[162,163] As an example, Cao et al. mixed MWCNTs with sulfur powder and $CdCl_2$ with the aid of ultrasonication.[164] The sulfur was first reduced with KBH_4 to form S^{2-} ions, which then reacted with the Cd^{2+} ions to form CdS nanoparticles on the surface of the CNTs. The authors observed a uniform distribution of the fibers, which caused a significant charge transfer to the CNTs and enhanced photovoltaic response. Robel et al. used a similar approach with CdI_2 and Na_2S.[165] A very uniform dispersion of metal nanoparticles was obtained by Li et al., who chose noncovalent functionalization with 1-aminopyrene and used electrostatic interactions for the deposition of Pt and CdS nanoparticles.[166] Under reaction conditions, the amino groups were slightly positively charged and thus attracted $(PtCl_6)^{2-}$ ions, which were then reduced with $NaBH_4$ to give Pt nanoparticles.

Sivvakkumar et al. deposited MnO_2 via chemical reduction of $KMnO_4$.[167] The authors suspended the CNTs in Na-*p*-toluene sulfonate and pyrrole, which polymerized with the aid of ultrasonication. $KMnO_4$ was then slowly added and reduced with acetonitrile to form hydrous MnO_2. A very elegant variation of this process is shown in Figure 9 and

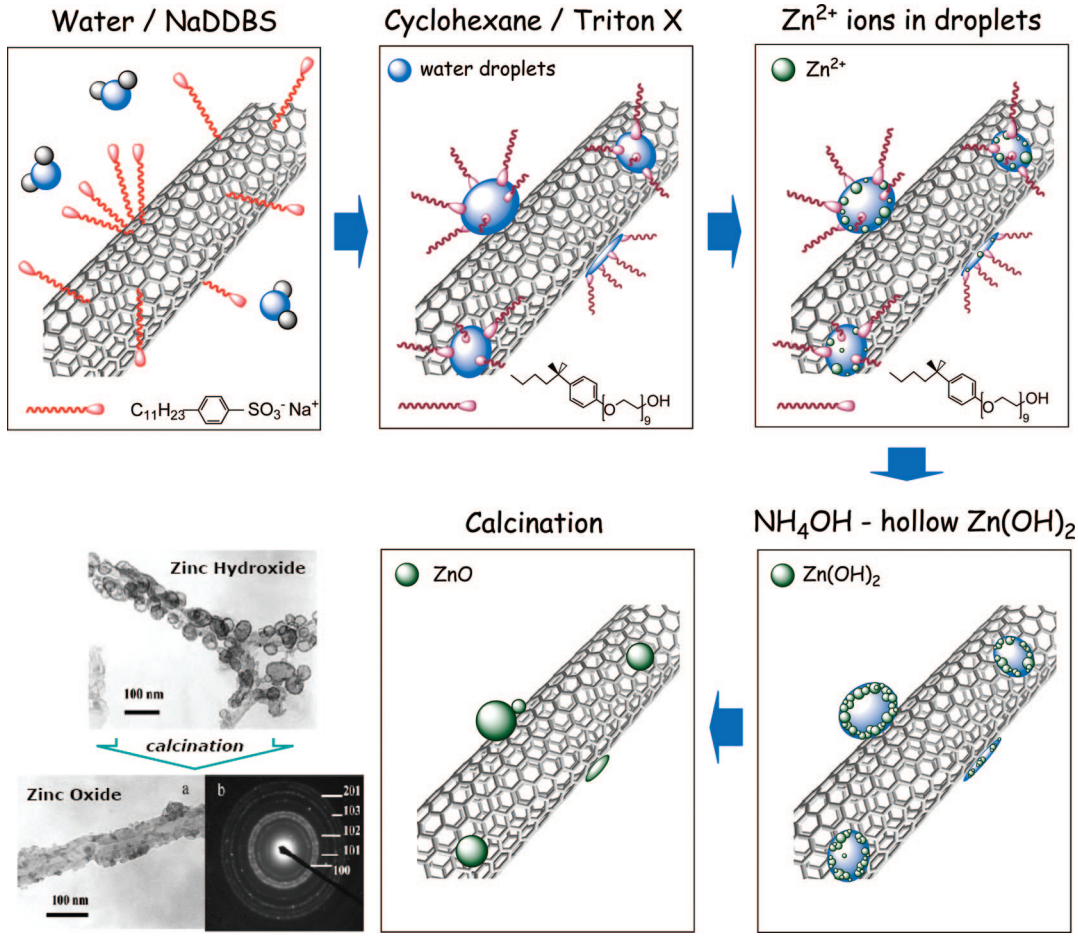

Figure 10. Example of a water-in-oil microemulsion technique. Formation of hollow $Zn(OH)_2$ spheres on CNTs and their subsequent calcination to dense ZnO nanoparticles. Redrawn from ref 178.

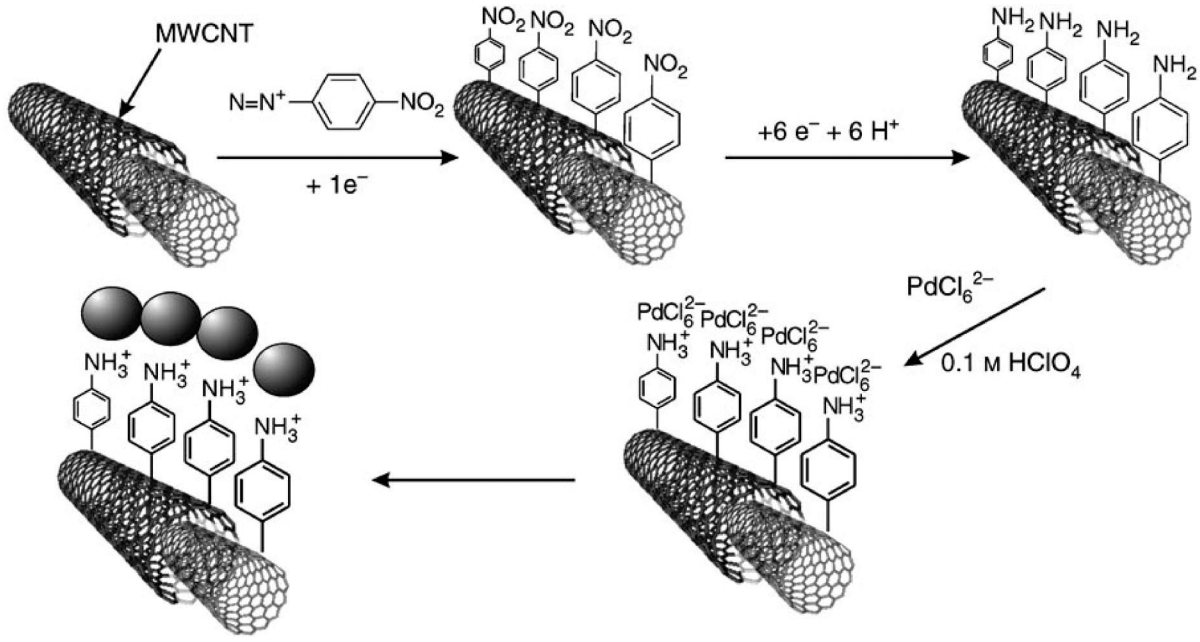

Figure 11. Electrodeposition of Pd nanoparticles on MWCNTs, via (1) covalent functionalization of CNTs with aminobenzyl groups via electrochemical reduction, (2) potentiostatic reduction of $PdCl_6^{2-}$ ions to Pd nanoparticles. Reprinted with permission from ref 152. Copyright 2004 Elsevier Publishing.

uses $KMnO_4$ as both the oxidizer and reactant.[168] In detail, pristine MWCNTs were first oxidized under reflux with $KMnO_4$, which introduced exclusively hydroxyl groups on the sidewalls of CNTs (step 1), in contrast to other oxidation treatments, e.g., with oxidizing acids. These hydroxyl groups then acted as anchors for Mn^{7+} ions (step 2), which subsequently were reduced to Mn^{4+} with citric acid (step 3) to form a coating of ϵ-MnO_2. For comparison, a pretreatment of the CNTs in strong acids, which induces the formation of carboxyl groups, resulted instead in γ-MnO_2.[169] Therefore, this work provides an interesting example of the effect of the CNT surface chemistry on the crystal structure of the inorganic coating.

In contrast to MnO_2, the deposition of other metal oxides typically requires oxidizing rather than reducing processes. For instance, Huang et al. added acid-treated CNTs to a solution containing ammonium metavanadate.[170] The adsorbed VO^{2+} ions were then oxidized with oxalic acid to V_2O_5.

Another common method involves the reduction of the adsorbed precursor at high temperatures under a hydrogen atmosphere. This approach has been applied to a variety of metal nanoparticles such as Pt,[171,172] Pd,[173] Rh, and Ru,[163,174] as well as to various carbides such as TiC, TaC, and NbC.[175] A different approach combined the reduction of cationic precursors by hydrogen with a water-in-oil microemulsion technique for the deposition of metal[157,176] or oxide nanoparticles.[177] Sun et al. used a slightly modified process, shown in Figure 10.[178] The authors mixed the CNTs first with an aqueous solution of sodium dodecylbenzene sulfonate (NaDDBS) and then with a mixture of Triton-X and cyclohexane, which resulted in very small water droplets on the CNT surface. Upon adding zinc acetate as the metal precursor, the Zn^{2+} ions concentrated in the aqueous phase and then reacted with NH_3 or LiOH to form spherical, hollow ZnOH nanoparticles. Subsequent calcinations oxidized them to create small and dense ZnO nanoparticles. In all cases, the microemulsion technique produced fine dispersions of small nanoparticles.

3.2.1.2. Electrodeposition. Many of the above-mentioned reduction/oxidation techniques are very time-consuming and as such allow impurities in the bath solution to be incorporated into the inorganic phase. In contrast, electrodeposited nanoparticles, especially noble metals such as Pt, Pd, or Au, are formed faster upon reduction of the corresponding metal salts under an applied potential and, thus, exhibit higher purities as well as a good adhesion to the CNT surface.[156,161] In most cases, simple van der Waals interactions between the CNTs and the nanoparticles seem to be sufficient to provide strong enough adhesion.

However, functionalization of CNTs can still enhance the dispersion and decrease the size of nanoparticles, as demonstrated by Guo et al. (Figure 11).[152] The authors functionalized MWCNTs covalently with 4-aminobenzene via the direct electrochemical reduction of the diazonium salt of nitrobenzene. These groups provided good electrostatic attractions for $[PdCl_6]^{2-}$ ions, which were then reduced to very small Pd nanoparticles (2.5 nm in diameter) via potentiostatic reduction in 0.1 M H_2SO_4.

Although most research currently concentrates on the electrodeposition of metal nanoparticles, there have also been a few reports on electrodeposited metal oxides. As an example, Lee et al. drop-casted acid-treated CNTs on a Ni working electrode and used Pt wires and saturated calomel as counter and reference electrodes, respectively.[179] By applying a potentiostatic method with $MnSO_4$ at pH 5.6 and a potential of 0.4 V, the authors deposited rather large aggregates of MnO_2, predominantly around the tips of the CNTs. Similarly, Frank et al. used pristine SWCNT bucky paper as a working electrode, using Pt wires as both reference electrodes and counterelectrodes.[180] $TiCl_3$ was used as a precursor and electrolyte and was kept at pH 2.5 with HCl/Na_2CO_3. The deposition was then carried out via galvanostatic oxidation with 1 mA/cm^2 and resulted in a rather irregular and partial coating of a mixture of anatase and TiO_2−B.

The galvanostatic approach (3 mA/cm^2) has also been applied to codeposit Ni and Co oxides from their nitrates,

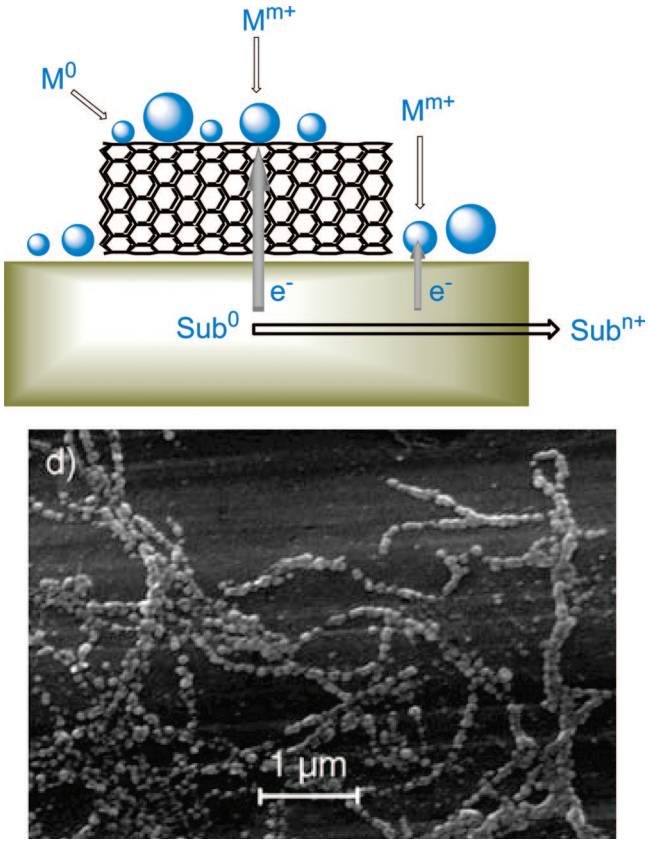

Figure 12. (a) Scheme of the substrate-enhanced electroless deposition (SEED) of nanoparticles using the CNT as cathode. (b) SEM image of Pt nanoparticles deposited on SWCNTs. Reprinted with permission from ref 185. Copyright 2005 American Chemical Society.

with Pt and saturated calomel as the counterelectrodes and reference electrodes, respectively.[181] By cycling the applied potential from 0 to 0.5 V, the authors could obtain a more uniform and stabilized coating. This was also demonstrated by Kim et al., who produced a continuous 3 nm thick coating of RuO_2 via the potential cycling method while varying the potential from −200 to 1000 mV with a scan rate of 50 mV/s.[182] They observed that the gas atmosphere during the postannealing process had a significant effect on the morphology of RuO_x. Furthermore, heating in argon produced more uniform, spherical nanoparticles, while annealing in O_2 resulted in elliptical RuO_2 nanoparticles.[183]

One advantage of this technique is that the electrodeposition occurs to the same extent on both the sidewalls of the tubes and the tips.[184] Consequently, the presence of carboxyl or hydroxyl groups as activators is not required. Furthermore, He et al. showed that the high purity is also of great advantage for the codeposition of bimetallic nanoparticles, which also exhibited enhanced electrocatalytic activity toward the oxidation of methanol.[156] The authors deposited Pt−Ru nanoparticles potentiostatically (−0.25 V) with diameters of 60−80 nm onto oxidized CNTs, starting from a solution containing ruthenium chloride and chloroplatinic acid in 0.5 M H_2SO_4. However, despite the simplicity and elegance of this technique for the deposition of metal nanoparticles especially, the major drawback of electrodeposition is that it is difficult to produce bulk quantities.

3.2.1.3. Electroless Metal Deposition. Electroless metal deposition was first mentioned by Qu et al.,[185] who observed that Au and Pt nanoparticles formed spontaneously on SWCNTs immediately after immersing the CNTs in a solution of $HAuCl_4$ or Na_2PtCl_2. Because of the absence of any reducing agent, the authors suggested that a direct redox reaction via electron transfer occurred between the metal ions and the CNTs, which acted as the cathode.[186,187] With the exception of MnO_2,[188,189] this substrate-enhanced electroless metal deposition (SEED) could only be successfully applied to noble metals, while Ag^+, Ni^{2+}, and Cu^{2+} had redox potentials too low to be reduced in the same way.

3.2.2. Sol−Gel Process

The sol−gel process is a versatile, solution-based process for producing various ceramic and glass materials in the form of nanoparticles, thin-film coatings, fibers, or aerogels and involves the transition of a liquid, colloidal "sol" into a solid "gel" phase.[190] Typical starting materials for the preparation of the sol include metal salts or metal organic compounds, such as metal alkoxides, which undergo a series of hydrolysis and condensation reactions to form a colloidal or polymeric sol. Upon aging, the sol forms a wet inorganic continuous network with oxo (M−O−M) or hydroxo (M−OH−M) bridges, creating a gel. Subsequent drying under supercritical conditions converts the gel into a low-density, highly porous aerogel, while drying induced by heating typically results in a xerogel (low temperature) or a dense ceramic (high temperature). The sol−gel process can be used to produce ultrafine and uniform ceramic powders, thin-film coatings, monolithic glasses and ceramics, membranes, and, with a suitable viscosity, ceramic fibers. It is, furthermore, a cheap and low-temperature technique that allows fine control of chemical composition and the introduction of lowest concentrations of finely dispersed dopants, such as organic dyes and rare earth metals. One of the major drawbacks is that the product typically consists of an amorphous phase rather than defined crystals and, thus, requires crystallization and postannealing steps.

In general, the sol−gel process has emerged as the most common technique to synthesize CNT−inorganic hybrids. Early attempts concentrated on the dispersion of CNTs within a matrix of inorganic nanoparticles. Vincent et al. synthesized TiO_2 nanoparticles using metal organic precursors and acetic acid as a gelator.[191] They observed that the dispersion of pristine CNTs was more stable when the TiO_2 nanoparticles had been produced in the presence of the CNTs (in situ) compared with the simple mixing of the two materials. Upon reducing the amount of TiO_2 with respect to CNTs, Jitianu et al. obtained a thin but rather irregular and partial coating of TiO_2 on CNTs.[192,193] Typically, the thickness of the coating can be controlled by various parameters, such as the reaction time,[194] the reaction composition, and the choice of metal precursor.[195] For instance, in the case of TiO_2, the use of titanium tetraisopropoxide (TTIP) produced irregular coatings,[192,196] while tetraethoxy orthotitanate (TEOT)[192] or tetrabutoxy orthotitanate (TBOT)[195,197] enabled a more uniform deposition. The sol−gel process was sometimes carried out under reflux,[194] or with the aid of ultrasonication,[198] microwave,[199] or magnetic agitation,[200] in order to enable faster and simultaneous nucleation resulting in a more homogeneous coating.

3.2.2.1. Covalent. These early works used pristine CNTs, whose hydrophobic nature provides little attractive interaction with the inorganic compound and thus limits the quality of the coating. Similar to the ex situ approach, the most common approach to change the surface chemistry of CNTs is to treat

them in strong oxidizing acids ($H_2SO_4-HNO_3$). This process introduces a variety of organic groups, with limited control over their number, type, and location, and causes surface etching and shortening of the tubes. Consequently, the inorganic coatings on acid-treated CNTs were often nonuniform, although they provided better interaction in comparison with pristine CNTs.

Despite these drawbacks, most researchers have used such acid-treated CNTs for various inorganic coatings, including SnO_2,[198,199,201−203] TiO_2,[197,204−206] RuO_2,[207,208] CeO_2,[200] NiO,[209] and mixed oxides (e.g., $Co_3O_4-SnO_2$).[210] Some oxide coatings were then heated at 800−900 °C in a carbon- or nitrogen-containing atmosphere (e.g., CH_4, NH_3) to produce metal nitride and carbide coatings such as TiN and Fe_2N,[211,212] TiC,[213] and WC.[214]

3.2.2.2. Noncovalent. In a similar way to the ex situ approach, noncovalent attractions and $\pi-\pi$ interactions can be used to grow the inorganic component on the surface of CNTs. For instance, Bourlinos et al. wetted pristine CNTs with vinyl silane molecules via noncovalent interactions between the vinyl groups and CNT surface.[215] After condensation to an oligomeric siloxane network and subsequent calcinations, the authors obtained small SiO_2 nanoparticles (5−12 nm), which were well-dispersed on the CNT surface. Another approach was used by Cao et al., who modified CNTs with surfactants such as sodium dodecylsulfate (SDS).[216] The hydrophobic aliphatic chain interacted with the surface of the CNTs, while the hydrophilic end attracted the metal ions of the $RuCl_3$ precursor, which then reacted to form RuO_2. Similarly, Wei et al. used metal nitrates and Na_2S to attach fibers such as CdS, Ag_2S, and HgS to the surface of pristine CNTs.[217]

Recently, this author has developed a nondestructive, simple process to coat pristine CNTs with TiO_2 by using benzyl alcohol as a surfactant.[55,195] Benzyl alcohol adsorbs onto the CNTs' surface via $\pi-\pi$ interactions with the alcohol's benzene ring (similar to pyrene derivatives), while simultaneously providing hydrophilic hydroxyl groups for the hydrolysis of the titanium precursor (TBOT) (Figure 13). In contrast to the sample without benzyl alcohol (Figure 13a), the addition of small amounts of benzyl alcohol resulted in a very uniform coating that covered the whole CNT surface. The work further showed that benzyl alcohol strongly affected the phase transition from anatase to rutile, providing very small and uniform rutile nanocrystals with very high specific surface areas (60−100 m^2/g) without too great a hindrance of the anatase to rutile transformation.

3.2.2.3. Electrostatic. In contrast to the ex situ approach, the use of electrostatic interactions for the in situ sol−gel route has been demonstrated only for a few metal oxides. As an example, Hernadi et al. used CNTs that had been pretreated with SDS, dried, and redispersed in 2-propanol.[218] Using metal halides as precursors, the authors could successfully produce coatings of Al_2O_3, SiO_2, and TiO_2. On the other hand, the use of metal organic precursors (aluminum isopropoxide (AIIP), TEOS, TEOT) did not produce any coating, but rather nanoparticles in solution. It appears that, in the latter example, the applied surfactant had a repressive role in the adhesion of the inorganic precursor due to different polarities between surfactant-treated CNTs (ionic) and the alkene groups of the precursor. This work provides yet another example of the importance of surface chemistry.

Seeger et al. modified the MWCNT with the polyelectrolyte PEI, which provided positive charges on the CNT surface.[219] Using the same metal organic precursor (TEOS) as the previous example, the negatively charged SiO_x colloids could then easily attach via electrostatic interactions to form a coating of amorphous SiO_2 (thickness ≈ 3−10 nm).

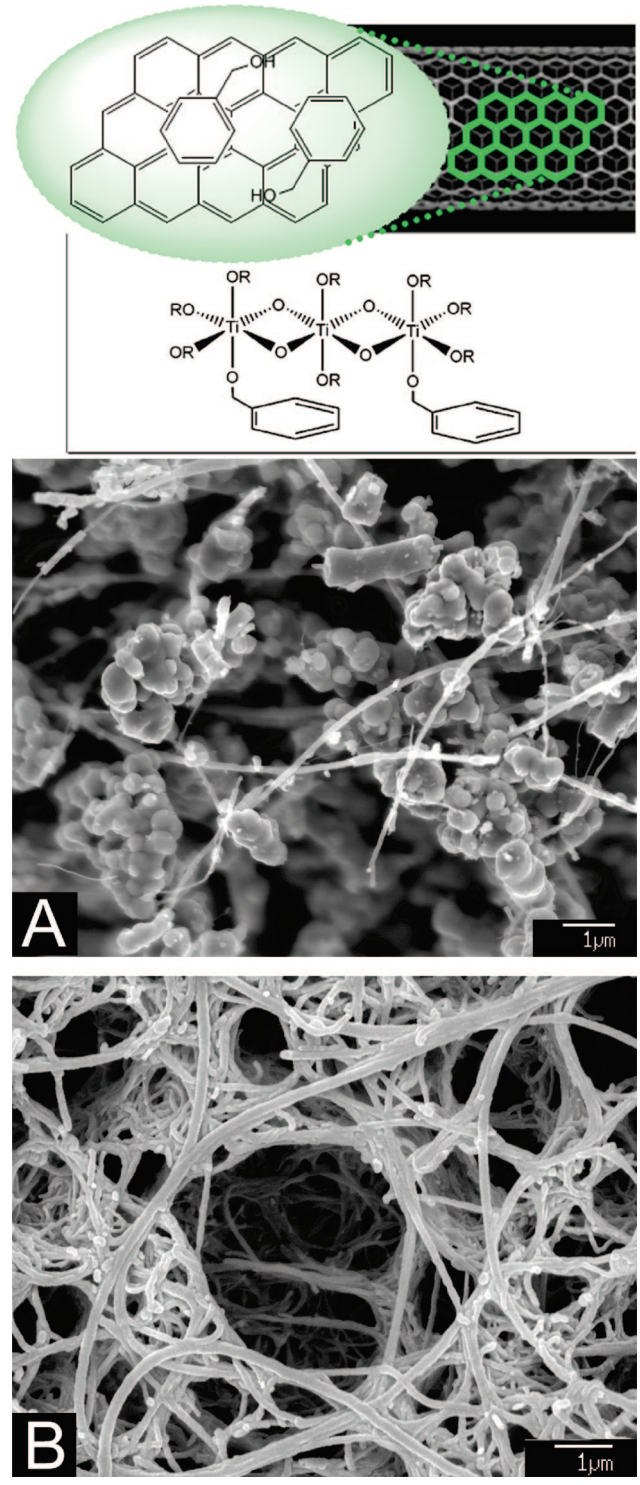

Figure 13. (Top) Scheme of the beneficial role of benzyl alcohol in the in situ coating of pristine CNTs with TiO_2. The benzene rings of the alcohol adsorb onto the CNT surface via $\pi-\pi$ interactions and at the same time provide a high density of hydroxyl groups for the hydrolysis of the titanium precursor directly on the CNT surface. (Bottom) SEM images of pristine MWCNTs (A) without the use of benzyl alcohol and (B) with a titanium-to-benzyl alcohol molar ratio of 5. Reprinted with permission from ref 55. Copyright 2008 Wiley-VCH.

However, since the reaction was carried out at room temperature, it was very time-consuming and exceeded 100 h.

In contrast, Vietmeyer et al. used acid-treated CNTs to attract Zn^{2+} ions (using zinc acetate), which then reacted with LiOH in an ice-water bath to form ZnO nanoparticles.[220] While some nanoparticles were attached to the CNT surface and tips, most of the nanoparticles formed large clusters rather than a continuous coating. For comparison, Jiang et al. enhanced the negative charge on the surface of acid-treated CNTs by simply depositing a thin layer of SDS and carried out the same reaction with zinc acetate and LiOH.[221] This surface modification significantly enhanced the attractive interactions with the metal ions and led to a more uniform coating with ZnO crystals.

3.2.3. Hydrothermal and Aerosol Techniques

In recent years, many organic−inorganic hybrids have been produced by hydrothermal techniques.[5,222] In contrast to standard sol−gel routes, the hydrothermal method typically enables the formation of crystalline particles or films without the need for postannealing and calcinations. Furthermore, the forced crystallization enables the formation of inorganic nanowires and nanorods.[223]

3.2.3.1. Vapor-Assisted, Polyol-Assisted Process. In this simplest case of hydrothermal synthesis, pristine or acid-treated CNTs were added to an aqueous solution of the precursor and treated in an autoclave at temperatures between 100 and 240 °C to produce crystalline films of ZnO,[224] TiO_2,[225] or Fe_2O_3.[226] These works consistently produced dense coatings of spherical or slightly elongated nanoparticles. Zhang et al. used aligned CNTs, which they precoated with a thin, amorphous layer of ZnO via magnetron sputtering[227] (see section 3.2.4.1). Then they dissolved a fine ZnO powder in NaOH at a pH of 10−12, which provided a saturated solution of $Zn(OH)_4^{2-}$. The modified CNT carpet was then placed top-down in an autoclave, floating on the precursor solution. By keeping the reaction at a temperature of 100 °C for several hours, the Zn precursor nucleated on the CNT−ZnO film to grow ZnO nanowires perpendicular to the CNTs, with a thickness of 30−70 nm and lengths of up to 0.5 μm (Figure 14).

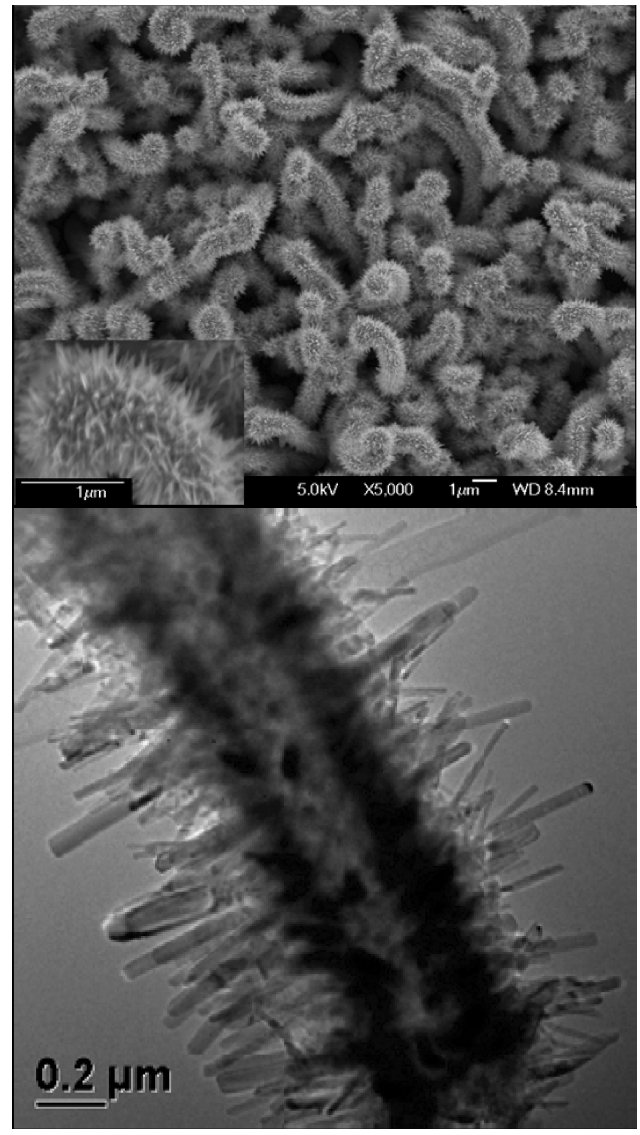

Figure 14. Example of the hydrothermal synthesis: growth of ZnO nanowires perpendicular to MWCNTs. Reprinted with permission from ref 227. Copyright 2006 Institute Of Physics.

The crystallinity of the inorganic compound typically depends on the reaction temperature and time. For instance, Du et al. showed that autoclaving a mixture of MWCNTs with $ZnCl_2$, ethanol, and thiourea[228] at 180 °C produced well-defined ZnS particles (diameter ≈ 40 nm) on the surface of the CNTs, while a reaction temperature of 80 °C only resulted in an amorphous coating.

In general, the use of specific molecules, which hinder the crystal growth by steric configuration (capping agents), provides efficient control of the crystal size of the nanoparticles. For example, Yu et al. dissolved copper acetate in water and diethylene glycol and added acid-treated CNTs.[229,230] Upon heating in an autoclave at 180 °C, the diethylene glycol-capped copper species condensed to CuO_x and nucleated to form small Cu_2O crystals. After a reaction time of 2 h, the crystals were 5−10 nm in diameter and covered by an amorphous layer. Similarly, small crystals of Fe_3O_4 were produced by Jia et al., who used polyethylene glycol (PEG) and $FeCl_3$ and a reaction temperature of 200 °C.[231] However, the 5 nm crystals agglomerated to about 180 nm aggregates (nanobeads), which attached preferably to the carboxyl groups on the surface of acid-treated CNTs. Consequently, the magnetite nanobeads were concentrated at the tips of the CNTs and acted as a glue to form heterojunctions between the CNTs (Figure 15).

3.2.3.2. Supercritical Solvent. A very important hydrothermal method involves the use of supercritical CO_2 as an antisolvent that reduces the solvent strength of ethanol, resulting in the precipitation of the oxide due to high saturation. Using metal nitrates or halides, this method has been applied to deposit Eu_2O_3,[232] CeO_2,[233] La_2O_3,[233] Al_2O_3,[233] SnO_2,[234,235] and Fe_2O_3[236] onto pristine CNTs. Sun et al. used supercritical ethylenediamine as a solvent to produce thin coatings of RuO_2.[237] They also observed various morphologies and structures of cerium oxide by simply changing the reaction temperature.[233] For instance, the authors could alter the composition of cerium oxide from preferentially Ce_2O_3 at 120 °C to CeO_2 at 150 °C. In contrast, a reaction temperature of 120 °C was needed to obtain a coating of SnO_2, while at 35 °C the oxide was only encapsulated.[235]

3.2.3.3. Liquid-Source Misted Chemical Deposition (LSMCD). In the LSMCD process, the liquid precursor is converted into submicrometer droplets with a monodisperse aerosol generator (atomizer). Electrostatic and fluid forces transport the droplets to the surface of CNTs, while preserv-

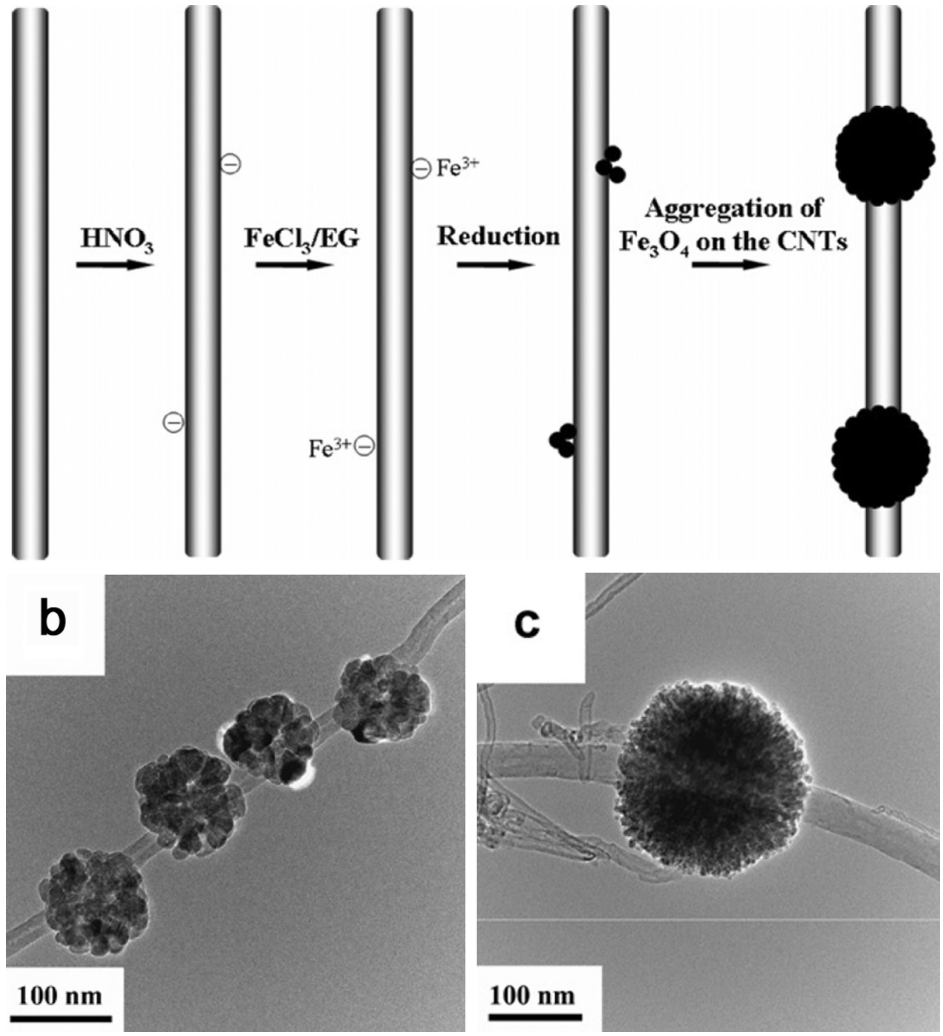

Figure 15. Example of a polyol-assisted hydrothermal deposition of Fe_3O_4 on acid-treated MWCNTs. Polyethylene glycol (PEG) was used to reduce $FeCl_2$ and to control the size of the magnetite nanoparticles, which formed large aggregates (nanobeads) near the carboxyl groups on the CNT surface. Reprinted with permission from ref 231. Copyright 2007 Elsevier Pubishing.

ing the precursor stoichiometry. After curing, conformal thin films with high uniformity can be achieved, as demonstrated by Kawasaki et al. for lead zirconium titanate (PZT) on vertically aligned individual CNTs.[238] A chemical deposition solution containing a Pb−Zr−Ti mixture of 1.1:0.4:0.6 was dissolved in methylethylketone, converted into mist with an atomizer, and sprayed at 140 °C vertically onto the CNTs, kept at 120 °C. The precursor reacted preferably with Stone-Walls defects on the surface of the CNTs and formed a uniform, still wet layer, which was then pyrolyzed at 300 °C to give an amorphous coating and subsequently heated to 650 °C to crystallize into PZT. The advantages of this technique include the use of commercially available chemical deposition solutions and the low reaction temperatures.

3.2.4. Gas-Phase Deposition

Chemical and physical vapor deposition techniques are among the most common methods to produce inorganic nanomaterials, as they provide excellent control over the size, shape, and uniformity of the inorganic material. Furthermore, it is possible to deposit thin, continuous films on carbon substrates, without altering the 3D integrity of vertically aligned CNTs. This section provides examples of the synthesis of various CNT−inorganic hybrids using physical techniques, such as evaporation, sputtering, and pulsed laser deposition (PLD), and chemical methods, including chemical vapor deposition (CVD) and atomic layer deposition (ALD).

3.2.4.1. Evaporation and Sputtering. Physical vapor deposition involves the evaporation of material in a crucible under high vacuum, using either resistive heating (thermal evaporation) or electron bombardment (electron beam deposition), which is generated from a hot filament and focused with a magnetic field. In contrast, sputtering (magnetron and radio frequency, RF) relies on plasma (typically argon) to bombard the target material, which can be kept at a relatively low temperature. Reactive sputtering involves a small amount of oxygen or nitrogen, which reacts with the sputtered material to deposit oxides or nitrides.

The deposition of metal oxides via thermal evaporation has been demonstrated by Kim et al., who mixed annealed CNTs with Zn powder in a ratio of 1:12.[239] Depending on the reaction temperature, the Zn particles reacted with oxygen impurities in argon to form a coating on the CNTs consisting either of spherical particles (450 °C), nanowires (800 °C), or short nanorods (900 °C). Similar results were obtained by Yu et al., who tested the hybrid materials in field emission devices and observed a significant improvement in emission spot density due to the one-dimensional shape of ZnO.[240]

Zhang et al. used an electron beam to deposit various metals on SWCNTs and observed that Ti, Ni, and Pd attached

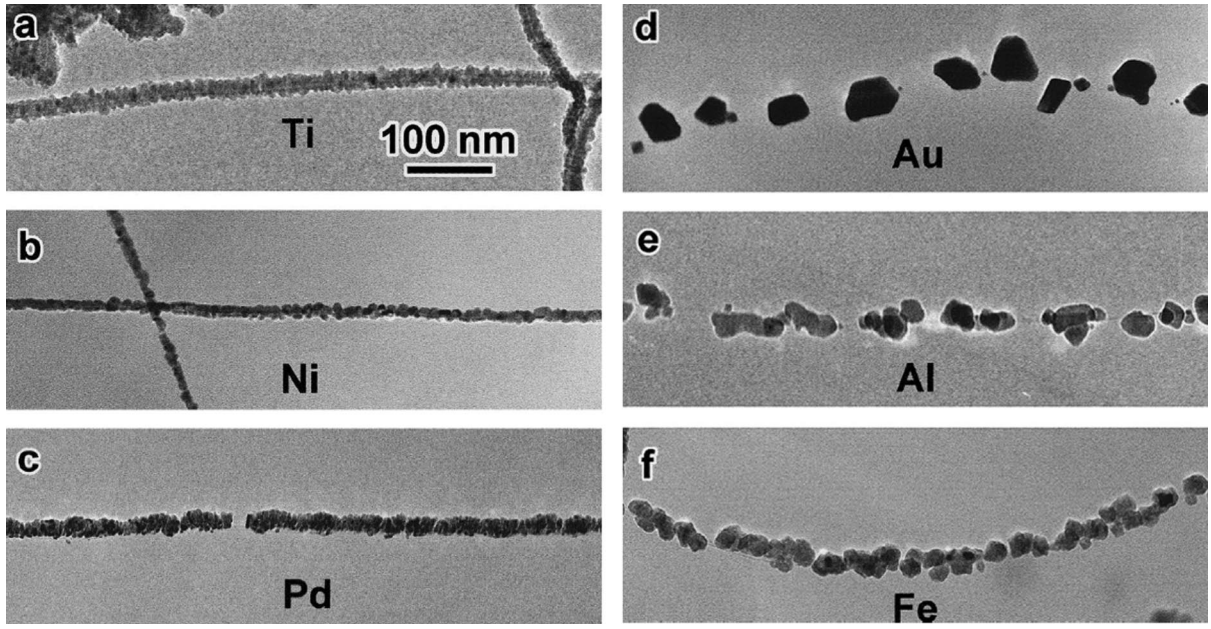

Figure 16. Examples of electron beam deposition showing the different morphologies of electron beam-deposited metals on CNTs. Reprinted with permission from ref 241. Copyright 2000 Elsevier Publishing.

strongly and formed metal nanowires, while Au, Al, and Fe interacted weakly with SWCNTs via van der Waals forces and formed isolated particles instead (Figure 16).[241] This technique can also be used to deposit oxides and nitrides, when using O_2 and NH_3 atmospheres, respectively, as demonstrated for MgO[242] and TiN.[211]

RF or magnetron sputtering has been used to deposit RuO_x,[158] SiO_2,[243] and ZnO.[227,244] Furthermore, Jin et al. have cosputtered Ba and Sr in an oxygen atmosphere to obtain a BaO/SrO coating.[245] In most of these works, the coating around the CNTs was generally conformal, although in the case of vertically aligned CNTs ("carpet"), the inorganic material was deposited predominantly along the top of the carpet. This is in contrast to other techniques such as electron beam deposition, where the thickness of the coating was found to increase from top to bottom.[242] The size of the particles can be controlled by adjusting the sputtering time, as demonstrated in Figure 17 by Zhu et al. for ZnO.[244]

Interestingly, Fang et al. observed that the distribution of RuO_2 particles on vertically aligned CNTs was significantly better on nitrogen-doped CNTs compared with pure CNTs.[246] It is well-known that the incorporation of nitrogen into the sp^2-type walls of CNTs causes many structural defects (pyridine-like bonding) due to the different valence of nitrogen ions. It seems that these defects are more reactive toward the adsorption of RuO_2 than the graphitic walls of pure CNTs and allow a uniform dispersion along the sidewalls of nitrogen-doped CNTs (Figure 18).

In summary, sputtered films typically have a better adhesion to the substrate than evaporated films and a composition closer to that of the source material. In contrast to evaporation techniques, sputtering also enables the deposition of materials with very high melting points and can be performed "top-down", while evaporation must be operated "bottom-up". On the other hand, evaporation techniques typically offer better structural and morphological control and more flexible deposition rates.

3.2.4.2. Pulsed Laser Deposition. Pulsed laser deposition (PLD) is related to the evaporation techniques described in the previous section but utilizes a high-power pulsed laser beam. The directed laser pulse is absorbed by the target, vaporizes the material, and creates a plasma plume containing various energetic species, such as atoms, molecules, electrons, ions, clusters, particulates, and molten globules, which then expand into the vacuum and deposit on a typically hot substrate to nucleate and grow as a thin film. This process can occur in ultrahigh vacuum or in the presence of a background gas, such as oxygen, which is commonly used when depositing oxides.

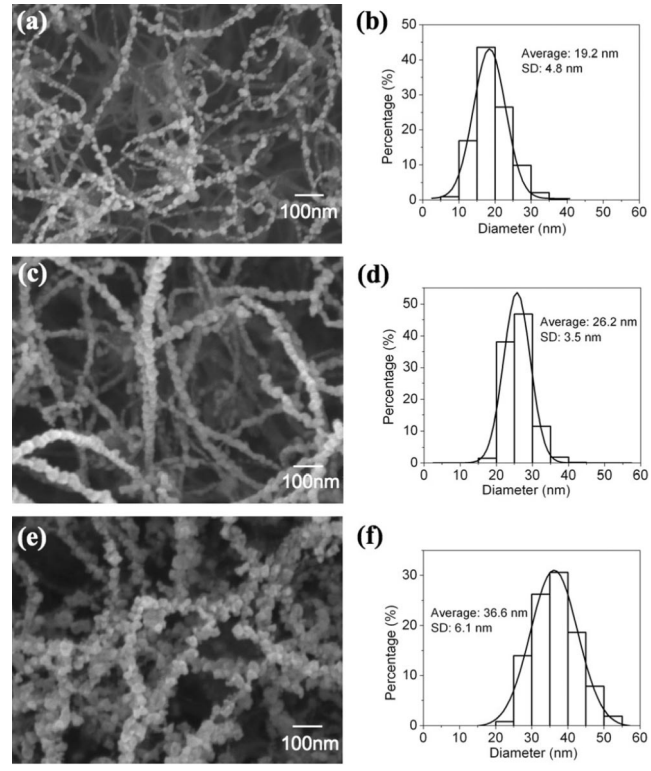

Figure 17. Example of the size control of ZnO nanoparticles deposited via magnetron sputtering: the average particle size increased from roughly 20 to 37 nm upon increasing the sputtering time from 1 to 3 min. Reprinted with permission from ref 244. Copyright 2006 Wiley-VCH.

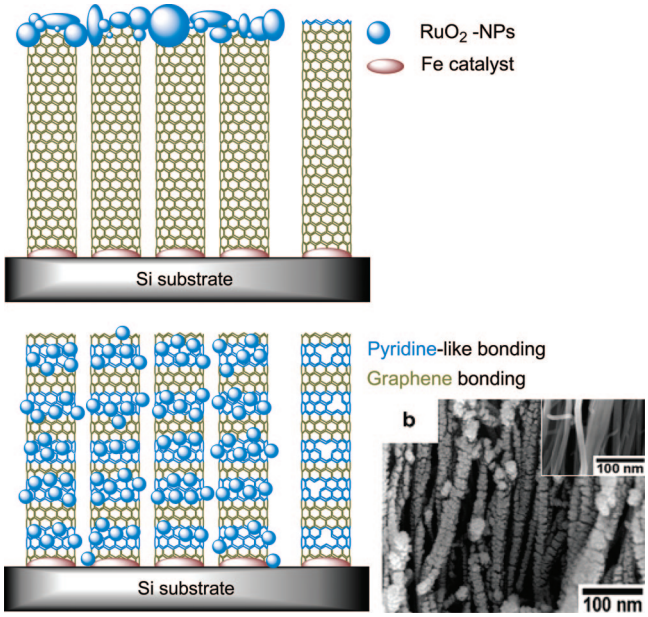

Figure 18. Scheme of the deposition of RuO_2 nanoparticles on aligned CNTs (top) and nitrogen-doped CNTs (N-CNT, bottom) via magnetron sputtering. The pyridine-like defects in the N-CNTs provide a stronger interaction with RuO_2 and a more uniform dispersion along the sidewalls. Redrawn from ref 246.

The work of Ikuno et al. provides an excellent example of the potential of PLD in coating CNTs.[247,248] The authors used individual MWCNTs (grown by arc discharge), which were attached to a molybdenum plate via electrophoresis. A pulsed Nd:YAG (yttrium aluminum garnet) laser with a wavelength of 355 nm (laser energy of 140 mJ and a pulse duration of 5 ns) was focused onto a target at a repetition rate of 10 Hz. A single-crystalline Si wafer and pellets of Zr, Hf, Al, ZnO, Au, and Ti were used as targets for the coating of SiO_x, ZrO_x, HfO_x, AlO_x, and ZnO_x. The experiment was carried out at room temperature and—for the oxide materials—with an oxygen pressure of 1.3×10^{-2} Pa.

The authors observed that all oxides covered the CNTs in a very uniform, dense, and continuous layer with a thickness between 6 and 11 nm, while Au adsorbed on the CNTs as nanoparticles (diameter $\approx$ 7 nm) (Figure 19). With the exception of the polycrystalline ZnO coating, the oxides of Zr, Hf, and Al were all amorphous. The differences in morphology were attributed to the different surface adhesions and diffusivities of the studied materials. The low mobility of the oxides on the CNT surface enabled a uniform wetting layer and prevented crystallization, while Au could diffuse easily and crystallized into nanoparticles. The authors further demonstrated the deposition of complex multilayers with nanometer accuracy, such as the SiO_x−Ti−SiO_x−CNT hybrid shown in Figure 19.

The advantages of this technique over other thin-film deposition methods include the relatively simple basic setup and the operation at room temperature. On the other hand, PLD has a lower average deposition rate than other deposition techniques, such as CVD or evaporation/sputtering techniques, but is faster than ALD. However, this enables a stable nucleation of smaller nucei (critical nuclei radius in the range of 1−2 atoms) and consequently higher nucleation rates and, hence, smoother films. Further information on PLD as a coating technique for CNTs can be found in a review by the same authors,[249] in which they also describe the possibility of etching the tips to leave CNTs free for nanoprobe and nanotip applications.

3.2.4.3. Chemical Vapor Deposition. Chemical vapor deposition (CVD) is a versatile technique often used in the semiconductor industry that involves the growth of a solid material from the gas phase via chemical reaction at the surface of a substrate. Volatile reaction byproducts are simply exhausted from the coating zone and sent to waste processing. In contrast to high-pressure/high-temperature synthesis, the CVD technique typically operates at medium temperatures (600−800 °C) and at slightly reduced atmospheric pressures. Because CVD utilizes reagents of very high purity, the technique is capable of synthesizing crystals with controlled purity and composition. Other advantages of CVD include the high deposition rate, good degree of control (purity and composition), and easy scalability. Tuning the process is simply a matter of manipulating the vapor flows in the coating zone. However, due to the fast deposition, it is difficult to achieve uniform and defect-free coatings when scaling down to a few nanometers.

Several groups have used CVD to synthesize CNT−inorganic hybrids with SnO_2,[250] RuO_2,[251] Si_3N_4,[252] and TiC.[213] These attempts can be separated into two categories: (a) coating of prepared CNTs and (b) in situ growth of CNTs onto or around inorganic nanoparticles, which act as the required catalyst.

(a) Kuang et al. deposited acid-treated MWCNTs on a Si waver and heated them to 550 °C in a SnH_4-containing N_2 atmosphere.[250] At this temperature, the precursor decomposed, attached to the functional groups of the CNTs, and reacted with the oxygen impurities to produce SnO_2. By altering the flow rate and the reaction time, the thickness of the layer could be increased from 3 nm (for 0.5 min) to 80 nm (for 3 min). In a similar way, CNTs have been coated with Si_3N_4 (T = 720 °C, precursor = H_2SiCl_2 and NH_3),[252] RuO_2 (T = 350 °C, precursor = $Ru(acac)_3$),[183] NiO, and Co_3O_4 (using metal nitrates).[253] In the case of RuO_2, the authors could also produce various morphologies, ranging from 1D single crystal nanorods with [001] growth direction to spherical nanoparticles of uniform size (10 nm), depending on the postannealing conditions.[183]

Chrissanthopoulos et al. used the carbothermal reduction of ZnO to coat MWCNTs.[254] The CNTs were placed a few centimeters downstream from the reaction zone (1000 °C) and close to the end of tube (850−950 °C) in order to achieve the desired temperature gradient. Following the reduction of ZnO, Zn vapor was transferred through the gaseous phase, attached to the defects on the CNT surface via Zn−C bonds, and reoxidized to ZnO. Depending on the temperature gradient, the authors observed either thick rods of ZnO (850 °C) or polypods of thin wires (950 °C).

A fascinating approach has been reported by Lazareck et al.[255,256] Aligned CNTs were synthesized within an anodized aluminum oxide (AAO) template, which was removed afterward with concentrated HNO_3. This acid treatment also produced carboxyl groups, predominantly on the tips of the CNTs, which were subsequently linked to a single-strand amine-terminated DNA. A complementary DNA strand, connected with a 20 nm Au nanoparticle, was then hybridized with the first strand to link Au nanoparticles to the tip of CNTs. Using CVD at 600 °C, these Au nanoparticles then acted as catalysts for the growth of ZnO via a vapor−liquid−solid (VLS) mechanism.

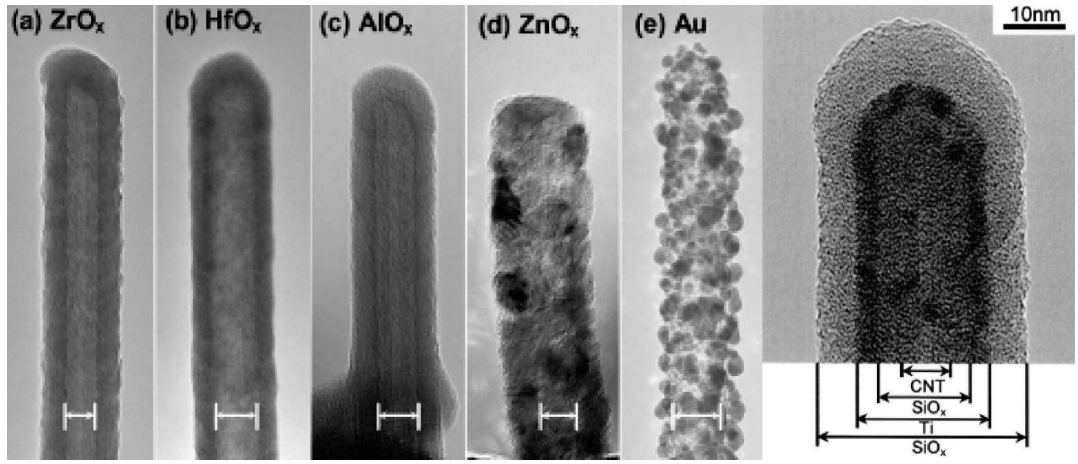

Figure 19. Examples of the deposition of various metals and metal oxides with different morphologies on free-standing CNTs via PVD. The far-right image shows a complex CNT−inorganic hybrid with a layer of Ti between two layers of amorphous SiO_2. Reprinted with permission from ref 247. Copyright 2007 Elsevier Publishing.

(b) An example of the in situ growth of CNTs is the work of Liu et al., who used a water-assisted CVD process to produce CNTs with a ZnO coating.[257] In detail, MWCNTs were synthesized on Zn foil via pyrolysis of C_2H_2 at 850 °C in a gas mixture of argon, hydrogen, and water. As the CNTs grew via a tip-growth mechanism, they carried up part of the Zn, which at the same time was oxidized by water vapor. Most of the ZnO coating was observed at the tip of the CNTs, which would suggest the use of this CNT-hybrid as an electron emitter (see section 4.4).

An interesting alternative to ZnO was demonstrated by Ho et al.[258] The authors used Ni catalyst particles, supported on MgO, which were deposited on a Si wafer and placed inside a tube furnace. ZnO powder was put inside a thin ceramic tube, whose ends were covered with Al foil, and placed inside the reactor tube, close to the catalyst powder. Upon reaching a certain temperature (300−350 °C), assisted via a plasma-enhanced CVD technique, CNTs began to grow on the Ni particles and kept growing as the temperature was steadily increased to 700 °C over a period of about 6−7 min. At this temperature, the Al foil melted and exposed the ZnO powder, which was instantaneously transformed to Zn vapor via carbothermal reduction and deposited on the still-growing CNTs as a thin coating of ZnO.

3.2.4.4. Atomic Layer Deposition. In contrast to CVD, the precursors for atomic layer deposition (ALD) are kept separate and exposed sequentially. Ideally, each precursor forms a monolayer on the substrate, and the excess vapor is removed before the next precursor is introduced. This process is then repeated until the deposited film reaches the desired thickness. Hence, ALD film growth is self-limiting and based on surface reactions, which enables deposition control on the atomic scale.

As an example, Gomathi et al. used metal chloride precursors to coat acid-treated MWCNTs with SiO_2, TiO_2, and Al_2O_3.[259] Their experimental setup consisted of three glass chambers, for the metal halide, reaction sample, and water, interconnected using high-vacuum stopcocks and maintained at 80 or 150 °C. The sample chamber was first evacuated with a diaphragm pump, then filled with metal halide for 5 min and evacuated again to remove the unreacted metal halide. The surface hydroxyl groups on the CNTs reacted with the metal precursor and formed metal−oxygen bonds. In the second step, water vapor was passed through the chamber, which hydrolyzed the residual metal−chlorine

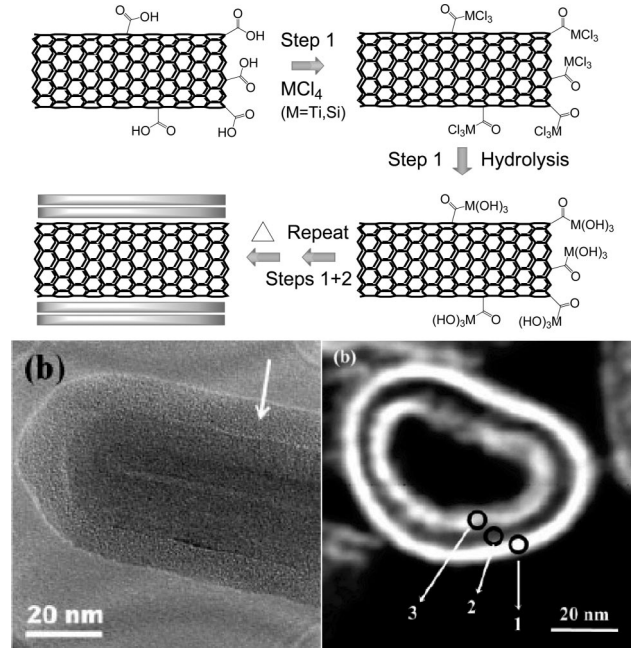

Figure 20. (a) Scheme of the deposition of amorphous layers of TiO_2 and SiO_2 on acid-treated CNTs via ALD and (b) corresponding SEM image for the case of SiO_2. (c) TEM image of vertically grown CNT coated with RuO_2 both outside and inside. Reprinted with permission from refs 259 and 261. Copyright 2003 and 2005 Wiley-VCH.

bonds. This two-step process (shown in Figure 20) was repeated until the thickness of the coating reached 1, 3, or 10 nm. As the coating at this stage consisted of amorphous, predominantly hydroxide species, the samples needed subsequent calcination at 350 °C to form the oxide 350 °C.

Javey et al. demonstrated coatings of ZrO_2 as thin as 8 nm covering the top of horizontally attached SWCNTs for device applications.[260] In contrast, Min et al. used vertically aligned arrays of MWCNTs, grown inside anodized aluminum oxide (AAO) via CVD using C_2H_2.[261] These CNTs were then treated in phosphoric acid, which not only etched away the AAO template but also opened the CNTs tips and introduced carboxyl groups that enabled attractive interaction with the ruthenium precursor. As shown in Figure 20c, the CNTs were coated both on the inside and on the outside. The authors also showed that the structure of the coating depends on the type of precursor. Although the reaction was

Table 6. List of Advantages and Disadvantages of the Various Synthesis Approaches for CNT−Inorganic Hybrids

	building blocks	in situ wet chemical	in situ gas phase
morphology	spherical particles	spheres, wires, films	spheres, wires, films
structure, crystallinity	good control of structure and crystallinity	often amorphous, requires heat treatment	nonstoichiometry possible
size control	capping agents, narrow size distribution	concentration and reaction time	reaction time good control in film thickness range in crystal sizes
coating	monolayer confocal	multilayer confocal directed (electrodeposition)	multilayer confocal (chemical) directed (physical)
interface	needs anchor molecules	pristine or functionalized CNTs possible	good coverage in pristine CNTs

carried out in an oxygen-containing atmosphere, the use of $Ru(od)_3$ (od = octane-2,4-dionate) resulted in a metallic Ru film, while Ru-β-diketonate produced RuO_x coatings.[261] Furthermore, upon oxidation at 500 °C, the CNTs were removed and the two coatings combined to form RuO_2 NTs.

ALD has unique advantages over other thin-film deposition techniques, as it can be operated at low temperatures (e.g., 80 °C) and allows exact control over the thickness of the deposited coating. Furthermore, ALD-grown films are very uniform, pinhole-free, and chemically bonded to the substrate. However, because of the sequential exposure of the precursors, the technique has the lowest deposition rate compared with CVD and PLD. As demonstrated, it is also possible to deposit various ceramics, from insulators to conductors, deep inside porous materials as well as around spherical particles and 3D architectures, such as aligned CNTs.

3.3. Comparison of Synthesis Techniques

Table 6 summarizes the advantages and disadvantages of the various synthesis techniques regarding the morphology, structure, and interface of CNT–inorganic hybrid materials. The building block approach synthesizes inorganic building blocks of defined size and shape and attaches them to the CNTs via linking agents that utilize covalent, noncovalent, or electrostatic interactions. Consequently, either the inorganic nanoparticles or the CNTs (or both) have to be modified with functional groups. The type of functionalization and, thus, the strength of interaction determine the distribution of the inorganic nanoparticles on the CNT surface. This wet-chemical technique is typically limited to the formation of monolayers of nanoparticles. Excess nanoparticles, not anchored to the CNTs, can easily be removed by filtration or centrifugation. Another advantage of this method is the control of particle size and distribution, which can be achieved by capping agents or by the addition of salts, which support heterogeneous nucleation and thus depress the growth of larger aggregates caused by homogeneous nucleation. The control of particle size and shape enables a better structure−property prediction.

In the in situ approach, the inorganic compound is directly formed on the surface of pristine or modified CNTs. The main advantage of this route is that the inorganic compound can be deposited as continuous amorphous or single-crystalline films with controlled thickness or as discrete units in the form of nanoparticles, nanorods, or nanobeads. In most cases, the inorganic particles are remarkably smaller when deposited on CNTs compared with amorphous carbon or graphite. For instance, CNTs can support TiO_2 nanoparticles during the reconstructive stresses of phase transformation from anatase to rutile at high temperatures, keeping the size of rutile particles small.[195,262] Hence, the CNTs can prevent crystal growth during crystallization and phase-transformation processes and may even stabilize uncommon or even novel crystal phases. Therefore, it is very possible with this synthesis route to develop novel materials with new properties.

Another advantage of the in situ approach is that a variety of chemical and physical synthesis techniques can be applied. The deposition can be carried out either in solution, via electrochemical reduction of metal salts, electro- or electroless deposition, sol−gel processing and hydrothermal treatment with supercritical solvents, or from the gas or vapor phase using chemical deposition (CVD, ALD) or physical deposition (laser ablation, electron beam deposition, thermal evaporation, sputtering).

In general, the wet chemical techniques are simple and cheap and can be performed at low temperatures but may need post-treatments to remove residues and to transform the amorphous product into a crystalline phase. Again, the size and shape of the particles can be controlled using capping agents. In contrast, the physical techniques enable excellent control of composition and size distribution but are limited by the availability of suitable precursors, the required high temperatures, the slow deposition rates, and the complex instrumentation.

4. Properties and Potential Applications of CNT−Inorganic Hybrids

This section presents several exciting examples of the improved performance of CNT−inorganic hybrids in applications, such as photocatalysis, electrocatalysis, and environmental catalysis, gas sensors, supercapacitors, and field emission devices. Furthermore, it describes how inorganic compounds can significantly increase or decrease the oxidation stability of CNTs, which is useful for the application of CNTs as a template for inorganic nanotubes.

4.1. Example 1: Photochemical and Photoelectrochemical Applications

Beginning in Japan in the early 1970s[263] with photoelectrochemical electrolysis, or "splitting", of water to produce hydrogen (a source of abundant clean energy), a tremendous amount of research has been carried out in the two closely related fields of semiconductor photoelectrochemistry and photocatalysis, both considered among the most important research areas.[264] Current research aims primarily at direct solar energy conversion as an alternative approach to solid-state junction photovoltaic cell (e.g., Graetzel dye-sensitized solar cell),[265−267] as well as the use of heterogeneous photocatalytic oxidation for water and air purification, decomposition of organic compounds, and self-cleaning surfaces.[264] The past few years saw a renewed interest in photocatalytic "water splitting", which was recently identified by the European Science Foundation as one of the world's emerging key research fields. The aim is to find new material

systems that enable conversion efficiencies beyond 10%, the U.S. Department of Energy's target for a commercially viable catalyst.

The majority of research currently focuses on the design of suitable materials (typically a semiconductor) that are able to efficiently harvest sunlight for the generation of electrons. In general, when the semiconductor is illuminated with photons having energies greater than that of the material's band gap, E_G, electron−hole pairs are generated and separated in a space-charge layer. In the case of water splitting, the electrons and holes are separated and the photogenerated electrons flow to the counterelectrode (usually platinum) and reduce protons, resulting in hydrogen gas evolution without an applied potential. This requires a semiconductor with a conduction band energy (ECB) of at least −0.4 V vs SHE in acid solution or 1.2 V in alkali solution.[264] In contrast, for the purpose of photocatalytic oxidation of harmful compounds, the reduction reaction is not necessarily hydrogen production and no counterelectrode is needed. In these cases, both the reduction and oxidation sites are located on the semiconductor surface. The holes (h^+) generated in TiO_2 are highly oxidizing, and most compounds are typically oxidized completely (to their final oxidation state). In addition, oxygen can act as an electron acceptor to form superoxide radical ions (O_2^-), while OH^- and H_2O are available as electron donors to yield the hydroxyl radical, which is very reactive, strongly oxidizing, and therefore capable of totally mineralizing organic pollutants.

TiO_2 is the most suitable material for industrial use in photoelectrochemical and photocatalytic applications due to its efficient photoactivity, chemical and biological inertness, nontoxicity, high photostability, cost effectiveness, and easy production.[268,269] The utilization of the strong photocatalytic oxidation potential of TiO_2 for the destruction of pollutants was shown in 1977 by Frank and Bard, who described the decomposition of cyanide in the presence of aqueous TiO_2 suspensions.[270] Using supported TiO_2 powders, detoxification of various harmful compounds in both water and air was demonstrated actively as a potential purification method of wastewater and polluted air.[271]

However, with band gaps of 3.25 and 3.0 eV for anatase and rutile, respectively,[268] TiO_2 needs photons with wavelengths smaller than 385 and 410 nm for efficient excitation. Consequently, TiO_2 only absorbs about 3% of the solar light it is exposed to and currently requires near-UV light to operate as an efficient photocatalyst.[272] Ideally, the band gap of the semiconductor is close to about 1.35 eV, which is required for optimum utilization of solar energy. However, semiconductors with such small band gaps, including CdS and CdSe, have shown considerably lower efficiencies and stabilities than TiO_2.[273]

Therefore, it is desirable to extend the absorption of TiO_2 into the visible region and thus improve its photocatalytic efficiency. So far, strategies have concentrated on the generation of defect structures, by doping with light ions (N, S, or halides)[274] or transition metal ions,[275−278] to induce space-charge separation and the modification of TiO_2 with noble metals or other semiconductors.[279] The use of organic dyes as photosensitizers is another approach, which is at present limited by the very low stabilities of the dye molecules.[264] Because of their electronic properties, chemical inertness, and stability, CNTs are considered promising candidates to improve the photoefficiency of semiconductors, and, as shown in the next section, some work has recently been directed toward investigating CNT−inorganic hybrids for photocatalytic applications.

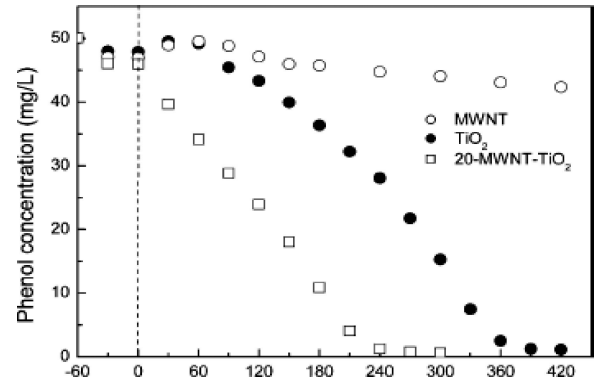

Figure 21. Kinetics of phenol removal under UV illumination in the presence of various photocatalysts. Reprinted with permission from ref 206. Copyright 2005 Elsevier Publishing.

4.1.1. Photocatalytic Production of Hydrogen

Ou et al. impregnated anatase−TiO_2 particles with small Ni clusters and used them as a catalyst to grow MWCNTs via CVD at 550 °C.[280] The hybrid materials were tested for water splitting under visible light and a methanol/water solution. The addition of organic alcohols as reducing agents considerably enhanced the reaction efficiency by preventing the H_2 and O_2 gases from recombining on the surface of TiO_2.

In contrast to the completely inactive TiO_2−Ni catalyst, the addition of 4.4 wt % CNTs produced significant amounts of hydrogen, with a reaction rate of 38 μmol g^{-1} h^{-1} (5 μmol g^{-1} h^{-1} in pure water). Increasing the amount of CNTs above 4.4 wt %, however, led to a decrease in the absorption of light and, thus, in the activity of water splitting. These initial results are especially promising, if one considers that the tested hybrids merely consisted of a network of CNTs, grown on and connected by TiO_2 particles, resulting in only a relatively small interfacial area. In this respect, this author believes that a uniform continuous coating of TiO_2 on CNTs, and hence an optimized interface, will lead to considerably higher hydrogen evolution rates.

4.1.2. Photocatalytic Decomposition of Organic Compounds

There have been quite a few studies concerning the photocatalytic activity of CNT−TiO_2 hybrids for the oxidation degradation of organic compounds, such as acetone,[196] propene,[281] and phenol[205,206,282] as well as the inactivation of bacterium anthraxium.[283] CNT−ZnO has been investigated for the decomposition of methylene blue,[221] while the decomposition of indigo carmine with both CNT−ZnO and CNT−TiO_2 has also been tested.[224] All of these studies observed superior photocatalytic performance by the hybrid over the individual component.

For instance, Wang et al. coated acid-treated MWCNTs with TiO_2 via sol−gel and investigated the degradation of phenol under UV light[206] and visible light.[205] In both cases, they observed a considerable acceleration of the oxidation reaction, with most of the phenol being transformed after 4 h (6 h in visible), while pure TiO_2 needed 6 h (9 h in visible) and pure MWCNTs only converted up to 5% (Figure 21). The maximum activity was observed with a CNT concentration of 20 wt % and was considerably higher than

the simple mechanical mixture of the same composition and surface area. A similar behavior was shown by Yu et al. for the oxidation of acetone (maximum activity at 5 wt % CNTs),[196] as well as by Lee et al. for the decomposition of methylene blue,[221] who observed a superior performance of CNT−ZnO hybrids over the mechanically mixed composite. The importance of the interface was further supported by the work of Yao et al., who compared MWCNT−TiO_2 hybrids with SWCNT−TiO_2 hybrids.[282] In contrast to MWCNTs, the higher flexibility and resilience of SWCNTs caused them to wrap around the TiO_2 particles, thus increasing the interfacial area. The authors believe that this enhanced interface was the reason for the higher photocatalytic activity observed in SWCNT−TiO_2 hybrids for the decomposition of phenol. All these works clearly demonstrated a synergistic effect of CNTs in enhancing the performance of TiO_2 or ZnO.

4.1.3. Photovoltaic Devices

The photocatalytic activity of semiconductors in photovoltaics has been successfully demonstrated in the so-called dye-sensitized solar cell (DSSC),[265,266] which utilizes nanostructured TiO_2 films modified with sensitizing dyes. The reported solar conversion efficiencies of up to 10% are indeed very encouraging; however, further improvement in the performance of DSSC has yet to be achieved. Currently, the photoconversion efficiency is mainly limited by the transport of photogenerated electrons across grain boundaries in the semiconductor particle network. Such a random transit path for the electrons also increases the probability of their recombination with oxidized sensitizer. To counter these drawbacks, networks of TiO_2 or ZnO nanotubes and nanowires have been used to direct the flow of photogenerated charge carriers, while the use of a redox couple such as I_3^-/I has been shown to facilitate the electron transport by rapid regeneration of the oxidized sensitizer.[264,284,285]

Another very promising approach has been demonstrated by Kamat et al., which involves the use of CNTs as support for light-harvesting semiconductor particles, such as CdS, CdSe, or CdTe QDs.[165,286] Upon irradiation with visible light, the authors observed induced charge transfer processes of the photogenerated electrons from excited semiconductors into semiconducting SWCNTs, whose electron-accepting ability further facilitated electron transport to the collecting electrode and thus increased the photoconversion efficiency of the solar cell. Guldi et al. used pyrene derivatives to attach CdTe QDs and investigated the electron-transfer chemistry in both the ground and excited states.[287] Using an excitation at 350 nm, the authors observed strong blue-shifts and luminescence quenching, which they attributed to strong electronic interactions between the two electroactive components. A charge transfer from the photoexcited electron donor (CdTe) to the electron acceptor (SWCNTs and MWCNTs) was also credited for the strong increase in charge lifetimes. Using femtosecond transient absorption and nanosecond laser flash photolysis, the decay rates decreased considerably from 3.5×10^7 s^{-1} for CdTe to 4.7×10^4 s^{-1} for CNT−pyrene$^+$−CdTe. The hybrid was then deposited on indium−tin oxide (ITO) to make a photoelectrochemical device, and very promising internal photoconversion efficiencies (IPCEs) of up to 2.3% were observed, which was about 6 times more efficient than a red CdTe cell.

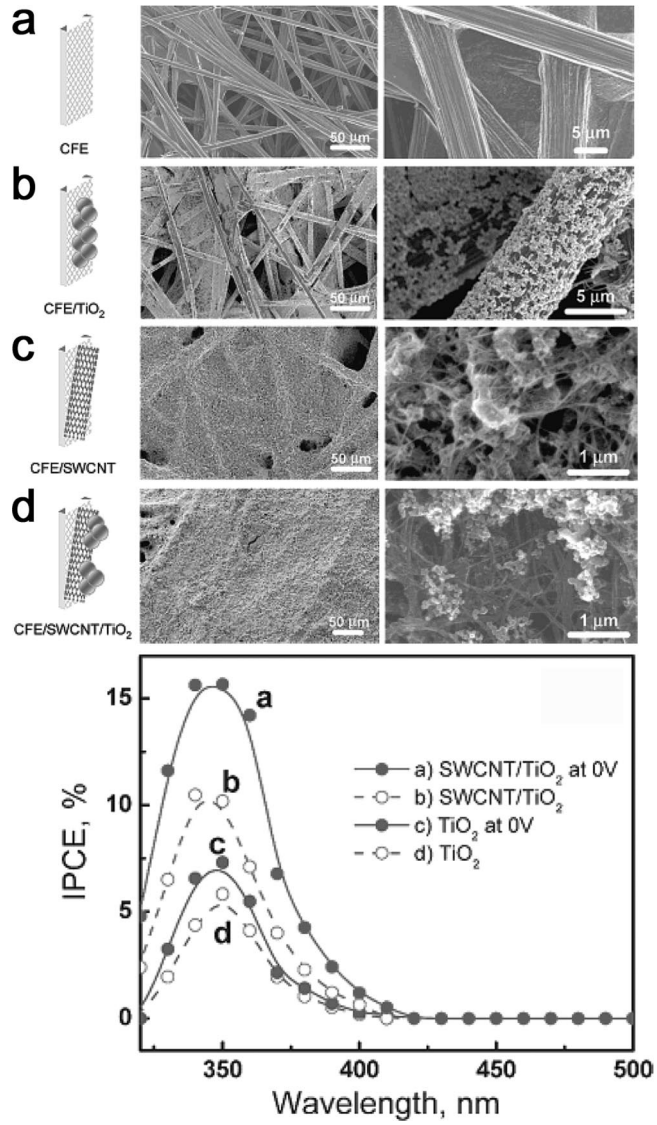

Figure 22. (Top) SEM images of various electrodes tested in a photelectrochemical cell: (a) pure carbon fiber electrode (CFE), (b) TiO_2 nanoparticles spray-coated on CFEs, (c) SWCNTs electrophoretically deposited on CFEs, and (d) the final hybrid. (Bottom) Incident photoconversion efficiency (IPCE) for various electrodes. Reprinted with permission from ref 112. Copyright 2007 American Chemical Society.

In view of these results, Kamat et al. also investigated SWCNT−TiO_2 and SWCNT−ZnO hybrids for use in photovoltaic devices.[112,220] The hybrid materials' SWCNTs were first refluxed in 5 M HNO_3 to remove any metal and organic impurities and to open the end of the tubes, then solubilized in tetrahydrofuran (THF) containing tetraoctylammonium bromide (TOAB) with the aid of ultrasonication, and assembled as a thin film on a carbon fiber electrode (CFE) using an electrophoretic deposition technique. A suspension of commercial TiO_2 powder (Degussa P25) in 1% acetic acid/methanol was slowly dropped onto the CFE and CFE/SWCNT electrodes and dried in air (Figure 22).

In the case of SWCNT−TiO_2, the authors observed that the photon conversion efficiency for the hybrid material was almost doubled compared with that of pure TiO_2. Further experiments revealed a positive shift in the flat-band potential of SWCNT−TiO_2, which indicates electron transfer between TiO_2 and SWCNTs. Although not directly participating in

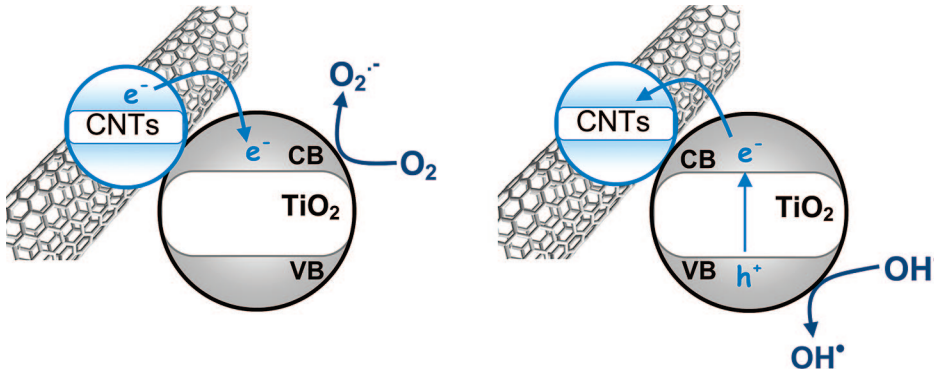

Figure 23. Schemes of CNTs as photosensitizers: (a) electron injection into the conduction band of TiO_2, (b) electron back-transfer to CNTs with the formation of a hole in the valence band of TiO_2 and reduction of the hole by oxidation of adsorbed OH^- species.

the photocurrent generation due to their low photocurrent efficiencies in visible light, the SWCNTs play a crucial role in the charge collection and charge transport processes and, thus, significantly enhance the photoconversion efficiency of the photovoltaic cell.

However, it can be expected that an improvement in morphology of the TiO_2 particles and control of the interface between CNT and TiO_2 will further enhance the performance of the hybrid. Additionally, acid treatment of the SWCNTs should be avoided in order to preserve their superior electronic properties, though separation of semiconducting and metallic CNTs may prove advantageous.

4.1.4. Synergistic Effects of CNTs

There are several possible explanations for the beneficial role of CNTs, depending on the inorganic material and choice of application.

(1) The first explanation is purely physical and can be described in terms of MWCNT acting as a dispersing agent that prevents TiO_2 from agglomerating, thus providing a higher active surface area for the resulting catalyst compared with the single-phase TiO_2. It is well-known that CNTs can affect the morphology of the deposited oxide, reducing its particle size and consequently increasing the specific surface area, even affecting the crystal size of several layers of TiO_2 nanoparticles.[195] Wang showed that, in first approximation, the decrease in TiO_2 particle size with increasing MWCNT−TiO_2 ratio correlated to the observed increase in photocatalytic activity, up to 20 wt % CNTs.[206] At higher CNT concentrations, however, the activities dropped, although the particle sizes decreased further. This suggests that the contribution of the particle size was not the only important factor. This was supported by Lee et al., who compared the hybrid and the pure TiO_2 with equal effective surface areas, using a comparably lower amount of the high specific surface area hybrid, and observed highly improved efficiencies in destroying bacteria anthraxium for the hybrid material compared with pure TiO_2.[283]

(2) CNTs are well-known for their enhanced adsorption properties for some gases[32,288] and thus may act as additional adsorbents for the organic compounds, which then diffuse to the TiO_2−CNT phase boundary to undergo degradation. This possibility was disproved by Wang et al.,[206] who observed similar adsorption capacities of phenol for the hybrid, the single compounds, and the mechanical mixture.

(3) The CNTs may act as photosensitizers for n-type semiconductors like TiO_2 (Figure 23). In this model, photoinduced electrons are easily transferred to the CNT−TiO_2 interface and injected into the TiO_2 conduction band. A similar electron transfer was observed between various other carbon materials and the TiO_2 semiconductor.[289] Simultaneously, a positively charged hole (h^+) can be formed by an electron migrating from the TiO_2 valence band to a MWCNT. With this understanding, the role played by CNTs can be illustrated by injecting electrons into the TiO_2 conduction band under visible light irradiation, triggering the formation of very reactive radicals such as superoxide radical ions ($O_2^{\bullet -}$) and hydroxyl radicals ($HO^{\bullet}$), which are then responsible for the degradation of the organic compound.

(4) Finally, CNTs could suppress the recombination of electrons and holes (Figure 23). Upon light irradiation, valence band electrons of the semiconductor are excited to its conduction band, leading to the formation of electron−hole pairs. CNTs then act as electron acceptors, promoting interfacial electron-transfer processes from the attached oxide to the nanotube. This separation of charges retards the recombination of photoinduced electrons and holes and hence improves the photocatalytic activity of the semiconductor. Wang et al. investigated this possibility by photoluminescence (PL) emission spectroscopy, which is generally used to measure the efficiency of charge carrier trapping, immigration, and transfer, and to understand the recombination mechanisms of e^-/h^+ pairs in semiconductor particles.[206] In the case of CNT−TiO_2, the intensity of the emission band at 525 nm decreased considerably with increasing CNT concentration. Since the emission in TiO_2 can be attributed to the radiative recombination process of self-trapped excitations,[264] the reduction of the PL intensity suggests a strong inhibition of e^-/h^+ recombination due to electron transfer.

In summary, the role of CNTs is presumably a combination of these effects. CNTs do not only photoinduce electrons and prevent e^-/h^+ pairs from recombining but also provide a large surface area for smaller nanoparticles.

4.2. Example 2: Heterogeneous Catalysis and Electrocatalysis

The major obstacle for the successful commercialization of direct alcohol fuel cells (DAFCs) is the slow kinetics of the electro-oxidation of alcohols (e.g., methanol or ethanol), which is agreed to be caused by poisoning of the surface of the platinum electrode with CO.[290] The most promising solution seems to be the addition of a second component, such as Ru or a transition metal oxide (RuO_2, TiO_2, SnO_2), which assists in the oxidation of CO to CO_2 by the

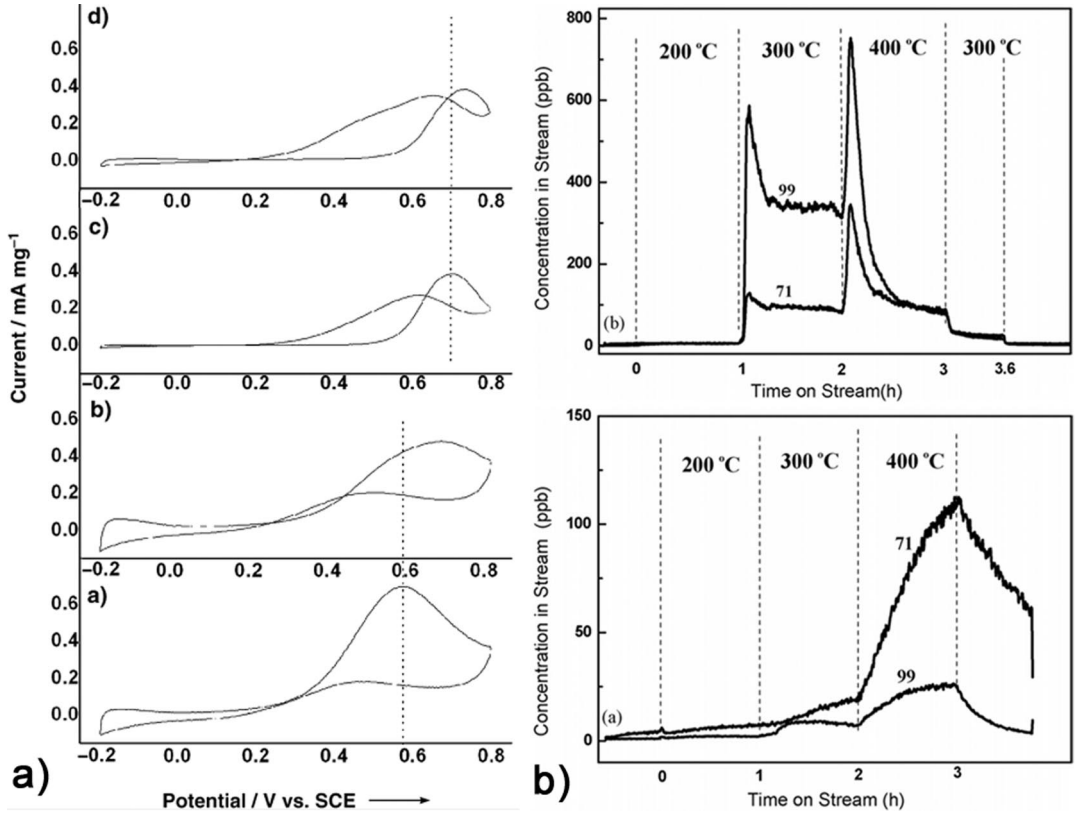

Figure 24. (a) Cyclic voltammograms for (a) Pt/RuO_2·0.56H_2O−CNT, (b) PtRu−C, (c) Pt−CNT, and (d) Pt−C (d), taken at 25 °C in 1 M CH_3OH + 1 M $HClO_4$ with a scan rate of 50 mVs^{-1}. The CNT−RuO_2 hybrid showed the lowest onset and peak potentials of all tested catalysts, indicating the highest activity for the electrooxidation of methanol. Reprinted with permission from ref 216. Copyright 2006 Wiley-VCH. (b) Partial oxidation of *n*-butane over (a) V_xO_y catalyst without CNTs and (b) the CNT−V_xO_y hybrid. The online proton transfer reaction mass spectrometry (PTR-MS) response for masses 71 and 99 amu, heated sequentially to 200, 300, and 400 °C, shows the activity of the CNT−V_xO_y hybrid at lower temperatures. Reprinted with permission from ref 299. Copyright 2007 Materials Research Society.

dissociation of water. Still, the electrocatalytic activities and CO tolerances of the catalysts need significant improvement, which may be achieved by the use of CNTs.

Indeed, noble metal particles show significantly higher power densities at higher backpressures, lower onset potentials, and higher anodic currents, when supported on CNTs rather than on activated carbon (AC) or other substrates. For instance, one of the current highest values of anodic currents for Pt−C has been reported by Motorola with 40 mA/cm^2 for 2.5 mg Pt/cm^2, while Pt−CNT catalysts exhibited currents as high as 54 mA/cm^2 for 0.43 mg Pt/cm^2 and 25 mA/cm^2 for 10 μg Pt/cm^2.[291] These high values suggest that the use of CNTs can significantly reduce the amount of expensive metal catalysts. Even higher currents and thus activities have been reported for the systems Pt/MoO_x−CNT,[292] Pt/TiO_2−CNT,[197,293] and Pt/RuO_2·H_2O−CNT.[294]

The role of CNTs is often attributed to their ability to stabilize highly dispersed oxide nanoclusters, resulting in higher specific surface areas. However, Cao et al. investigated the role of CNTs in more detail and chose the bifunctional system of Pt/RuO_2·H_2O.[216] The authors observed that, with almost identical Pt loadings and surface areas, Pt/RuO_2·0.56H_2O−CNT showed a 50% higher current density and, thus, a higher activity for methanol electrooxidation, compared with the PtRu−C catalyst (Figure 24a). Further analysis revealed that the CNT-containing sample required only eight scanning cycles for activation, compared with 32 cycles needed for the PtRu−C. Thus, CNTs can dramatically reduce the induction period of the electrocatalyst. Furthermore, the onset potential for CO oxidation was considerably lower for the CNT-hybrid (223 mV) than for the PtRu−C catalyst (338 mV). This is attributed to the exceptional electronic properties of CNTs causing electron transfer to the RuO_2 crystals.

The beneficial role of CNTs has also been demonstrated for application in heterogeneous catalysis. For instance, Pd showed significantly higher catalytic activities toward hydrogenation of nitrobenzene when supported on CNTs than on activated carbon,[295] with nearly complete conversion after 5 h, while at the same time Pd/C showed a conversion of only 10%. While not all materials showed such enhanced catalytic activities, the hybrids typically developed excellent selectivities toward a certain product. For example, in the case of the hydrogenation of cinnamaldehyde, Pd and Ru showed high selectivities toward hydrocinnamaldehyde[296] and cinnamyl aldehyde,[297] respectively, when supported on CNTs, while metals supported on activated carbon produced mixtures with phenyl propanol.

There have also been a few reports on CNT hybrids with transition metal oxides for heterogeneous catalysis, such as RuO_2,[298] V_xO_5,[170,299] WO_x,[300] ZnO,[301] and sulphated ZrO_2,[113] as well as for electrocatalysis, such as SnO_2.[302] For instance, Fu et al. synthesized hydrous RuO_2 nanoparticles supported on CNTs via a homogeneous oxidation−precipitation (HOP) method using H_2O_2 as both the oxidant and precipitant at room temperature.[298] The hybrid was very active in the aerobic oxidation of various aromatic, saturated, and cyclic alcohols and quite selective toward the corresponding aldehydes or ketones in liquid phase under mild conditions. The

improvement was attributed to a better dispersion of RuO_2 nanoparticles on the CNT surface compared with other substrates, like γ-Al_2O_3 and activated carbon. Huang et al. investigated the activity of V_2O_5 catalysts toward the selective catalytic reduction (SCR) of NO with NH_3 in the presence of excess oxygen.[170] In supporting V_2O_5 on CNTs, the authors could decrease the required reaction temperature significantly to temperatures well below 200 °C, which is important for increasing the lifetime of the catalyst and saving energy.

Other examples involve solid acid catalysts such as WO_3 and ZrO_2, which play an important role in the petrochemical industry for the conversion of hydrocarbon, including cracking, isomerization, and alkylation, which are important in the chemical and petrol industries. Using WO_3, Pietruszka et al. demonstrated the use of CNT as an active support for skeletal isomerization reactions.[300] Furthermore, the CNT−WO_3 hybrids exhibited very high skeletal isomerization selectivity exclusively toward olefin reactions. In this example, the improved performance of the CNT−WO_3 hybrid was not only attributed to a more uniform dispersion of WO_3; CNTs also prevented the complete reduction of WO_3 to metallic tungsten, a process that typically causes complete deactivation of the catalyst.

Another example of a successful application of CNT hybrids has been demonstrated by Chen et al., who investigated the catalytic performance of CNT−VO_x in the partial oxidation of *n*-butane.[303] Such dehydrogenation reactions are often highly exothermic, and the heat is typically released to the catalyst surface, causing sintering of the particles and decreased catalytic activities. Because of their high thermal conductivity, the CNTs can act as a heat sink, thus keeping the crystal size small (see section 4.1.4). Indeed, the authors observed higher activities at lower reaction temperatures in the CNT−VO_x hybrids compared with unsupported VO_x as well as a very high selectivity toward the formation of maleic anhydride.

In summary, the role of CNTs in heterogeneous catalysis is predominantly a support for small catalyst particles with excellent dispersion and high surface areas, which can dramatically increase the activity and affect the selectivity of the catalysts. Recently, Schlögl, Su, and co-workers demonstrated that, by modifying their surface chemistry, the CNTs alone can be active for the oxidative dehydrogenations (ODH) of 1-butene,[304,305] ethylbenzene,[306] and styrene.[307] In all cases, quinine groups were identified as the active functional groups, which can be introduced by gradually heating in oxygen. A contribution of this catalytic behavior of functionalized CNTs should be considered in order to understand the role of CNTs in heterogeneous catalysis.

4.3. Example 3: Gas Sensors, Chemical Sensors

Metal oxide semiconductors (MOS) are prominent examples of sensing materials in gas sensors, as their electrical properties are highly affected by the surrounding gas environment. For instance, tungsten trioxide (WO_3) shows sensitivity to pollutants such as SO_2, H_2S, NO, and NH,[308,309] while SnO_2 is sensitive to NOx, CO, ethanol, and C_2H_4.[310] The surface reactivity of the metal oxides toward reducing and oxidizing gases is associated with the formation of oxygen vacancies and the transfer of *d*-electrons into adsorbates.[311] Hence, the mechanism for gas detection is controlled by the change in surface conductivity caused by the release/trapping of electrons during gas interaction with the surface. In general, the specific surface area, morphology, crystallinity, and chemical composition (e.g., dopants, impurities) have an impact on the sensing properties. Consequently, gas sensors based on MOS nanoparticles and structures would benefit from a small grain size, high surface-to-volume ratio, and increased surface activities. When their size becomes comparable to that of the space-charge layer, the electron transport properties of nanoparticles can be strongly modulated by adsorption and desorption processes, resulting in high gas sensitivities to ambient gases. However, their sensing properties often suffer degradation due to growth and aggregation.

Improvements in metal oxide based sensors, such as enhanced sensitivity and selectivity to target gases, reduced response and recovery times, and lowered operating temperature, have been achieved by adding small amounts of catalytically active metals onto the oxide surface, by producing core−shell materials, by doping with n-type or p-type ions, and by adding a sacrificial component (mostly liquid) as an electron donor.[308,312−314] However, it is desirable for gas-detection purposes to operate the metal oxide-based sensors at room temperature, in order to reduce the power consumption of the device and to enable safer detection of flammable gases.[297]

In contrast with metal oxide sensors, CNTs exhibit excellent adsorption properties due to their high specific surface area, which provides a large number of active surface sites.[288,315−317] As the CNTs' electric properties are effectively altered by very small amounts of adsorbed gas molecules, the CNT gas sensor can be operated at temperatures close to room temperature. However, as MWCNTs are not very sensitive to ambient gas, the use of CNTs as gas sensors is mainly restricted to SWCNTs. Furthermore, due to their long recovery times, CNT-based sensors typically need reactivation, e.g., by UV light irradiation, which purges the surface from adsorbed gas molecules.

Similar to core/shell heterostructures like MOS/CdS, MOS–CNT hybrids have shown improved photoluminescent quantum efficiencies and enhanced gas-sensing properties including reduced response and recovery times.[201,318] So far, CNT−SnO_2 has been tested for detection of CO,[210] NO_2,[201,203] NH_3,[319] formaldehyde,[320] and ethanol,[321] while glucose was detected with CNT hybrids containing SiO_2,[322] clay,[323] and Fe_3O_4.[324]

Wei et al. used a sol−gel process to coat pristine SWCNTs with SnO_2 and investigated the gas-sensing performance for NO_2 at room temperature.[203] They observed considerably enhanced sensitivities ($\Delta R/\Delta C$, Figure 25) compared with the pure SnO_2 sensor. Because the morphology and surface area of the hybrid sensors were similar to those of the pure SnO_2, and the observed sensitivities increased with increasing CNT loading, the authors concluded that the advanced sensing behavior originated from a common interface with CNTs. In contrast to conventional SnO_2 sensors, which typically operate at temperatures between 200 and 500 °C, the SWCNT/SnO_2 hybrid gas sensors could indeed be operated at room temperature.

When the NO_2 gas molecules adsorb on the surface of pure SnO_2, they extract electrons, leaving the oxide surface positively charged. This leads to the formation of a depletion zone and to an increase in the sensor resistance. In the CNT−SnO_2 hybrid sensor, the electric properties of the oxide are strongly enhanced by the highly conducting CNTs. Consequently, the sensor resistance is dominated by the

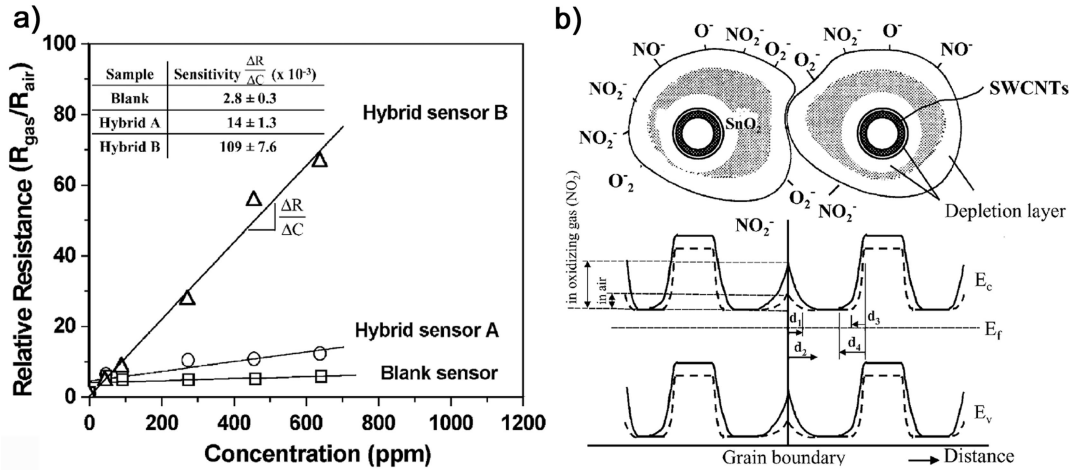

Figure 25. Example of CNT−SnO_2 hybrid in gas sensors. (a) Relative resistances versus NO_2/air gas concentrations of SnO_2 and hybrids with low (A) and high (B) concentrations of CNTs at room temperature. The sensitivities ($\Delta R/\Delta C$) increase considerably with increasing CNT concentration. (b) Scheme of the presence of depletion zones near the CNT−oxide interface. Reprinted with permission from ref 203. Copyright 2004 Elsevier Publishing.

Schottky barrier at the interface between the n-type SnO_2 grains and the p-type CNTs, causing the formation of additional depletion layers, which then amplifies the increase in resistance upon NO_2 adsorption and enables the operation of the gas sensor at room temperature.

The barrier height between the SnO_2 grains and the MWCNTs seems to vary for different gases. In contrast with NO_2,[201] exposure to ethanol,[321] NH_3,[319] or acetylene[201] has been shown to release electrons and consequently reduce the sensor resistance. This effect was observed only for the hybrid sensors; the pure SnO_2 sensor did not show any response to ethanol or acetylene at room temperature. This underlines the importance of the CNT–SnO_2 interface. Furthermore, Chen et al. showed that the response and recovery times of the CNT–SnO_2 hybrid sensor were considerably improved over pure SnO_2 sensors.[321]

In summary, hybrid SWCNTs–SnO_2 gas sensors can successfully combine the advantages of both components to produce significantly higher sensitivities in detecting both oxidizing (e.g., NO_2) and reducing (e.g., ethanol, C_2H_4) gases. Furthermore, the sensors exhibit shorter response times, enhanced recovery properties, and better stability and reproducibility, and can indeed be operated at room temperature. There is still plenty of room for improvement toward successful application as gas sensors, including the control of morphology and the maximization of the surface area and interfacial area. It would also be useful to investigate other MOS in CNT hybrid materials.

4.4. Example 4: Supercapacitors and Batteries

Reliable and affordable electricity storage is a prerequisite for optimizing the integration of renewable energy systems. Energy storage, therefore, has a pivotal role to play in the effort to combine a future, sustainable energy supply with the standards of technical services and products. For both stationary and transport applications, energy storage is of growing importance as it enables the smoothing of transient and/or intermittent loads and the downsizing of base-load capacity with substantial potential for energy and cost savings. The extended lifetime of batteries in handheld devices is credited not only to higher energy densities but also to a simultaneous reduction of energy consumption of the portable devices. In contrast, the electric vehicle has failed to become the accepted mode of transportation mainly because of the battery. Short distances between recharging and a limited service life of the battery are to blame, but also the incredible weight and volume of the batteries.

Electrochemical capacitors (ECs) are energy-storage devices that possess higher energy and power density than conventional dielectric capacitors and batteries and are used in applications including electric vehicles, noninterruptible power supplies, dc power systems, lightweight electronic fuses, memory backups, and solar batteries.[325] The challenges for these applications concern limitations in volumetric/gravimetric power densities and RC time, long life, safety, simplicity of design, cost, and the possibility of recharging, and can only be accomplished by specially designed materials.

According to the mechanism of energy storage, ECs can be categorized into two classes:[325] (a) electrochemical double layer capacitors (EDLC), based on double-layer capacitance due to charge separation at the electrode/electrolyte interface, which thereby need materials with high specific surface area (e.g., activated carbon, CNTs), and (b) pseudocapacitors or supercapacitors, based on the pseudocapacitance of faradaic processes in active electrode materials such as transition metal oxides and conducting polymers.

Because of their exceptional electronic properties, which allow ballistic transport of electrons over long nanotube lengths, CNTs have been considered a most promising candidate for electrochemical capacitors.[326,327] However, pure CNTs possess a rather low specific capacitance, typically about 10−40 F/g, which depends on the microtexture, purity, and electrolyte.[327] A considerable enhancement can be expected from the combination of CNTs with an electroactive material, which provides the additional pseudocapacitance while each tube acts as a minute electrode. For instance, capacitance values up to 170 F/g have been obtained by coating CNTs with conducting polymers, such as polypyrrole.[328,329] However, these materials do not withstand the high cycle life (>100 000) due to the strong propensity of conducting polymers toward degradation, which may be further decreased by overcharge and overdischarge misuse. In this context, the electrochemical stability of transition metal oxides makes them a better choice, provided they are highly conducting. A wide range of oxides has been investigated for use in CNT hybrids, including NiO,[209,330,331]

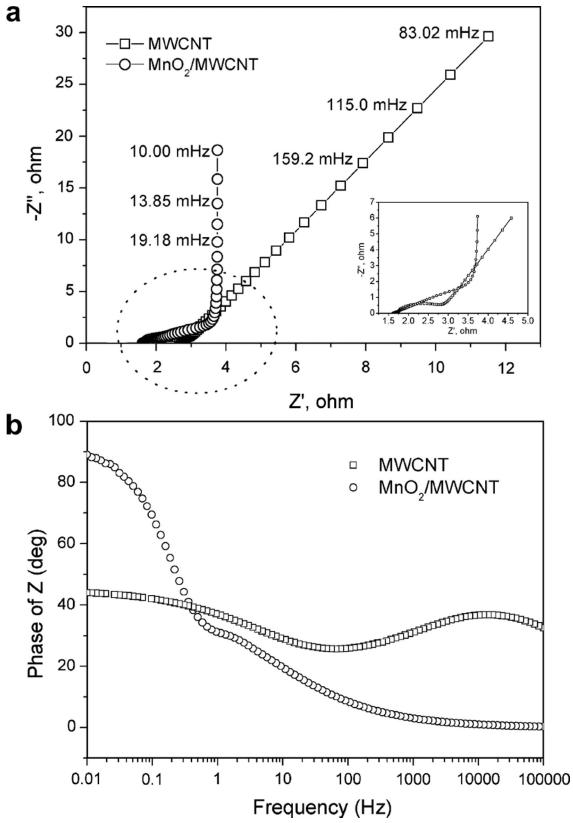

Figure 26. Example of the supercapacitive performance of CNT−MnO_2 hybrids. Nyquist (a) and Bode plots (b) of pure MWCNT and the hybrid electrode in 1 M KOH aqueous solution (inset is the amplification of the high-frequency region), recorded between 10^5 and 0.01 Hz with a perturbation of 5 mV. Reprinted with permission from ref 168. Copyright 2007 Elsevier Publishing.

MnO_2,[110,188,332−335] V_2O_5,[336,337] and RuO_2.[207,237,251,338] In all of these studies, the synergistic effects of CNT−oxide hybrids have shown a considerable improvement of the otherwise poor electric properties and deficient charge transfer channels of the pure oxide.

Among these transition metal oxides, ruthenium oxides are regarded as the most promising electrode material for supercapacitor applications due to their high specific capacitance, highly reversible redox reactions, wide potential window, and very long cycle life.[237] Park et al. reported a specific capacitance for CNT−RuO_2 (13 wt %) of 450 F/g at a potential scan rate of 20 mV s^{-1}, which could be further enhanced, by using hydrous ruthenium oxide and functionalized CNTs, to 800 F/g.[208] Reducing the thickness of the RuO_2 layer to 3 nm led to an even higher capacitance (1170 F/g at a potential scan rate of 10 mV s^{-1}).[182] All of these studies also demonstrated longer lifetimes and greater stabilities and rate capabilities, while the specific capacitances were in general considerably higher than those observed for pure MWCNTs (<80 F/g) or pure RuO_2 (<400 F/g).

In view of the rather high costs and environmental issues concerning RuO_2, and despite the lower specific capacitances, there has been a clear trend toward the use of hydrous manganese oxides in the past few years.[188] Xie et al. produced a CNT−MnO_2 hybrid by in situ reduction of $KMnO_4$ on MWCNTs with citric acid and observed that the specific capacitance increased from 18 to 190 F/g (Figure 26a).[168] while Ma et al. reported 250 F/g[188] at a large current density of 1 Ag^{1-}, both for scan rates of 10 mV/s. Zhang et al. electrodeposited MnO_2 "nanoflowers" onto the surface of vertical CNT arrays and obtained capacitances of about 200 F/g, as well as excellent rate capabilities (50.8%, capacity retention at 77 A/g) and a long cycle life (3% capacity loss after 20 000 charge/discharge cycles).[334] The authors proposed a model for the improved electrochemical storage characteriztics based on high electronic conductivity in CNTs (Figure 26b). In this model, the geometry of the MnO_2 nanoflowers and their hierarchical localization at CNT junctions limits the diffusion length of ions within the MnO_2 phase during the charge/discharge process and enhances the ionic conductivity of the hybrid.

To maximize the electrochemical utilization of the supercapacitor, it is desirable to (a) use a low loading of metal oxide and (b) increase the interfacial area between CNTs and metal oxide. Consequently, the preparation of a thin, uniform, connected coating on CNTs is expected to improve the specific capacitance significantly. This was confirmed by Nam et al., who observed increasing capacitances with decreasing NiO content and thus coating thickness.[331]

A promising approach to enhance the capacitive performance has recently been reported by Sivakkumar et al., who synthesized a ternary hybrid of CNT/polypyrrole/hydrous MnO_2, which showed a significantly higher specific capacitance (280 F/g) compared to the binary CNT/MnO_2 (150 F/g).[167] The increase in capacitance is believed to be due to the better dispersion of hydrous MnO_2 in the composite electrode. However, the presence of the polymer also accounts for the poor cyclability behavior.

Fang et al. chose a different approach by depositing RuO_2 on N-doped CNT,[246] for which they measured considerably higher specific capacitances. The authors showed that the RuO_2 particles were considerably better dispersed on N-doped CNTs than on pure CNTs (Figure 18), due to the presence of structural defects in N-CNTs. Consequently, the hybrids with N-doped CNTs had an enhanced interface, which resulted in their better performance as a supercapacitor (Figure 27).

A good cyclability is crucial to a successful application as an anode material for lithium-ion batteries, as demonstrated by Chen et al. for CNT−SnO_x hybrids.[202] Pure CNTs typically show good cycle stability, but also a large and irreversible capacity loss in the first cycle. The authors showed that well-dispersed SnO_x on CNTs enhanced the electrochemical performance significantly as the capacity fade of the hybrid electrode was strongly reduced compared to unsupported SnO_x or pure CNT. The authors attributed the improvement in performance to the enhanced conductivity and ductility of the hybrid. This is in line with Zheng et al., who observed a 5-fold increase in electronic conductivity and thus enhanced cycling rate and stability in CNT−CuO hybrids compared to pure CuO.

In summary, electrochemical devices have been among the first applications for which CNT−inorganic hybrids were tested. In the long run, CNT hybrids are expected to strongly enhance the batteries' intrinsic capacities, stabilities, and lifetimes, as well as the charging/discharging characteristics. Furthermore, the substitution of part of the heavy oxide material (e.g., in car batteries) with the lightweight CNTs will significantly reduce the weight of the batteries.

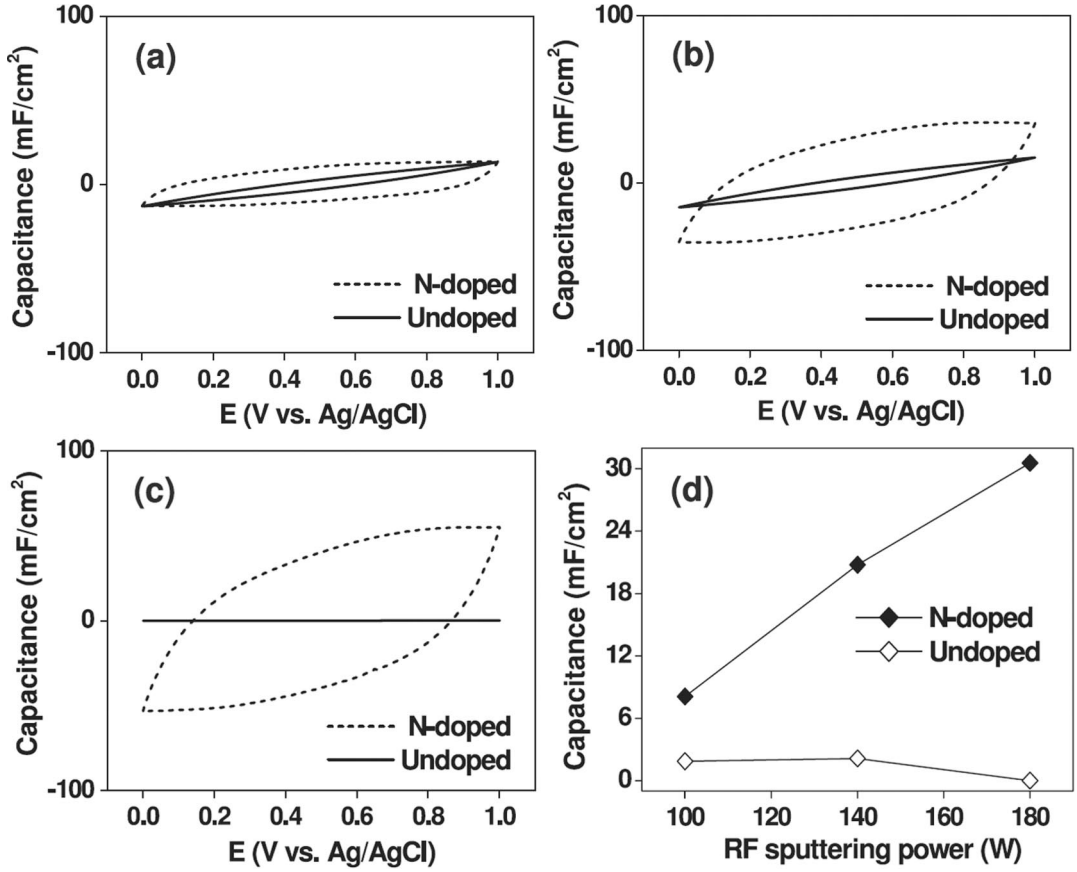

Figure 27. Capacitance−voltage diagrams of hybrids with RuO_2 using undoped and nitrogen-doped CNTs (Figure 18); (a) light (RF power = 100 W), (b) moderate (RF power = 140 W), and (c) heavy (RF power = 180 W) loading of RuO_2. (d) Capacitance of hybrids as a function of RF sputtering power. In contrast to the undoped CNTs, the N-doped CNTs are coated completely with RuO_2, resulting in a larger interfacial area and an improved capacitance. Reprinted with permission from ref 437. Copyright 2007 Institute of Physics.

4.5. Example 5: Photonics and Field Emission Devices

Since the early days of CNT research, the prospect of new CNT-based electronic and photonic devices has attracted tremendous interest for both fundamental and applied science. For instance, as ideal one-dimensional systems, semiconducting CNTs are direct-bandgap materials, which can be used to both generate and detect light simply by changing the applied voltage. In this respect, extensive research has been conducted on studying the electronic and optical properties of pure CNTs and applying them in transistors, field emission devices, and nonlinear optics, and has been summarized recently by Avouris et al.[339,340] On the other hand, only a few works have been directed toward CNT−inorganic hybrids. Recently, the importance of the oxide substrate for measuring the electrical and optical properties of CNTs has been highlighted by Lin et al.[341] The authors observed that the electrical noise ($1/f$) was one magnitude higher in supported CNTs than in suspended CNT, thus demonstrating that the noise amplitude $1/f$ is dominated by the trapped charges at the CNT−oxide interface. Another example has been shown by Zhu et al., who observed that the optical properties of CNTs can be affected by a charge transfer between CNTs and the ZnO coating, which enables an ultrafast nonlinear optical switching behavior.[244] Furthermore, the combination of the three-photon absorption properties of ZnO with the saturable absorption properties of CNTs creates a multifunctional nanohybrid with promising applications in saturable absorber devices that offer a simple and cost-efficient solution for passive optical regeneration, long error-free optical transmission distances, and high noise-suppression capabilities.

Most other works on CNT−inorganic hybrids have concentrated on field emission properties (secondary electron emission, thermionic emission), which have attracted extensive attention because of their potential application in flat-panel displays and compact X-ray tubes, high-power microwave devices, and fluorescence lamps.[342−344] For these applications, CNTs are typically grown vertically via a CVD technique, which allows both positional control and the growth of well-aligned CNTs (carpets). This unique geometry and the high aspect ratio of CNTs enable the creation of very high, localized electric fields, characterized by the electric field enhancement factor β. Most of the studies have so far focused on improving the β factor of CNTs.[344,345] However, CNTs also have a relatively high work function (4.5 eV), which typically increases the barrier for electron tunnelling and thus limits the current density. Ideally, one would want to have an emitter that has both a high β factor and a low work function. This has been achieved by coating CNTs with a thin layer of a low work function material, such as SiO_x,[346] ZnO,[347,348] Cr_2O_3,[349] MgO,[242,350] $BaSrO_x$,[245,351,352] and TiC.[213]

As an example, Yi et al. employed electron beam deposition to coat well-aligned CNTs with a uniform layer of MgO with thickness ranging between 100 and 500 nm.[342] Following the creation of secondary electrons, they observed sensationally high secondary electron emission (>1 × 10^4),[353,354] compared to ~10^3 for pure CNT,[355] which

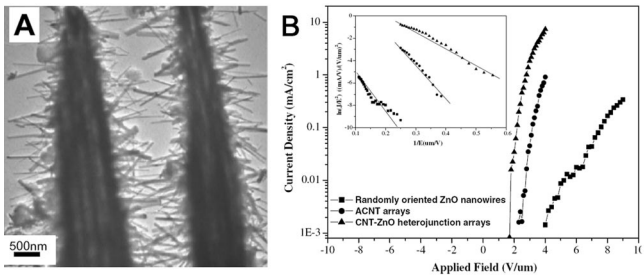

Figure 28. (Left) TEM image of a CNT−ZnO heterojunction, composed of vertically aligned CNTs and perpendicularly grown ZnO nanowires. (Right) Field emission current density as a function of the applied electric field for the randomly oriented ZnO nanowires, the pristine CNT arrays, and the ordered CNT−ZnO heterojunction arrays, respectively. The inset corresponds to Fowler−Nordheim (F−N) plots. The CNT−ZnO hybrid has the best field emission properties with the lowest turn-on field of 1.8 V/μm and the lowest threshold field of 2.7 V/μm. Reprinted with permission from ref 347. Copyright 2008 Elsevier Publishing.

strongly depended on the thickness of the coating.[350] When the layer was too thick, the electrons experienced difficulties in escaping the oxide, while in a layer that was too thin the few created secondary electrons caused only a small potential difference. The highest emission values were observed for a thickness of 200 nm.[350] Hence, the authors concluded that both the geometry of the hybrid and the intrinsic properties of MgO are crucial to the design of electron emission devices.

Huang et al. deposited a 200 nm thick ZnO layer around the tips of aligned CNTs via the filtered cathodic vacuum arc technique,[348] while other researchers used the vapor-phase transport method to produce either a thick film of ZnO[240] or a heterojunction array of CNTs with ZnO nanowires (Figure 28a).[347] In all these works, the improved geometries resulted in higher and stable emission currents of secondary electrons, as well as lower turn-on and threshold fields and stable emission currents compared with pure CNTs and pure ZnO. The thermionic emission of an oxide-modified CNT device has been investigated by Jin et al.,[245,351,352] who used magnetron sputtering to deposit a 100 nm thick layer of barium strontium oxide onto CNTs. Because of the decreased work function of the hybrid (2.1 eV), the current densities were about 50 times higher than for the pure CNTs (Figure 28b).

Most of these studies have in common that they deposited rather thick layers of inorganic materials (100−200 nm), which typically reduced the field enhancement factor β and, hence, the performance of CNTs as an emitter. An alternative hybrid material for field emission has been demonstrated by Pan et al., who used the electron beam technique to deposit layers of MgO or TiC, which were considerably thinner (1−10 nm).[213,242] Consequently, these thin films did not alter the geometry and, hence, the β factor of the CNT emitter. Instead, the electrons were transferred from the CNTs into the TiC coating (due to the low work function−2.8 eV−of TiC) and emitted easily without barrier. Therefore, the coating increased the current density of the CNTs considerably, while also reducing the turn-on voltage from 411 V for pure CNTs to 267 V in the hybrid.

Another problem for CNT emitters arises from the fact that emitted electrons tend to ionize surrounding gas molecules, which then bombard the CNT surface and slowly degrade their structure and peel them off the substrate. As a result, the field emission characteristics and emission stability

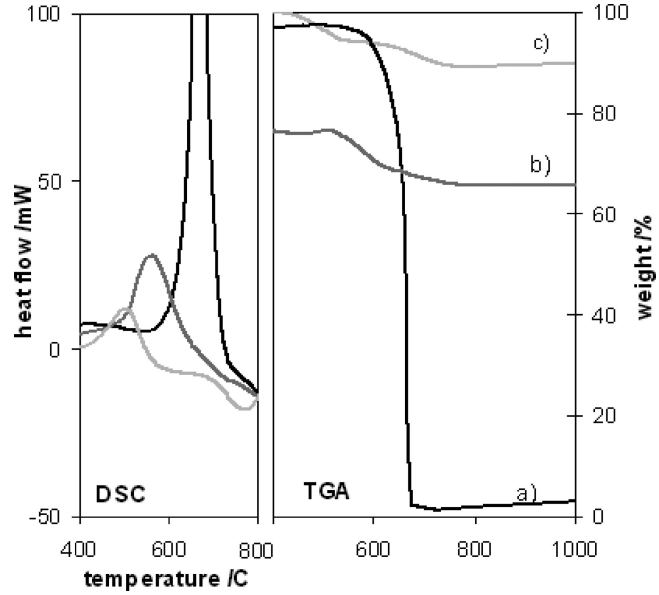

Figure 29. Differential scanning calorimetry (DSC) and thermogravimetric analysis (TGA) of uncoated CNTs and CNT−TiO_2 hybrid materials, taken in air in a temperature range from 25 to 1000 °C (10 °C/min). The exothermic peak at around 550−600 °C indicates the oxidation of CNTs (675 °C) and shifts to lower temperature when coated with anatase (565 °C) or rutile (520 °C), indicating a reduced oxidation resistance in the hybrid materials. Reprinted with permission from ref 195. Copyright 2008 Royal Society of Chemistry.

could be affected.[356] Coating the CNTs with materials such as SiO_x or MgO was shown to protect the CNTs from reactive sputter etching. Moon et al. showed that even a very thin layer of amorphous SiO_x (1−2 nm) could improve the lifetime of the CNT emitter by a factor of 2.5.[346] Although SiO_x improved the current density by a factor of 3, it is this author's opinion that a slightly thicker but uniform coating, covering the whole CNT surface, would improve the performance even more.

4.6. Example 6: Oxidation Resistance

For many applications, it is important to know about the oxidation resistance of CNTs in CNT−inorganic hybrids, since a reduced stability can limit the operation temperature. In general, CNTs oxidize in air at temperatures above 700 °C.[357] However, the presence of defects, catalyst residues, and amorphous carbon can considerably reduce their oxidation temperature. In contrast, the oxidation resistance of CNTs can be significantly increased by annealing in an inert atmosphere at 2000 °C, which produces very pure and crystalline CNTs with low defect concentration.

A conformal coating of a dense layer of inorganic material around the CNTs, such as in CNT−inorganic hybrids, can dramatically affect the oxidation resistance of CNTs. For instance, the present author observed that a coating of TiO_2−anatase decreased the oxidation temperature to 565 °C (Figure 29), which was about 100 °C lower than that required for pristine, uncoated CNTs (675 °C).[195] Interestingly, the observed oxidation temperature was even lower when the CNTs were coated with TiO_2 in the rutile phase (520 °C).[195]

A similar behavior was reported for RuO_2 (570 °C)[294] and MnO_2, for which an oxidation temperature as low as 350 °C was reported.[150] So far, the lowest oxidation temperature, 320 °C, was observed by the present author

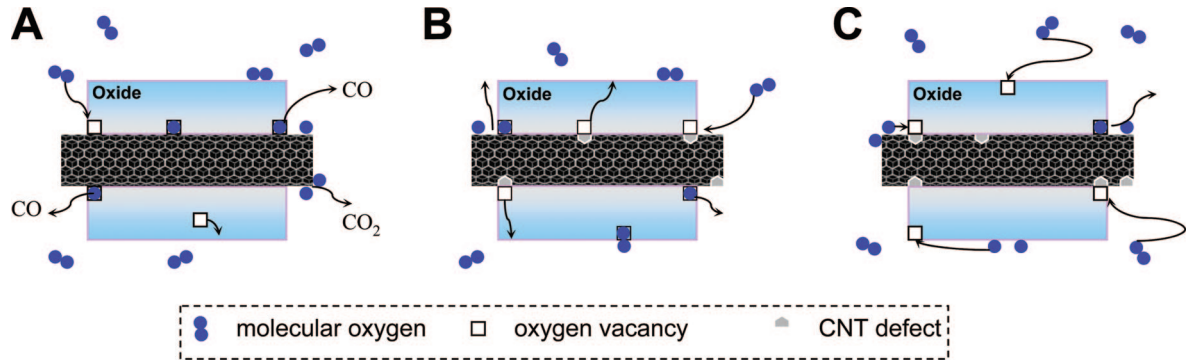

Figure 30. Scheme of Mars−van Krevelen mechanism, involving (a) the reaction of a TiO_2−lattice oxygen with carbon to CO or CO_2, (b) the diffusion of an oxygen vacancy to the surface of TiO_2, and (c) the reoxidation of the vacancy with gaseous oxygen.

for Bi_2O_3, a promising material for electrochemical applications. On the other hand, the deposition of a thin layer of SiO_2 was shown to hinder the combustion of CNTs, increasing their oxidation temperature by at least 60 °C,[215] while Al_2O_3 and ZrO_2 increased the oxidation temperature to about 800 °C.[358]

Reducible oxides like TiO_2, CeO_2, V_2O_5, and MnO_2 can provide lattice oxygen in promoting the C−O bond formation to produce CO or CO_2, similar to the Mars−van Krevelen mechanism (Figure 30).[359] Upon reaction with CNTs, the lattice oxygen is consumed and produces an oxygen vacancy, a reduced Ti^{3+} species, and an electron, via[360,361]

$$C + Ti^{4+} + O^{2-} \rightarrow CO + VO + Ti^{3+} + e^-$$

The oxygen vacancy then diffuses to the surface or triple phase boundary to be reoxidized by the gaseous oxygen. The oxygen diffusion is believed to be the rate-limiting step and is, in the case of TiO_2, faster in rutile than in anatase.[362] Consequently, the oxidation temperature and heat evolution in rutile-coated CNTs are lower than those in the CNT−anatase hybrid (Figure 29). This effect obviously depends on the reducibility of the oxide. Therefore, the nonreducible SiO_2 and ZrO_2 do not catalyze the CNT oxidation; on the contrary, a complete coverage of CNTs hinders the access of gaseous oxygen and consequently their oxidation.

4.7. Example 7: Synthesis of Inorganic Nanotubes

A reduced oxidation stability can be advantageous for another application of CNT−inorganic hybrids: the fabrication of inorganic nanotubes, for which CNTs can be used as a template.[363−365,195,262,366] In general, a thin film of the desired material is deposited on the CNTs, which are subsequently removed by oxidation in air at the temperature required for the specific hybrid. This approach was first demonstrated by Ajayan and co-workers for the synthesis of V_2O_5 nanotubes[357] and has since been used to generate tubular forms of a variety of oxides, including SiO_2 and Al_2O_3,[367,368] MoO_3 and ZrO_2,[369] and RuO_2[370] and TiO_2.[195,262,366] Recent examples include nanotubes of In_2O_3,[371] Co_3O_4,[372] Fe_2O_3,[236] and Eu_2O_3.[373] The advantage of oxides in nanotubular morphology is their three-dimensional mechanically coherent architecture, which allows ready gas access to a very high specific surface area.[195,262,366] Consequently, most of the above-mentioned nanotubes showed excellent performance in gas sensing or photocatalysis.[374−376]

Besides their role as a template, the CNTs can further act as a support during crystallization and phase transformation, which led to the first TiO_2 nanotubes in rutile phase, as demonstrated recently by this author.[195,262] Out of the polymorphs of TiO_2, anatase is the kinetically favored phase, while rutile has to be transformed from anatase via heat treatment at temperatures between 600 and 900 °C.[377] These high temperatures generally induce grain growth and cause collapse of the tubes' structure, thus reducing the specific surface area considerably. However, when the phase transformation was conducted in an inert atmosphere, the preserved CNTs could act as a support so that the stresses associated with the reconstruction of the phase did not destroy the nanotube morphology (Figure 31). Furthermore, the CNTs prevented the grain growth typical for the anatase to rutile transition, affecting several layers of rutile crystals (diameter ≈ 10 nm) within a distance of about 50 nm. Consequently, the subsequent oxidation of the CNT template produced phase-pure rutile nanotubes with high surface area.[195,262]

This template-based synthesis route has yet another, very promising potential: the synthesis of electronically modified inorganic nanotubes.[278] The addition of benzyl alcohol (see section 3.2.2.2) has enabled the use of pristine CNTs as templates without the need for covalent functionalization.[55] Pristine, and thus unpurified, CNTs still contain metal (e.g., Fe) catalyst residues (see section 2.2.1), which are often encapsulated within the tubes' walls. Recently, the present author demonstrated that, upon oxidative removal of the CNT template, these iron residues can be used to produce iron-doped anatase and rutile nanotubes.[378−380] In contrast to other doping routes, this unique process does not require postannealing, it enables a uniform distribution of iron at high concentrations as a solute in anatase and rutile nanotubes without the formation of secondary phases. This iron-doping has enabled a considerable extension of light absorption into the visible region (red-shift) as well as a reduced electron−hole recombination rate.[379] These advantages, combined with the high surface and illumination area of the anatase and rutile nanotubes, have led to an improved performance in photocatalytic applications, such as water splitting.

In summary, the template-directed synthesis provides a simple, versatile, and cost-effective procedure for pure and modified inorganic nanotubes. Furthermore, since the CNTs can be produced with lengths of millimeters, this approach can be adopted for fabricating very long nanotubes from a rich pool of materials.

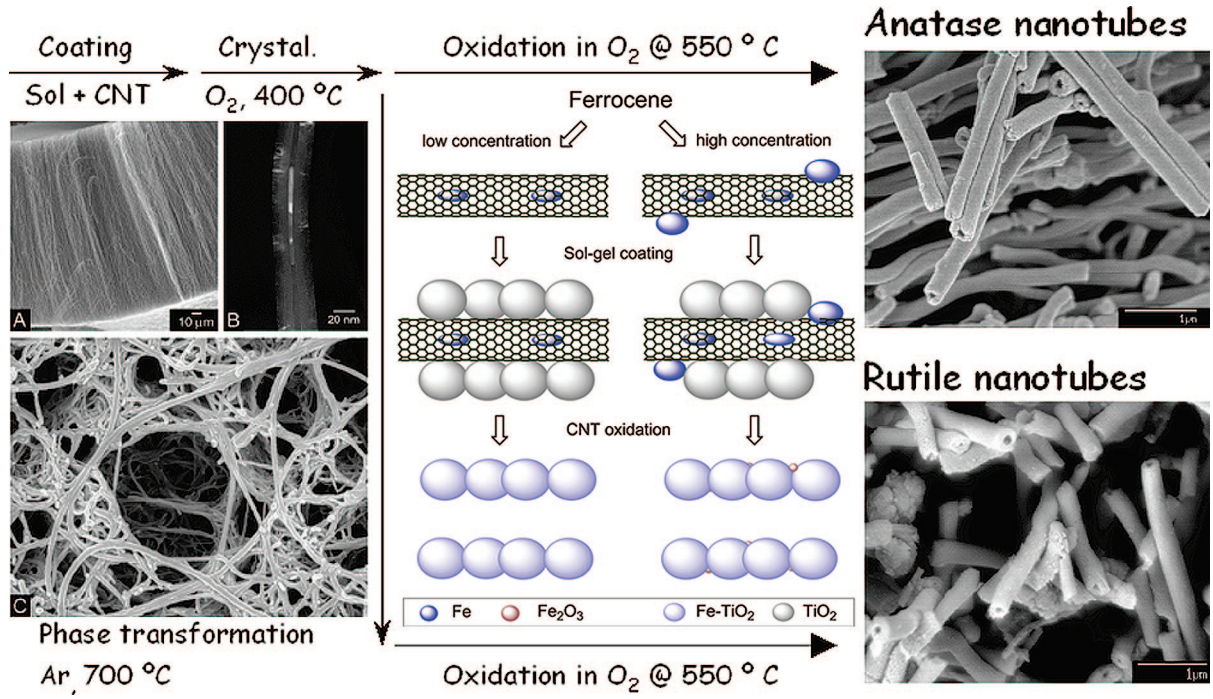

Figure 31. Scheme for the synthesis of iron-doped anatase and rutile nanotubes, using the catalyst residues within CNTs as iron source (A, B) involving coating of pristine CNTs with TiO_2 via sol−gel process (C), heat treatment in argon to either anatase or rutile, and oxidation of the CNT template in air at 550 °C, during which the iron oxidizes and enters the TiO_2 lattice as substituents (Fe^{3+}) for Ti^{4+} ions.

5. Challenges and Outlook

This review introduces CNT−inorganic hybrids as a new and very promising class of functional materials that combine the multiphase characteristics of nanocomposites with the synergistic functions of hybrid frameworks. In these materials, a synergistic effect in CNT−hybrids arises through size domain effects and charge transfer processes through the CNT−inorganic interface. The beneficial role of CNTs is manifold, ranging from photosensitizers and electron traps to magnetic shields, intrinsic capacitors, and electrodes. Because of their high surface area and their excellent thermal conductivity, CNTs can also support very small nanoparticles, hinder their growth during postannealing treatments, and even stabilize new phases, so creating new functional materials with new properties.

This review provides a comprehensive description of the various synthesis approaches of CNT−inorganic hybrids and also demonstrates their outstanding potential for a wide range of applications concerning energy and the environment. Despite being at a very early stage of research, CNT−inorganic hybrids have demonstrated considerably enhanced activities and selectivity in photo- and environmental catalysts, markedly improved sensitivities, and lower operation temperatures in gas and biosensors, as well as increased capacitances and extended recyclability, stability, and lifetime in batteries. Among the many applications described in this review, gas sensors and batteries have so far enjoyed the greatest attention and are very likely to become commercially feasible. Considering the outstanding results of some preliminary studies, I see the greatest potential of CNT−inorganic hybrids in their use in photocatalytic applications, including water and air purification, the production of hydrogen from water, and the direct energy conversion of sunlight.

The development of these and other applications from laboratory devices to industrial prototypes, however, will require further optimization toward designing the ideal hybrid material. Among the most important challenges is the control of the interface, especially for applications that involve charge transfer processes. However, most hybrid materials tested for applications have been produced simply by mechanically mixing the compounds or by growing the inorganic material on pristine CNTs, both of which often resulted in irregular and partial coatings and thus a poor interface. An increased interfacial area and a uniform coating can considerably improve the performance of the hybrid materials. This can be achieved with a variety of synthesis techniques by modifying the surface chemistry by covalent (functional groups) or noncovalent (surfactant, biomolecules) means or by using ionic polymers as a glue. Each of these techniques has advantages and disadvantages that will have to be considered for designing a new hybrid material. For instance, covalent functionalization often involves harsh chemical reactions that, especially when involving ultrasonication, typically shorten the tubes, roughen the surface, and even alter the intrinsic (mostly electronic) properties of CNTs due to the formation of structural defects. In contrast, noncovalent attraction is nondestructive but may not be sufficient to guarantee a mechanically stable coating. The length of the surfactants, capping agents, and other linkers can be used to control the extent of charge transfer, while the choice of CNTs (metallic vs semiconducting) may cause additional barriers at the interface (e.g., metal−insulator junctions).

The second challenge involves the control of the morphology and phase composition of the inorganic compounds, which can be deposited either as an amorphous or single crystalline thin film or as a layer of small polycrystalline nanoparticles. Consequently, the material can be designed with either high specific surface area or a decreased number of grain boundaries. Photovoltaics is a good example of the importance of these properties, as a high surface area enables

the adsorption of more dye molecules, while grain boundaries limit the charge transfer in the oxide. As mentioned above, CNTs can support small particle sizes, while also directing their growth orientation. Most importantly, CNTs can even stabilize new, otherwise unstable phases, leading to novel CNT−hybrid materials with yet unknown properties. Furthermore, the design of the functionality of the inorganic component may involve layer-by-layer or core−shell structures of mixed inorganic compounds as well as complex structures (e.g., mixed oxide solutions, perovskites) and electronically modified materials (e.g., using dopants). In this respect, exploration and control of the hybrid's phase composition and morphology will likely extend its impact in various applications.

There are also challenges concerning the type and quality of the CNTs, which must be controlled to further understand the beneficial role of CNTs in the hybrid materials. For instance, some applications like photovoltaics or gas sensors may favor thin SWCNTs with high aspect ratio over MWCNTs. Semiconducting SWCNTs may perform better in charge transfer processes than metallic ones, and consequently the separation techniques need further improvements in yield, selectivity, and total conversion. Other important issues are the purification of the CNTs from metal residues and carbonaceous species (e.g., amorphous carbon, fullerenes, aromatic debris) and the reproducibility of CNT synthesis with respect to graphitization and defect concentration. This requires the standardization of synthesis and purification techniques. I further recommend the use of other carbonaceous nanomaterials, such as graphene or fullerenes, as well as fibers and transparent thin films made from CNTs, which are very likely to enhance the diversity and adaptability of CNT−inorganic hybrids and also facilitate new applications.

Finally, a successful application of CNT−inorganic hybrids and their implementation into the market requires a strong improvement in methodology to ensure reproducibility and better understanding of the structure−property relationship. Equally important is addressing the biocompatibility of the hybrid materials for use in biological and medical applications. Health and safety regulations further require detailed studies on toxicology and exposure, and research directed toward those issues has just started.

Although at the early stage of research, this new class of materials offers great potential for use in a wide variety of applications, including sustainable energy, environmental, and medical applications. As a multidisciplinary research field, the further development and successful implementation strongly requires the expertise of researchers from chemistry, physics, and nanotechnology, but also from various areas in engineering and medicine. In this respect, the purpose of this review is to increase the visibility of CNT−inorganic hybrids and to offer a comprehensive overview of recent advances for both academia and industry.

6. Abbreviations

3Y-TZP	tetragonal ZrO_2, stabilized with 3 mol % Y_2O_3
AAO	anodized aluminum oxide
AIIP	aluminum isopropoxide
ALD	atomic layer deposition
CFE	carbon fiber electrode
CTAB	cetyltrimethyl ammoniumbromide
CVD	chemical vapor deposition
DAFC	direct alcohol fuel cell
DMFC	direct methanol fuel cell
DSSC	dye-sensitized solar cell
DTAB	dodecyl dimethylammonium bromide
EC	electrochemical capacitors
EDLC	electrochemical double-layer capacitor
ECB	conduction band energy
EG	ethylene glycol
FED	field emission display
FET	field effect transistor
ITO	indium tin oxide
IPCE	internal photoconversion efficiencies
LSMCD	liquid-source misted chemical deposition
NaDDBS	sodium dodecylbenzene sulfonate
NPs,NWs	nanoparticles, nanowires
P2 VP	poly-2-vinylpyridine
PAA	polyacrylic acid
PDDA	poly(diallyl dimethyl ammonium chloride)
PECVD	plasma-enhanced chemical vapor deposition
PEG	poly(ethylene glycol)
PEI	poly(ethylene imine)
PLD	pulsed laser deposition
PV	photovoltaics
PVD	physical vapor deposition
PPh3	triphenylphosphine
PSS	poly(sodium 4-styrenesulfonate)
SDS	sodium dodecylsulfate
SEE	secondary electron emission
SEED	substrate-enhanced electroless metal deposition
SET	single electron transistor
SHE	standard hydrogen electrode
SPS	scanning probe spectroscopy
TAA	thioacetamide
THF	tetrahydrofuran
TBOT	tetrabutyl orthotitanate/titanium(iv) butoxide
TEOS	tetraethyl orthosilicate/silicon(iv) ethoxide
TEOT	tetraethyl orthotitanate/titanium(iv) ethoxide
TOAB	tetraoctylammonium bromide
TOPO	trioctylphosphine oxide
TTIP	titanium(iv) isopropoxide
VLS	vapor−liquid−solid mechanism
QDs	quantum dots

7. Acknowledgments

I would like to thank Profs. A. K. Cheetham, U. Schubert, U. Steiner, and A. H. Windle for helpful discussions and A. White for proofreading. I am further grateful to the Austrian Academy of Science for financial support via the Austrian Programme for Advanced Research and Technology (APART).

8. References

(1) Roco, M. C.; Williams, R. S.; Alivisatos, A. P. *Nanotechnology Research Directions*; Kluwer Academic Publishers: Boston, 2000.
(2) Rao, C. N. R.; Cheetham, A. K. *J. Mater. Chem.* **2001**, *11*, 2887–2894.
(3) Wolf, S. A.; Awschalom, D. D.; Buhrman, R. A.; Daughton, J. M.; Molnar, S. v.; Roukes, M. L.; Chtchelkanova, A. Y.; Treger, D. M. *Science* **2001**, *294*, 1488.
(4) On, D. T.; Desplantier-Giscard, D.; Danumah, C.; Kaliaguine, S. *Appl. Catal. A: Gen.* **2001**, *222*, 299.
(5) Kickelbick, G. *Hybrid Materials: Synthesis, Characterization and Application*; Wiley-VCH: Weinheim, Germany, 2007.
(6) Sanchez, C.; Gomez-Romero, P. *Functional Hybrid Materials*; Wiley VCH: Weinheim, Germany, 2004.
(7) Sanchez, C.; Julian, B.; Belleville, P.; Popall, M. *J. Mater. Chem.* **2005**, *15*, 3559–3592.
(8) *Organic−Inorganic Hybrids forPhotonics*; Hubert, L., Najafi, S. I., Eds.; SPIE: Bellingham, WA, 1998; Vol. 3469.
(9) Schubert, U.; Huesing, N.; Lorenz, A. *Chem. Mater.* **1995**, *7*, 2010.
(10) Judenstein, P.; Sanchez, C. *J. Mater. Chem.* **1996**, *6*, 511.
(11) Cheetham, A. K.; Rao, C. N. R. *MRS Bull.* **2005**, *30*, 93.
(12) Holland, B. T.; Blanford, C. F.; Stein, A. *Science* **1998**, *281*, 538.
(13) Stein, A.; Schroden, R. C. *Curr. Opin. Solid State Mater. Sci.* **2001**, *5*, 553.

(14) Ferey, G. *Chem. Mater.* **2001**, *13*, 3084.
(15) Ferey, G.; Mellot-Draznieks, C.; Serre, C.; Millange, F. *Acc. Chem. Res.* **2005**, *38*, 217.
(16) Templin, M.; Franck, A.; Chesne, A. D.; Leist, H.; Zhang, Y.; Ulrich, R.; Schädler, V.; Wiesner, U. *Science* **1997**, *278*, 1795.
(17) Warren, S. C.; Messina, L. C.; Slaughter, L. S.; Kamperman, M.; Zhou, Q.; Gruner, S. M.; DiSalvo, F. J.; Wiesner, U. *Science* **2008**, *320*, 1748.
(18) Yang, P.; Zhao, D.; Margolese, D. I.; Chmelka, B. F.; Stucky, G. D. *Nature* **1998**, *396*, 152.
(19) Yaghi, O. M.; O'Keeffe, M.; Ockwig, N. W.; Chae, H. K.; Eddaoudi, M.; Kim, J. *Nature* **2003**, *423*, 705.
(20) Yaghi, O. M.; Li, G.; Li, H. *Nature* **1995**, *378*, 703.
(21) Mellot-Draznieks, C.; Dutour, J.; Ferey, G. *Angew. Chem., Int. Ed.* **2004**, *43*, 6290.
(22) Loiseau, T.; Serre, C.; Huguenard, C.; Fink, G.; Taulelle, F.; Henry, M.; Bataille, T.; Ferey, G. *Chem.—Eur. J.* **2004**, *10*, 1373.
(23) Terrones, M. *Annu. Rev. Mater. Sci.* **2003**, *33*, 419.
(24) Aliev, A. E.; Oh, J.; Kozlov, M. E.; Kuznetsov, A. A.; Fang, S.; Fonseca, A. F.; Ovalle, R.; Lima, M. D.; Haque, M. H.; Gartstein, Y. N.; Zhang, M.; Zakhidov, A. A.; Baughman, R. H. *Science* **2009**, *323*, 1575.
(25) Pugno, N. M. *J. Phys.: Condens. Matter* **2006**, *18*, S1971.
(26) Iijima, S. *Nature* **1991**, *354*, 56.
(27) Iijima, S. *Nature* **1993**, *363*, 603.
(28) Harris, P. J. F. *Carbon Nanotubes and Related Structures*; Cambridge University Press: Cambridge, U.K., 2003.
(29) Kroto, H. W.; Heath, J. R.; O'Brien, S. C.; Curl, R. F.; Smalley, R. E. *Nature* **1985**, *318*, 162.
(30) Dai, H. *Acc. Chem. Res.* **2002**, *35*, 1035.
(31) Moisala, A.; Nasibulin, A. G.; Kauppinen, E. I. *J. Phys.: Condens. Matter* **2003**, *15*.
(32) Ajayan, P. M. *Chem. Rev.* **1999**, *99*, 1787.
(33) *Carbon Nanotubes: Synthesis, Structure, Properties, and Applications*; Dresselhaus, M. S., Dresselhaus, G., Avouris, P., Eds.; Springer: New York, 2000.
(34) Saito, R.; Dresselhaus, G.; Dresselhaus, M. S. *Physical Properties of Carbon Nanotubes*; Imperial College Press: London, 1998.
(35) Terrones, M. *Annu. Rev. Mater. Res.* **2003**, *33*, 419.
(36) Dresselhaus, M. S.; Dresselhaus, G.; Charlier, J. C.; Hernandez, E. *Philos. Trans. R. Soc. London, A* **2004**, *362*, 2065.
(37) Wei, B. Q. *Appl. Phys. Lett.* **2001**, *79*, 1172.
(38) Robertson, D. H.; Brenner, D. W.; Mintmire, J. W. *Phys. Rev. B* **1992**, *45*, 12592.
(39) Yu, M. F. *Phys. Rev. Lett.* **2000**, *84*, 5552.
(40) Pugno, N. *Acta Materialia* **2007**, *55*, 5269.
(41) Xie, X. L.; Mai, Y. W.; Zhou, X. P. *Mater. Sci. Eng. R: Reports* **2005**, *49*, 89.
(42) Berber, S.; Kwon, Y. K.; Tomanek, D. *Phys. Rev. Lett.* **2000**, *84*, 4613.
(43) Hone, J.; Batlogg, B.; Benes, Z.; Johnson, A. T.; Fischer, J. E. *Science* **2000**, *289*, 1730.
(44) Salzmann, C. G.; Llewellyn, S. A.; Tobias, G.; Ward, M. A. H.; Huh, Y.; Green, M. L. H. *Adv. Mater.* **2007**, *19*, 883.
(45) Banerjee, S.; Hemraj-Benny, T.; Balasubramanian, M.; Fischer, D. A.; Misewich, J. A.; Wong, S. S. *ChemPhysChem* **2004**, *5*, 1416.
(46) Pillai, S. K.; Ray, S. S.; Moodley, M. *J. Nanosci. Nanotechnol.* **2007**, *7*, 3011.
(47) Park, T. J.; Banerjee, S.; Hemraj-Benny, T.; Wong, S. S. *J. Mater. Chem.* **2006**, *16*, 141.
(48) Moon, J. M.; An, K. H.; Lee, Y. H.; Park, Y. S.; Bae, D. J.; Park, G. S. *J. Phys. Chem. B* **2001**, *105*, 5677.
(49) Fei, B.; Lu, H.; Hu, Z.; Xin, J. H. *Nanotechnology* **2006**, *17*, 1589.
(50) Hou, P.-X.; Liu, C.; Cheng, H.-M. *Carbon* **2008**, *46*, 2003.
(51) Jeong, T.; Kim, W. Y.; Haha, Y. B. *Chem. Phys. Lett.* **2001**, *344*, 18.
(52) Tobias, G.; Shao, L. D.; Salzmann, C. G.; Huh, Y.; Green, M. L. H. *J. Phys. Chem. B* **2006**, *110* (45), 22318.
(53) Li, Y.; Zhang, X. B.; Luo, J. H.; Huang, W. Z.; Chen, J. P.; Luo, Z. Q. *Nanotechnology* **2004**, *15*, 1645.
(54) Andrews, R.; Jacques, D.; Qian, D.; Dickey, E. C. *Carbon* **2001**, *39*, 1681.
(55) Eder, D.; Windle, A. H. *Adv. Mater.* **2008**, *20*, 1787.
(56) Chattopadhyay, D.; Galeska, L.; Papadimitrakopoulos, F. *J. Am. Chem. Soc.* **2003**, *125*, 3370.
(57) Strano, M. S.; Dyke, C. A.; Usrey, M. L.; Barone, P. W.; Allen, M. J.; Shan, H. W.; Kittrell, C.; Hauge, R. H.; Tour, J. M.; Smalley, R. E. *Science* **2003**, *301*, 1519.
(58) Zheng, M.; Jagota, A.; Strano, M. S.; Santos, A. P.; Barone, P.; Chou, S. G.; Diner, B. A.; Dresselhaus, M. S.; McLean, R. S.; Onoa, G. B.; Samsonidze, G. G.; Semke, E. D.; Usrey, M.; Walls, D. J. *Science* **2003**, *302*, 1545.
(59) Arnold, M. S.; Stupp, S. I.; Hersam, M. C. *Nano Lett.* **2005**, *5*, 713.
(60) Feng, Q.-P.; Xie, X. M.; Liu, Y.-T.; Gao, Y.-F.; Wang, X.-H.; Ye, X.-Y. *Carbon* **2001**, *45*, 11.
(61) Arnold, M. S.; Green, A. A.; Hulvat, J. F.; Stupp, S. I.; Hersam, M. C. *Nat. Nanotechnol.* **2006**, *1*, 60.
(62) Krupke, R.; Hennrich, F.; Lohneysen, H. v.; Kappes, M. M. *Science* **2003**, *301*, 344.
(63) Krupke, R.; Hennrich, F.; Weber, H. B.; Kappes, M. M.; Lohneysen, H. v. *Nano Lett.* **2003**, *3*, 1019.
(64) Krupke, R.; Hennrich, F. *Adv. Eng. Mater.* **2005**, *7*, 111.
(65) Tasis, D.; Tagmatarchis, N.; Bianco, A.; Prato, M. *Chem. Rev.* **2006**, *106*, 1105.
(66) Prato, M.; Kostarelos, K.; Bianco, A. *Acc. Chem. Res.* **2008**, *41*, 60.
(67) Kuzmany, H.; Kukovecz, A.; Simona, F.; Holzweber, M.; Kramberger, C.; Pichler, T. *Synth. Met.* **2004**, *41*, 113.
(68) Hirsch, A.; Vostrowsky, O. *Funct. Mol. Nanostruct.* **2005**, *245*, 193.
(69) Klein, K. L.; Melechko, A. V.; McKnight, T. E.; Retterer, S. T.; Rack, P. D.; Fowlkes, J. D.; Joy, D. C.; Simpson, M. L. *J. Appl. Phys.* **2008**, *103*, 061301.
(70) Hirsch, A. *Angew. Chem., Int. Ed.* **2002**, *41*, 1853.
(71) Li, W. W.; Gao, C.; Qian, H. F.; Ren, J. C.; Yan, D. Y. *J. Mater. Chem.* **2006**, *16*, 1852.
(72) He, P. G.; Dai, L. M. *Chem. Commun.* **2004**, *3*, 348.
(73) Lee, C. S.; Baker, S. E.; Marcus, M. S.; Hamers, W. S. J. *Nano Lett.* **2004**, *4*, 1713.
(74) Daniel, S.; Raoa, T. P.; Raob, K. S.; Rani, S. U.; Naidu, G. R. K.; Lee, H.-Y.; Kawai, T. *Sens. Actuators, B* **2007**, *122*, 672.
(75) Fu, K. F.; Sun, Y. P. *J. Nanosci. Nanotechnol.* **2005**, *3*, 351.
(76) Tasis, D.; Tagmatarchis, N.; Georgakilas, V.; Prato, M. *Chem.—Eur. J.* **2003**, *9*, 4000.
(77) Cui, D. X. *J. Nanosci. Nanotechnol.* **2007**, *7*, 1298.
(78) Katz, E.; Willner, I. *Chem. Phys. Chem.* **2004**, *5*, 1085.
(79) Giordani, S.; Bergin, S. D.; Nicolosi, V.; Lebedkin, S.; Kappes, M. M.; Blau, W. J.; Coleman, J. N. *J. Phys. Chem. B* **2006**, *110*, 15708.
(80) Cambre, S.; Wenseleers, W.; Culin, J.; Doorslaer, S. V.; Fonseca, A.; Nagy, J.; Goovaerts, E. *Chem. Phys. Chem.* **2008**, *9* (13), 1930.
(81) Jurkschat, K.; Wilkins, S. J.; Salter, C. J.; Leventis, H. C.; Wildgoose, G. G.; Jiang, L.; Jones, T. G. J.; Crossley, A.; Compton, R. G. *Small* **2005**, *2*, 95.
(82) Ajayan, P. M.; lijima, S. *Nature* **1993**, *361*, 333.
(83) Ajayan, P. M.; Ebbesen, T. W.; Ichihashi, T.; Iijima, S.; Tanigaki, K.; Hiura, H. *Nature* **1993**, *362*, 522.
(84) Seraphin, S.; Zhou, D.; Jiao, J.; Withers, J. C.; Loufty, R. *Nature* **1993**, *362*, 503.
(85) Saito, Y.; Yoshikawa, T. *J. Cryst. Growth* **1993**, *134*, 154.
(86) Sloan, J.; Hammer, J.; Zwiefka-Sibley, M.; Green, M. L. H. *Chem. Commun.* **1998**, *3*, 347.
(87) Monthioux, M.; Flahaut, E.; Cleuziou, J. P. *J. Mater. Res.* **2006**, *21*, 2774.
(88) Smith, B. W.; Monthioux, M.; Luzzi, D. E. *Nature* **1998**, *296*, 323.
(89) Ugarte, D.; Chatelain, A.; Heer, W. A. d. *Science* **1996**, *274*, 1897.
(90) Thamavaranukup, N.; Höppe, H. A.; Ruiz-Gonzalez, L.; Costa, P. M. F. J.; Sloan, J.; Kirkland, A.; Green, M. L. H. *Chem. Commun.* **2004**, *15*, 1686.
(91) Watts, P. C. P.; Hsu, W. K.; Kotzeva, V.; Chen, G. Z. *Chem. Phys. Lett.* **2002**, *366*, 42.
(92) Satishkumar, B. C.; Govindaraj, A.; Mofokeng, J.; Subbanna, G. N.; Rao, C. N. R. *J. Phys. Ber. Bunsenges. Phys. Chem.* **1996**, *29*, 4925.
(93) Ugarte, D.; Stöckli, T.; Bonard, J. M.; Châtelain, A.; Heer, W. A. d. *Appl. Phys. A: Mater. Sci. Process.* **1998**, *67*, 101.
(94) Chancolon, J.; Archaimbault, F.; Pineau, A.; Bonnamy, S. *J. Nanosci. Nanotechnol.* **2006**, *6*, 1.
(95) Brown, G.; Bailey, S.; Sloan, J.; Xu, C.; Friedrichs, S.; Flahaut, E.; Coleman, K. S.; Hutchison, J. L.; Dunin-Borkowski, R. E.; Green, M. L. H. *Chem. Commun.* **2001**, 845.
(96) Dujardin, E.; Ebbesen, T. W.; Hiura, H.; Taginaki, K. *Science* **1994**, *265*, 1850.
(97) Kim, B. M.; Qian, S.; Bau, H. H. *Nano Lett.* **2005**, *5*, 873.
(98) Monthioux, M. *Carbon* **2002**, *40*, 1809.
(99) Zhang, B.; Liu, C.; Cheng, H. M.; Cai, Q. K. *New Carbon Mater.* **2003**, *18*, 174.
(100) Carter, R.; Sloan, J.; Kirkland, A. I.; Meyer, R. R.; Lindan, P. J. D.; Lin, G.; Green, M. L. H.; Vlandas, A.; Hutchison, J. L.; Harding, J. *Phys. Rev. Lett.* **2006**, *96*, 215501.
(101) Georgakilas, V.; Gournis, D.; Tzitzios, V.; Pasquato, L.; Guldi, D. M.; Prato, M. *J. Mater. Chem.* **2007**, *17*, 2679.
(102) Wildgoose, G. G.; Banks, C. E.; Compton, R. G. *Small* **2006**, *2*, 182.
(103) Chen, J.; Hamon, M. A.; Hu, H.; Chen, Y. S.; Rao, A. M.; Ecklund, P. C.; Haddon, R. C. *Science* **1998**, *282*, 95.
(104) Haremza, J. M.; Hahn, M. A.; Krauss, T. D.; Chen, S.; Calcines, J. *Nano Lett.* **2002**, *2*, 1253.
(105) Banerjee, S.; Wong, S. S. *Nano Lett.* **2002**, *2*, 195.

(106) Ravindran, S.; Chaudhary, S.; Colburn, B.; Ozkan, M.; Ozkan, C. S. *Nano Lett.* **2003**, *3*, 447.
(107) Daniel, M. C.; Astruc, D. *Chem. Rev.* **2004**, *104*, 293.
(108) Azamian, B. R.; Coleman, K. S.; Davis, J. J.; Hanson, N.; Green, M. L. H. *Chem. Commun.* **2002**, 366.
(109) Zanella, R.; Basiuk, E. V.; Santiago, P.; Basiuk, V. A.; Mireles, E.; Puente-Lee, I.; Saniger, J. M. *J. Phys. Chem. B* **2005**, *109*, 16290.
(110) Wang, G.-X.; Zhang, B.-L.; Yu, Z.-L.; Qu, M.-Z. *Solid State Ionics* **2005**, *176*, 1169.
(111) Liu, B.; Chen, J. H.; Xiao, C. H.; Cui, K. Z.; Yang, L.; Pang, H. L.; Kuang, Y. F. *Energy Fuels* **2007**, *21*, 1365.
(112) Kongkanand, A.; Dominguez, R. M.; Kamat, P. V. *Nano Lett.* **2007**, *7*, 676.
(113) Juan, J. C.; Jiang, Y.; Meng, X.; Cao, W.; Yarmo, M. A.; Zhang, J. *Mater. Res. Bull.* **2007**, *42*, 1278.
(114) Sainsbury, T.; Fitzmaurice, D. *Chem. Mater.* **2004**, *16*, 3780.
(115) Lee, C.-L.; Ju, Y.-C.; Chou, P.-T.; Huang, Y.-C.; Kuo, L.-C.; Oung, J.-C. *Electrochem. Commun.* **2004**, *7*, 453.
(116) Wei, X.-W.; Xu, J.; Song, X.-J.; Ni, Y.-H. *Zhongguo Youse Jinshu Xuebao* **2004**, *14*, 236.
(117) Whitsitt, E. A.; Moore, V. C.; Smalley, R. E.; Barron, A. R. *J. Mater. Chem.* **2005**, *15*, 4678.
(118) Whitsitt, E. A.; Barron, A. R. *Nano Lett.* **2003**, *3*, 775.
(119) Ellis, A. V.; Vijayamohanan, K.; Goswami, R.; Chakrapani, N.; Ramanathan, L. S.; Ajayan, P. M.; Ramanath, G. *Nano Lett.* **2003**, *3*, 279.
(120) Rahman, G. M.; Guldi, D. M.; Zambon, E.; Pasquato, L.; Tagmatarchis, N.; Prato, M. *Small* **2005**, *1*, 527.
(121) Han, L.; Wu, W.; Kirk, F. L.; Luo, J.; Maye, M. M.; Kariuki, N. N.; Lin, Y.; Wang, C.; Zhong, C.-J. *Langmuir* **2004**, 20.
(122) Sainsbury, T.; Fitzmaurice, D. *Chem. Mater.* **2004**, *16*, 2174.
(123) Yang, D. Q.; Hennequin, B.; Sacher, E. *Chem. Mater.* **2006**, *18*, 5033.
(124) Guldi, D. M.; Rahman, G. M. A.; Jux, N.; Tagmatarchis, N.; Prato, M. *Angew. Chem., Int. Ed.* **2004**, *43*, 5526.
(125) Chen, R. J.; Zhang, Y.; Wang, D.; Dai, H. *J. Am. Chem. Soc.* **2001**, *123*, 3838.
(126) Murakami, H.; Nomura, T.; Nakashima, N. *Chem. Phys. Lett.* **2003**, *378*, 481.
(127) Satake, A.; Miyajima, Y.; Kobuke, Y. *Chem. Mater.* **2005**, *17*, 716.
(128) Rahman, G. M. A.; Guldi, D. M.; Campidelli, S.; Prato, M. *J. Mater. Chem.* **2006**, *16*, 62.
(129) Wang, X.; Liu, Y.; Qiu, W.; Zhu, D. *J. Mater. Chem.* **2002**, *12*, 1636.
(130) D'Souza, F.; Chitta, R.; Sandanayaka, A. S. D.; Subbaiyan, N. K.; D'Souza, L.; Araki, Y.; Ito, O. *Chem.—Eur. J.* **2007**, *13*, 8277.
(131) Mu, Y.; Liang, H.; Hu, J.; Jiang, L.; Wan, L. *J. Phys. Chem. B* **2005**, *109*, 22212.
(132) Liu, L.; Wang, T.; Li, J.; Guo, Z.-X.; Dai, L.; Zhang, D.; Zhu, D. *Chem. Phys. Lett.* **2003**, *367*, 747.
(133) Ou, Y. Y.; Huang, M. H. *J. Phys. Chem. B* **2006**, *110*, 2031.
(134) Li, C. S.; Tang, Y. P.; Yao, K. F.; Zhou, F.; Ma, Q.; Lin, H.; Tao, M. S.; Liang, J. *Carbon* **2006**, *44*, 2021.
(135) Georgakilas, V.; Tzitzios, V.; Gournis, D.; Petridis, D. *Chem. Mater.* **2005**, *17*, 1613.
(136) Zhou, J.; Zhou, X.; Sun, X.; Lib, R.; Murphy, M.; Ding, Z.; Sun, X.; Sham, T.-K. *Chem. Phys. Lett.* **2007**, *437*, 229.
(137) Guldi, D. M.; Taieb, H.; Rahman, G. M. A.; Tagmatarchis, N.; Prato, M. *Adv. Mater.* **2005**, *17*, 871.
(138) Correa-Duarte, M. A.; Liz-Marzán, L. M. *J. Mater. Chem.* **2006**, *16*, 22.
(139) Chen, H.; Donga, S. *Talanta* **2006**, *71*, 1752.
(140) Ostranger, J. W.; Mamedov, A. A.; Kotov, N. A. *J. Am. Chem. Soc.* **2001**, *123*, 1101.
(141) Jiang, K.; Eitan, A.; Schadler, L. S.; Ajayan, P. M.; Siegel, R. W.; Grobert, N.; Mayne, M.; Reyes-Reyes, M.; Terrones, H.; Terrones, M. *Nano Lett.* **2003**, *3*, 275.
(142) Correa-Duarte, M. A.; Perez-Juste, J.; Sanchez-Iglesias, A.; Giersig, M. *Angew. Chem., Int. Ed.* **2005**, *44*, 4375.
(143) Kim, B.; Sigmund, W. M. *Langmuir* **2004**, *20*, 8239.
(144) Grzelczak, M.; Correa-Duarte, M. A.; Salgueirino-Maceira, V.; Giersig, M.; Diaz, R. *Adv. Mater.* **2006**, *18*, 415.
(145) Correa-Duarte, M. A.; Liz-Marzan, L. M. *J. Mater. Chem.* **2006**, *16*, 22.
(146) Hu, X.; Wang, T.; Qu, X.; Dong, S. *J. Phys. Chem. B* **2006**, *110*, 853.
(147) Wang, J.; Musameh, M.; Lin, Y. *J. Am. Chem. Soc.* **2003**, *125*, 2408.
(148) Fullam, S.; Cottell, D.; Rensmo, H.; Fitzmaurice, D. *Adv. Mater. Chem. Phys.* **2000**, *12*, 1430.
(149) Sun, J.; Gao, L. *J. Electroceram.* **2006**, *17*, 91.
(150) Sun, J.; Iwasa, M.; Gao, L.; Zhang, Q. *Carbon* **2004**, *42*, 895.
(151) Stoffelbach, F.; Aqil, A.; Jerome, C.; Jerome, R.; Detrembleur, C. *Chem. Commun.* **2005**, 4532.
(152) Guo, D. J.; Li, H. L. *Electrochem. Commun.* **2004**, *6*, 999.
(153) Day, T. M.; Unwin, P. R.; Wilson, N. R.; Macpherson, J. V. *J. Am. Chem. Soc.* **2005**, *127*, 10639.
(154) Quinn, B. M.; Dekker, C.; Lemay, S. G. *J. Am. Chem. Soc.* **2005**, *127*, 6147.
(155) Qu, J.; Shen, Y.; Qu, X.; Dong, S. *Chem. Commun.* **2004**, 34.
(156) He, Z.; Chen, J.; Liu, D.; Zhou, H.; Kuang, Y. *Diamond Relat. Mater.* **2004**, *13*, 1764.
(157) Yoon, B.; Wai, C. M. *J. Am. Chem. Soc.* **2005**, *127*, 17174.
(158) Ye, J. S.; Cui, H. F.; Liu, X.; Lim, T. M.; Zhang, W. D.; Sheu, F. S. *Small* **2005**, *1*, 560.
(159) Kong, J.; Chapline, M. G.; Dai, H. *Adv. Mater.* **2001**, *13*, 1384.
(160) Kim, H. S.; Lee, H.; Han, K. S.; Kim, J. H.; Song, M. S.; Park, M. S.; Lee, J. Y.; Kang, J. K. *J. Phys. Chem. B* **2005**, *109*, 8983.
(161) Guo, D. J.; Li, H. L. *J. Electroanal. Chem.* **2004**, *573*, 197.
(162) Xing, Y. *J. Phys. Chem. B* **2004**, *108*, 19255.
(163) Lin, Y.; Cui, X.; Yen, C.; Wai, C. M. *J. Phys. Chem. B* **2005**, *109*, 14410.
(164) Cao, J.; Sun, J. Z.; Hong, J.; Li, H. Y.; Chen, H. Z.; Wang, M. *Adv. Mater.* **2004**, *16*, 84.
(165) Robel, I.; Bunker, B. A.; Kamat, P. V. *Adv. Mater.* **2005**, *17*, 2458.
(166) Li, X. L.; Liu, Y. Q.; Fu, L.; Cao, L. C.; Wei, D. C.; Wang, Y. *Adv. Funct. Mater.* **2006**, *16*, 2431.
(167) Sivakkumar, S. R.; Ko, J. M.; Kim, D. Y.; Kim, B. C.; Wallace, G. G. *Electrochim. Acta* **2007**, *52*, 7377.
(168) Xie, X.; Gao, L. *Carbon* **2007**, *45*, 2365.
(169) Huang, X. P.; Pan, C. X.; Huang, X. T. *Mater. Lett.* **2007**, *61*, 934.
(170) Huang, B.; Huang, R.; Jin, D.; Ye, D. *Catal. Today* **2007**, *126*, 279.
(171) Huang, H.; Zhang, W.; Li, M.; Gan, Y.; Chen, J.; Kuang, Y. *J. Colloid Interface Sci.* **2005**, *284*, 593.
(172) Kyotani, T.; Tsai, L.-f.; Tomita, A. *Chem. Commun.* **1997**, 701.
(173) Carmo, M.; Paganin, V. A.; Rosolen, J. M.; Gonzalez, E. R. *J. Power Sources* **2005**, *142*, 169.
(174) Ye, X. R.; Lin, Y.; Wai, C. M. *Chem. Commun.* **2003**, *9*, 642.
(175) Fukunaga, A.; Chu, S.; McHenry, M. E. *J. Mater. Sci. Lett.* **1999**, *18*, 431.
(176) Giordano, R.; Serp, P.; Kalck, P.; Kihn, Y.; Schreiber, J.; Marhic, C.; Duvail, J.-L. *Eur. J. Inorg. Chem.* **2003**, 610.
(177) Moriguchi, I.; Hidaka, R.; Yamada, H.; Kudo, T.; Murakami, H.; Nakashima, N. *Adv. Mater.* **2006**, *18*, 69.
(178) Sun, J.; Gao, L.; Iwasa, M. *Chem. Commun.* **2004**, 832.
(179) Lee, C. Y.; Tsai, H. M.; Chuang, H. J.; Li, S. Y.; Lin, P.; Tseng, T. Y. *J. Electrochem. Soc.* **2005**, *152*, A716.
(180) Frank, O.; Kalbac, M.; Kavan, L.; Zukalova, M.; Prochazka, J.; Klementova, M.; Dunsch, L. *Phys. Status Solidi* **2007**, *244*, 4040.
(181) He, K.-X.; Wu, Q.-F.; Zhang, X.-G.; Wang, X.-L. *J. Electrochem. Soc.* **2006**, *153*, A1568.
(182) Kim, I.-H.; Kim, J.-H.; Lee, Y.-H.; Kim, K.-B. *J. Electrochem. Soc.* **2005**, *152*, A2170.
(183) Kim, J. D.; Kang, B. S.; Noh, T. W.; Yoon, J.-G.; Baik, S. I.; Kim, Y.-W. *J. Electrochem. Soc.* **2005**, *152*, D23.
(184) Wang, C.; Waje, M.; Wang, X.; Tang, J. M.; Haddon, R. C.; Yan, Y. *Nano Lett.* **2004**, *4*, 345.
(185) Qu, L.; Dai, L. *J. Am. Chem. Soc.* **2005**, *127*, 10806.
(186) Choi, H. C.; Shim, M.; Bangsaruntip, S.; Dai, H. *J. Am. Chem. Soc.* **2002**, *124*, 9058.
(187) Qu, L.; Dai, L.; Osawa, E. *J. Am. Chem. Soc.* **2006**, *128*, 5523.
(188) Ma, S.-B.; Nam, K.-W.; Yoon, W.-S.; Yang, X.-Q.; Ahn, K.-Y.; Oh, K.-H.; Kim, K.-B. *J. Power Sources* **2008**, *178*, 483.
(189) Ma, S.-B.; Nam, K.-W.; Yoon, W.-S.; Yang, X.-Q.; Ahn, K.-Y.; Oh, K.-H.; Kim, K.-B. *Electrochem. Commun.* **2007**, *9*, 2807.
(190) Brinker, C. J.; Scherer, G. W. *Sol—Gel Science—The Physics and Chemistry of Sol—Gel Processing*; Academic Press: New York, 1990.
(191) Vincent, P.; Brioude, A.; Journet, C.; Rabaste, S.; Purcell, S. T.; Brusq, J. L.; Plenet, J. C. *J. Non-Cryst. Solids* **2002**, *311*, 130.
(192) Jitianu, A.; Cacciaguerra, T.; Benoit, R.; Delpeux, S.; Beguin, F.; Bonnamy, S. *Carbon* **2004**, *42*, 1147.
(193) Jitianu, A.; Cacciaguerra, T.; Berger, M. H.; Benoit, R.; Beguin, F.; Bonnamy, S. *J. Non-Cryst. Solids* **2004**, *345—46*, 596.
(194) Zhao, L. P.; Gao, L. *Carbon* **2004**, *42*, 1858.
(195) Eder, D.; Windle, A. H. *J. Mater. Chem.* **2008**, *18*, 2036.
(196) Yu, Y.; Yu, J. C.; Yu, J.-G.; Kwok, Y.-C.; Che, Y.-K.; Zhao, J.-C.; Ding, L.; Ge, W.-K.; Wong, P.-K. *Appl. Catal., A* **2005**, *289*, 186–196.
(197) Song, H.; Qiu, X.; Li, F.; Zhu, W.; Chen, L. *Electrochem. Commun.* **2007**, *9*, 1416.
(198) Han, W.-Q.; Zettl, A. *Nano Lett.* **2003**, *3*, 681.
(199) Bai, J. Y.; Xu, Z. D.; Zheng, Y. F. *Chem. Lett.* **2006**, *35*, 96.
(200) Li, Y.; Ding, J.; Chen, J.; Xu, C.; Wei, B.; Liang, J.; Wu, D. *Mater. Res. Bull.* **2002**, *37*, 313.
(201) Liang, Y. X.; Chen, Y. J.; Wanga, T. H. *Appl. Phys. Lett.* **2004**, *85*, 666.
(202) Chen, M. H.; Huang, Z. C.; Wu, G. T.; Zhu, G. M.; You, J. K.; Lin, Z. G. *Mater. Res. Bull.* **2003**, *38*, 831.

(203) Wei, B.-Y.; Hsu, M.-C.; Su, P.-G.; Lin, H.-M.; Wu, R.-J.; Lai, H.-J. *Sens. Actuators, B* **2004**, *101*, 81.
(204) Wang, W. D.; Serp, P.; Kalck, P.; Silva, C. G.; Faria, J. L. *Mater. Res. Bull.* **2008**, *43*, 958.
(205) Wang, W. D.; Serp, P.; Kalck, P.; Faria, J. L. *J. Mol. Catal. A: Chem.* **2005**, *235*, 194.
(206) Wang, W. D.; Serp, P.; Kalck, P.; Faria, J. L. *Appl. Catal., B* **2005**, *56*, 305.
(207) Arabale, G.; Wagh, D.; Kulkarni, M.; Mulla, I. S.; Vernekar, S. P.; Vijayamohanan, K.; Rao, A. M. *Chem. Phys. Lett.* **2003**, *376*, 207.
(208) Park, J. H.; Ko, J. M.; Parka, O. O. *J. Electrochem. Soc.* **2003**, *150*, A864.
(209) Lee, J. Y.; Liang, K.; Ana, K. H.; Lee, Y. H. *Synth. Met.* **2005**, *150*, 153.
(210) Wu, R.-J.; Wu, J.-G.; Yu, M.-R.; T, T.-K; Yeh, C.-T. *Sens. Actuators, B* **2008**, *131*, 306.
(211) Jiang, L. Q.; Gao, L. *J. Am. Ceram. Soc.* **2006**, *89*, 156.
(212) Jiang, L. Q.; Gao, L. *J. Mater. Chem.* **2005**, *15*, 260.
(213) Pan, L.; Shoji, T.; Nagataki, A.; Nakayama, Y. *Adv. Eng. Mater.* **2007**, *9*, 584.
(214) Shi, X.; Yang, H.; Sun, P.; Shao, G.; Duan, X.; Zhen, X. *Carbon* **2007**, *45*, 1735.
(215) Bourlinos, A. B.; Georgakilas, V.; Zboril, R.; Dallas, P. *Carbon* **2007**, *45*, 2136.
(216) Cao, L.; Scheiba, F.; Roth, C.; Schweiger, F.; Cremers, C.; Stimming, U.; Fuess, H.; Chen, L.; Zhu, W.; Qiu, X. *Angew. Chem., Int. Ed.* **2006**, *45* (32), 5315.
(217) Wei, X. W.; Song, X. H.; Xu, J.; Ni, Y. H.; Zhang, P. *Mater. Chem. Phys.* **2005**, *92*, 159.
(218) Hernadi, K.; Ljubovic, E.; Seo, J. W.; Forro, L. *Acta Mater.* **2003**, *51*, 1447.
(219) Seeger, T.; Kohler, T.; Frauenheim, T.; Grobert, N.; Ruhle, M.; Terrones, M.; Seifert, G. *Chem. Commun.* **2002**, 34.
(220) Vietmeyer, F.; Seger, B.; Kamat, P. V. *Adv. Mater.* **2007**, *19*, 2935–2940.
(221) Jiang, L.; Gao, L. *Mater. Chem. Phys.* **2005**, *91*, 313.
(222) Yoshimura, M.; Byrappa, K. *J. Mater. Sci.* **2008**, *43*, 2085.
(223) Menzel, R.; Peiró, A. M.; Durrant, J. R.; Shaffer, M. S. P. *Chem. Mater.* **2006**, *18*, 6059.
(224) Byrappa, K.; Dayananda, A. S.; Sajan, C. P.; Basavalingu, B.; Shayan, M. B.; Soga, K.; Yoshimura, M. *J. Mater. Sci.* **2008**, *43*, 2348.
(225) Lee, Y.; Song, H. J.; Shin, H. S.; Shin, H. J.; Choi, H. C. *Small* **2005**, *1*, 975.
(226) Huang, Y.; Lin, J.; Ding, X. X.; Tang, C.; Gu, C. Z.; Qi, S. R. *Mater. Lett.* **2007**, *61*, 697.
(227) Zhang, W. D. *Nanotechnology* **2006**, *17*, 1036–1040.
(228) Du, J.; Fu, L.; Liu, Z.; Han, B.; Li, Z.; Liu, Y.; Sun, Z.; Zhu, D. *J. Phys. Chem. B* **2005**, *109*, 12772.
(229) Yu, Y.; Ma, L. L.; Huang, W. Y.; Li, J. L.; Wong, P. K.; Yu, J. C. *J. Solid State Chem.* **2005**, *178*, 1488.
(230) Yu, Y.; Ma, L. L.; Huang, W. Y.; Du, F. P.; Yu, J. C.; Yu, J. G.; Wang, J. B.; Wong, P. K. *Carbon* **2005**, *43*, 670.
(231) Jia, B. P.; Gao, L.; Sun, J. *Carbon* **2007**, *45*, 1476.
(232) Fu, L.; Liu, Z. M.; Liu, Y. Q.; Han, B. X.; Wang, J. Q.; Hu, P. A.; Cao, L. C.; Zhu, D. B. *Adv. Mater.* **2004**, *16*, 350.
(233) Sun, Z. Y.; Zhang, X. R.; Han, B. X.; Wu, Y. Y.; An, G. M.; Liu, Z. M.; Miao, S. D.; Miao, Z. J. *Carbon* **2007**, *45*, 2589.
(234) Sun, X.; Chu, Y.; Wang, D. W.; Du, J. H.; Zhang, B. Y.; Wang, F. P. *Rare Metals* **2007**, *26*, 191.
(235) Sun, Z.; Liu, Z.; Han, B.; An, G. *Mater. Lett.* **2007**, *61*, 4565.
(236) Sun, Z.; Yuan, H.; Liu, Z.; Han, B.; Zhang, X. *Adv. Mater.* **2005**, *17*, 2993.
(237) Sun, Z.; Liu, Z.; Han, B.; Miao, S.; Du, J.; Miao, Z. *Carbon* **2006**, *44*, 888.
(238) Kawasaki, S.; Scott, J. F.; Fan, H.; Catalan, G.; Saad, M. M.; Gregg, J. M.; Correa, M. A.; Morrison, F. D.; Tatsuta, T.; Tsuji, O. *Integr. Ferroelectr.* **2007**, *95*, 180.
(239) Kim, H.; Sigmund, W. *Appl. Phys. Lett.* **2002**, *81*, 2085.
(240) Yu, K.; Zhang, Y. S.; Xu, F.; Li, Q.; Zhua, Z. Q. *Appl. Phys. Lett.* **2006**, *88*, 153123.
(241) Zhang, Y.; Franklin, N. W.; Chen, R. J.; Dai, H. *Chem. Phys. Lett.* **2000**, *331*, 35.
(242) Pan, L.; Konishi, Y.; Tanaka, H. *J. Vac. Sci. Technol., B* **2007**, *25*, 1581.
(243) Kim, H. W.; Shim, S. H.; Lee, J. W. *Carbon* **2007**, *45*, 2695.
(244) Zhu, Y. W.; Elim, H. I.; Foo, Y. L.; Yu, T.; Liu, Y. J.; Ji, W.; Lee, J. Y.; Shen, Z. X.; Wee, A. T. S.; Thong, J. T. L.; Sow, C. H. *Adv. Mater.* **2006**, *18*, 587.
(245) Jin, F.; Liu, Y.; Day, C. M. *Appl. Phys. Lett.* **2007**, *90*, 143114.
(246) Fang, W.-C.; Chyan, O.; Sun, C.-L.; Wu, C.-T.; Chen, C.-P.; Chen, K.-H.; Chen, L.-C.; Huang, J.-H. *Electrochem. Commun.* **2007**, *9*, 239.
(247) Ikuno, T.; Yasuda, T.; Honda, S. I.; Oura, K.; Katayama, M.; Lee, J. G.; Mori, H. *J. Appl. Phys.* **2005**, *98*, 114305.
(248) Ikuno, T.; Katayama, M.; Kamada, K.; Honda, S.; Lee, J. G.; Mori, H.; Oura, K. *Jpn. J. Appl. Phys. Lett.* **2003**, *42*, L1356.
(249) Kawasaki, S.; Catalan, G.; Fan, H.; Saad, M. M.; Gregg, J. M.; Correa-Duarte, M. A.; Rybczynski, J.; Morrison, F. D.; Tatsuta, T.; Tsuji, O.; Scott, J. F. *Appl. Phys. Lett.* **2008**, *92*, 053109.
(250) Kuang, Q.; Li, S. F.; Xie, Z. X.; Lin, S. C.; Zhang, X. H.; Xie, S. Y.; Huang, R. B.; Zheng, L. S. *Carbon* **2006**, *44*, 1166.
(251) Deng, G. H.; Xiao, X.; Chen, J. H.; Zeng, X. B.; He, D. L.; Kuang, Y. F. *Carbon* **2005**, *43*, 1557.
(252) Peng, H. B.; Golovchenko, J. A. *Appl. Phys. Lett.* **2004**, *84*, 5428.
(253) Fan, Z.; Chen, J.; Cui, K.; Sun, F.; Xu, Y.; Kuang, Y. *Electrochim. Acta* **2007**, *2007*, 2959.
(254) Chrissanthopoulos, A.; Baskoutas, S.; Bouropoulos, N.; Dracopoulos, V.; Tasis, D.; Yannopoulos, S. N. *Thin Solid Films* **2007**, *515*, 8524.
(255) Lazareck, A. D.; Kuo, T.-F.; Xu, J. M.; Taft, B. J.; Kelley, S. O.; Cloutier, S. G. *Appl. Phys. Lett.* **2006**, *89*, 103109.
(256) Lazareck, A. D.; Cloutier, S. G.; Kuo, T.-F.; Taft, B. J.; Kelley, S. O.; Xu, J. M. *Nanotechnology* **2006**, *17*, 2661.
(257) Liu, J.; Li, X.; Dai, L. *Adv. Mater.* **2006**, *18*, 1740.
(258) Ho, Y. M.; Liu, J. W.; Qi, J. L.; Zheng, W. T. *J. Phys. D: Appl. Phys.* **2008**, *41*, 665308.
(259) Gomathi, A.; Vivekchand, S. R. C.; Govindaraj, A.; Rao, C. N. R. *Adv. Mater.* **2005**, *17*, 2757.
(260) Javey, A.; Kim, H.; Brink, M.; Wang, Q.; Ural, A.; Guo, J.; Mcintyre, P.; McEuen, P.; Lundstrom, M.; Dai, H. *Nat. Mater.* **2002**, *1*, 241.
(261) Min, Y.-S.; Bae, E. J.; Jeong, K. S.; Cho, Y. J.; Lee, J.-H.; Choi, W. B.; Park, G.-S. *Adv. Mater.* **2003**, *15*, 1019.
(262) Eder, D.; Kinloch, I. A.; Windle, A. H. *Chem. Commun.* **2006**, *13*, 1448.
(263) Fujishima, A.; Honda, K. *Nature* **1972**, *238*, 37.
(264) Tryk, D. A.; Fujishima, A.; Honda, K. *Electrochim. Acta* **2000**, *45*, 2363.
(265) Graetzel, M.; Rotzinger, F. P. *Chem. Phys. Lett.* **1985**, *118*, 474.
(266) Graetzel, M. *Nature* **2001**, *414*, 338.
(267) O'Regan, B.; Graetzel, M. *Nature* **1991**, *353*, 737.
(268) Carp, O.; Huisman, C. L.; Reller, A. *Prog. Solid State Chem.* **2004**, *32*, 33.
(269) Diebold, U. *Surf. Sci. Rep.* **2003**, *48*, 53.
(270) Frank, S. N.; Bard, A. J. *J. Am. Chem. Soc.* **1977**, *99*, 303.
(271) Aguado, M. A.; Anderson, M. A.; Hill, C. G. *J. Mol. Catal.* **1994**, *89* (1–2), 165.
(272) Hoffmann, M. R.; Martin, S. T.; Choi, W. Y.; Bahnemann, D. W. *Chem. Rev.* **1995**, *95*, 69.
(273) Zhang, Z. B.; Wang, C. C.; Zakaria, R.; Ying, J. Y. *J. Phys. Chem. B* **1998**, *102*, 10871.
(274) Asahi, R.; Morikawa, T.; Ohwaki, T.; Aoki, K.; Taga, Y. *Science* **2001**, *293*.
(275) Zhang, Y. H.; Reller, A. *J. Mater. Chem.* **2004**, *11*, 2537.
(276) Wang, J.; Una, S.; Klabunde, K. J. *Appl. Catal., B* **2004**, *48*, 151.
(277) Eder, D.; Motta, M. S.; Windle, A. H. *Nanotechnology* **2009**, *20*, 055602.
(278) Eder, D.; Motta, M. S.; Windle, A. H. *Acta Mater.* submitted for publication.
(279) Anpo, M.; Ichihashi, Y.; Takeuchi, M.; Yamashita, H. *Res. Chem. Intermed.* **1998**, *24*, 143.
(280) Ou, Y.; Lin, J.; Fang, S.; Liao, D. *Chem. Phys. Lett.* **2006**, *429*, 199.
(281) Bouazza, N.; Ouzzine, M.; Lillo-Ródenas, M. A.; Eder, D.; Linares-Solano, A. *Appl. Catal. B: Environ.* **2009**, *92* (3–4), 377.
(282) Yao, Y.; Li, G.; Ciston, S.; Lueptow, R. M.; Gray, K. A. *Environ. Sci. Technol.* **2008**, *42*, 4952.
(283) Lee, S.-H.; Pumprueg, S.; Moudgil, B.; Sigmund, W. *Colloids Surf., B* **2005**, *40*, 93.
(284) Jayadevan, K. P.; Tseng, T. Y. *J. Nanosci. Nanotechnol.* **2005**, *5*, 1768.
(285) Baxter, J. B.; Walker, A. M.; Ommering, K. v.; Aydil, E. S. *Nanotechnology* **2006**, *17*, S304.
(286) Kamat, P. V. *J. Phys. Chem. C* **2007**, *111*, 2834.
(287) Guldi, D. M.; Rahman, G. M. A.; Sgobba, V.; Kotov, N. A.; Bonifazi, D.; Prato, M. *J. Am. Chem. Soc.* **2006**, *128*, 2315.
(288) Varghese, O. K.; Kichambre, P. D.; Gong, D.; Ong, K. G.; Dickey, E. C.; Grimes, C. A. *Sens. Actuators, B* **2001**, *81*, 32.
(289) Huang, H.-C.; Huang, G.-L.; Chen, H.-L.; Lee, Y.-D. *Thin Solid Films* **2006**, *511−512*, 203.
(290) Jusys, Z.; Behm, R. J. *J. Phys. Chem. B* **2001**, *105*, 10874.
(291) Rajesh, B.; Thampi, K. R.; Bonard, J. M.; Viswanathan, B. *J. Mater. Chem.* **2000**, *10*, 1757.
(292) Wang, M.-Y.; Chen, J.-H.; Cui, K.-Z.; Liu, B.; Zhou, H.-H.; Kuang, Y.-Z. *Chin. J. Chem.* **2006**, *24*, 881.
(293) Song, H.; Qiu, X.; Li, F. *Electrochim. Acta* **2008**, *53*, 3708.
(294) Yu, H.; Zeng, K.; Fu, X.; Zhang, Y.; Peng, F.; Wang, H.; Yang, J. *J. Phys. Chem. C* **2008**, *112*, 11875.

(295) Li, C.-H.; Yu, Z.-X.; Yao, K.-F.; Ji, S.-F.; Liang, J. *J. Mol. Catal. A: Chem.* **2005**, *226*, 101.
(296) Tessonnier, J. P.; Pesant, L.; Ehret, G.; Ledoux, M. J.; Huu, C. P. *Appl. Catal., A* **2005**, *288*, 203.
(297) Planeix, J. M.; Coustel, N.; Coq, B.; Brotons, V.; Kumbhar, P. S.; Dutartre, R.; Geneste, P.; Bernier, P.; Ajayan, P. M. *J. Am. Chem. Soc.* **1994**, *116*, 7935.
(298) Fu, X.; Yu, H.; Peng, F.; Wang, H.; Qian, Y. *Appl. Catal., A* **2007**, *321*, 190.
(299) Chen, X.-W.; Zhu, Z.; Haevecker, M.; Su, D. S.; Schloegl, R. *Mater. Res. Bull.* **2007**, *42*, 354.
(300) Pietruszka, B.; DiGregorio, F.; Keller, N.; Keller, V. *Catal. Today* **2005**, *102*−*103*, 94.
(301) Yang, H.-M.; Liao, P.-H. *Appl. Catal., A* **2007**, *317*, 226.
(302) Zhang, D.; Pan, C.; Shi, L.; Mai, H.; Gao, X. *Appl. Surf. Sci.* **2009**, *255*, 4907.
(303) Chen, X. W.; Zhu, Z.; Hävecker, M.; Su, D. S.; Schlögl, R. *Mater. Res. Bull.* **2007**, *42*, 354.
(304) Liu, X.; Su, D. S.; Schloegl, R. *Carbon* **2008**, *46*, 547.
(305) Zhang, J.; Liu, X.; Blume, R.; Zhang, A. H.; Schlogl, R.; Su, D. S. *Science* **2008**, *322*, 73.
(306) Zhang, J.; Su, D. S.; Zhang, A.; Wang, D.; Schlögl, R.; Hebert, C. *Angew. Chem., Int. Ed.* **2007**, *46*, 7319.
(307) Mestl, G.; Maksimova, N.; Keller, N.; Roddatis, V. V.; Schlögl, R. *Angew. Chem., Int. Ed.* **2001**, *40*, 2066.
(308) Jimenez, I.; Centeno, M. A.; Scotti, R.; Morazzoni, F.; Cornet, A.; Morante, J. R. *J. Electrochem. Soc.* **2003**, *150*, H72.
(309) Frühberger, B.; Grunze, M.; Dwyer, D. J. *Sens. Actuators, B* **1996**, *31*, 167.
(310) Wu, N. L.; Wang, S. Y.; Rusakova, I. A. *Science* **1999**, *285*, 1375.
(311) Ottaviano, L.; Bussolotti, F.; Lozzi, L.; Passacantando, M.; Rosa, S. L.; Santucci, S. *Thin Solid Films* **2003**, *436*, 9.
(312) Gao, T.; Wang, T. H. *Chem. Commun.* **2004**, 2558.
(313) Cabot, A.; Marsal, A.; Arbiol, J.; Morante, J. R. *Sens. Actuators, B* **2004**, *99*, 74.
(314) Chen, L.; Tsang, S. C. *Sens. Actuators, B* **2003**, *89*, 68.
(315) Collins, P. G.; Bradley, K.; Ishigami, M.; Zettl, A. *Science* **2000**, *287*, 1801.
(316) Sinha, N.; Ma, J. Z.; Yeow, J. T. W. *J. Nanosci. Nanotechnol.* **2006**, *6*, 573.
(317) Kong, J.; Franklin, N. R.; Zhou, C.; Chapline, M. G.; Peng, S.; Cho, K.; Dai, H. *Science* **2000**, *287*, 622.
(318) Sun, Z.; Zhang, X.; Na, N.; Liu, Z.; Han, B.; An, G. *J. Phys. Chem. B* **2006**, *110*, 13410.
(319) Van Hieu, N.; Thuy, L. T. B.; Chien, N. D. *Sens. Actuators, B* **2008**, *129*, 888.
(320) Liu, J.; Guo, Z.; Meng, F.; Jia, Y.; Liu, J. *J. Phys. Chem. C* **2008**, *112*, 6119.
(321) Chen, Y.; Zhu, C.; Wang, T. *Nanotechnology* **2006**, *17*, 3012.
(322) Kang, X.; Maia, Z.; Zou, X.; Cai, P.; Moa, J. *Talanta* **2008**, *74*, 879.
(323) Hsu, H.-L.; Jehng, J.-M. *Mat. Chem. Phys.* **2009**, *113* (1), 166.
(324) Liu, Z.; Wang, J.; Xie, D.; Chen, G. *Small* **2008**, *4*, 462.
(325) Conway, B. E. *J. Electrochem. Soc.* **1991**, *138*, 1539.
(326) Niu, C.; Sichel, E. K.; Hoch, R.; Moy, D.; Tennet, H. *Appl. Phys. Lett.* **1997**, *70*, 1480.
(327) Lota, G.; Lota, K.; Frackowiak, E. *Electrochem. Commun.* **2007**, *9*, 1828.
(328) Hughes, M.; Shaffer, M. S. P.; Renouf, A. C.; Singh, C.; Chen, G. Z.; Fray, D. J.; Windle, A. H. *Adv. Mater.* **2002**, *14*, 382.
(329) Hughes, M.; Chen, G. Z.; Shaffer, M. S. P.; Fray, D. J.; Windle, A. H. *Chem. Mater.* **2002**, *14*, 1610.
(330) Yi, W.; Yu, S. G.; Lee, W. T.; Han, I. T.; Jeong, J. T.; Woo, Y. S.; Lee, J. H.; Jin, S. W.; Choi, W. B.; Heo, J. N.; Jeon, D.; Kim, J. M. *J. Appl. Phys.* **2001**, *89*, 4091.
(331) Nam, K. W.; Kim, K. H.; Lee, E. S.; Yoon, W. S.; Yang, X. Q.; Kim, K. B. *J. Power Sources* **2008**, *182*, 642.
(332) Subramanian, V.; Zhu, H. W.; Wei, B. Q. *Electrochem. Commun.* **2006**, *8*, 827.
(333) Deng, M. G.; Yang, B. C.; Zhang, Z. A.; Hu, Y. D. *J. Mater. Sci.* **2005**, *40*, 1017.
(334) Zhang, H.; Cao, G.; Wang, Z.; Yang, Y.; Shi, Z. *Nano Lett.* **2008**, *8*, 2664.
(335) Reddy, A. L. M.; Shaijumon, M. M.; Gowda, S. R.; Ajayan, P. M. *Nano Lett.* **2009**, *9*, 1002.
(336) Wu, G.-M.; Wang, A.-R.; Zhang, M.-X.; Yang, H.-Y.; Zhou, B.; Shen, J. *J. Sol*−*Gel Sci. Technol.* **2008**, *46*, 79.
(337) Fang, W.-C. *J. Phys. Chem. C* **2008**, *112*, 11552.
(338) Kim, Y.-T.; Tadai, K.; Mitani, T. *J. Mater. Chem.* **2005**, *15*, 4914.
(339) Avouris, P.; Chen, J. *Mater. Today* **2006**, *9*, 46.
(340) Avouris, P.; Freitag, M.; Perebeinos, V. *Nat. Photonics* **2008**, *2*, 341.
(341) Lin, Y.-M.; Tsang, J. C.; Freitag, M.; Avouris, P. *Nanotechnology* **2007**, *18*, 295202.
(342) Yi, W. K.; Jeong, T.; Yu, S. G.; Heo, J.; Lee, C.; Lee, J.; Kim, W.; Yoo, J. B.; Kim, J. *Adv. Mater.* **2002**, *14*, 1464.
(343) Zhang, Y. B.; Lau, S. P.; Huang, L.; Tanemura, M. *Appl. Phys. Lett.* **205**, *86*, 123115.
(344) Shih, A.; Yater, J.; Hor, C.; Abrams, R. *Appl. Surf. Sci.* **1997**, *111*, 251.
(345) Besteman, K.; Lee, J. O.; Wiertz, F. G. M.; Heering, H. A.; Dekker, C. *Nano Lett.* **2003**, *3*, 727.
(346) Moon, J. S.; Alegaonkar, P. S.; Han, J. H.; Lee, T. Y.; Yoo, J. B.; Kim, J. M. *J. Appl. Phys.* **2006**, *100*, 104303.
(347) Yan, X.; Tay, B.-K.; Miele, P. *Carbon* **2008**, *46*, 753.
(348) Huang, L.; Lau, S. P.; Yang, H. Y.; Yu, S. F. *Nanotechnology* **2006**, *17*, 1564.
(349) Huo, K.; Outlaw, R. A.; Wang, S.; Zhu, M.; Quinlan, R. A.; Manos, D. M.; Kordesch, M. E.; Arp, U.; Holloway, B. C. *Appl. Phys. Lett.* **2008**, *92*, 133112.
(350) Heo, J. N.; Kim, W. S.; Jeong, T. W.; Yu, S.; Lee, J. H.; Lee, C. S.; Yi, W. K; Lee, Y. H.; Yoo, J. B.; Kim, J. M. *Physica B* **2002**, *323*, 174.
(351) Jin, F.; Liu, Y.; Day, C. M.; Little, S. A. *Carbon* **2007**, *45*, 587.
(352) Jin, F.; Liu, Y.; Day, C. M. *Appl. Phys. Lett.* **2006**, *88*, 163116.
(353) Nam, K. W.; Kim, K. B. *J. Electrochem. Soc.* **2002**, *149*, A346.
(354) Kim, W. S.; Lee, J.; Jeong, T. W.; Heo, J. N.; Kong, B. Y.; Jin, Y. W.; Kim, J. M. *Appl. Phys. Lett.* **2005**, *87*, 163112.
(355) Collins, P. G.; Zettl, A. *Phys. Rev. B* **1997**, *55*, 9391.
(356) Milne, W. I.; Teo, K. B. K.; Chhowalla, M.; Amaratunga, G. A. J.; Lee, S. B.; Hasko, D. G.; Ahmed, H.; Groening, O.; Legagneux, P.; Gangloff, L.; Schnell, J. P.; Pirio, G.; Pribat, D.; Castignolles, M.; Loiseau, A.; Semet, V.; Binh, V. T. *Diamond Relat. Mater.* **2003**, *12*, 422.
(357) Ajayan, P. M.; Stephan, O.; Redlich, P.; Colliex, C. *Nature* **1995**, *375*, 564.
(358) Eder, D. 2009, submitted for publication.
(359) Mars, P.; Krevelen, D. W. v. *Chem. Eng. Sci. (Special issue)* **1954**, *3*, 41.
(360) Haerudin, H.; Bertel, S.; Kramer, R. *J. Chem. Soc., Faraday Trans.* **1998**, *94*, 1481.
(361) Eder, D.; Kramer, R. *Phys. Chem. Chem. Phys.* **2003**, *5*, 1314.
(362) Eder, D.; Kramer, R. *J. Phys. Chem. B* **2004**, *108*, 14823.
(363) Caruso, R. A.; Antonietti, M. *Chem. Mater.* **2001**, *13*, 3272.
(364) Patzke, G. R.; Krumeich, F.; Nesper, R. *Angew. Chem., Int. Ed.* **2002**, *41*, 2446.
(365) Rao, C. N. R.; Nash, M. *Dalton Trans.* **2003**, *1*, 1.
(366) Eder, D.; Motta, M. S.; Kinloch, I. A.; Windle, A. H. *Physica E* **2007**, *37*, 245.
(367) Satishkumar, B. C.; Govindaraj, A.; Vogl, E. M.; Baumallick, L.; Rao, C. N. R. *J. Mater. Res.* **1997**, *12*, 604.
(368) Kim, M.; Hong, J.; Lee, J.; Hong, C. K.; Shim, S. E. *J. Colloid Interface Sci.* **2008**, *322*, 321.
(369) Rao, C. N. R.; Satishkumar, B. C.; Govindaraj, A. *Chem. Commun.* **1997**, 1581.
(370) Satishkumar, B. C.; Govindaraj, A.; Nath, M.; Rao, C. N. R. *J. Mater. Chem.* **2000**, *10*, 2115.
(371) Du, N.; Zhang, H.; Chen, B.; Ma, X.; Liu, Z.; Wu, J.; Yang, D. *Adv. Mater.* **2007**, *19*, 1641.
(372) Du, N.; Zhang, H.; Chen, B.; Wu, J. B.; Ma, X. Y.; Liu, Z. H.; Zhang, Y. Q.; Yang, D.; Huang, X. H.; Tu, J. P. *Adv. Mater.* **2007**, *19*, 4505.
(373) Yang, H.; Zhang, D.; Shi, L.; Fang, J. *Acta Mater.* **2008**, *56*, 955.
(374) Mor, G. K.; Varghese, O. K.; Paulose, M.; Grimes, C. A. *Sens. Lett.* **2003**, *1*, 42.
(375) Adachi, M.; Murata, Y.; Okada, I.; Yoshikawa, S. *J. Electrochem. Soc.* **2003**, *150*, G488.
(376) Lin, C. H.; Lee, C. H.; Chao, J. H.; Kuo, C. Y.; Cheng, Y. C.; Huang, W. N.; Chang, H. W.; Huang, Y. M.; Skih, M. K. *Catal. Lett.* **2004**, *98*, 61.
(377) Yoganarasinhan, S. R.; Rao, C. N. R. *Trans. Faraday Soc.* **1962**, *58*, 1579.
(378) Deleted in proof.
(379) Eder, D.; Motta, M. S.; Windle, A. H. *Nanotechnology* **2009**, *20*, 055602.
(380) Eder, D.; Sandeman, K. G.; Windle, A. H. *Phys. Rev. B* **2009**, in press.
(381) Ijima, S. *Nature* **1991**, *354*, 56.
(382) Ebbesen, T. W.; Ajayan, P. M. *Nature* **1992**, *358*, 220.
(383) Guo, T.; Nikolaev, P.; Thess, A.; Colbert, D. T.; Smalley, R. E. *Chem. Phys. Lett.* **1995**, *1,2*, 243.
(384) Hsu, W. K.; Hare, J. P.; Terrones, M.; Kroto, H. W.; Walton, D. R.; Harris, P. J. F. *Nature* **1995**, *377*, 687.
(385) Endo, M.; Takeuchi, K.; Igarashi, S.; Susumu, K.; Kiyoharu, S. M.; Kroto, H. W. *J. Phys. Chem. Solids* **1993**, *12*, 54.
(386) Hernadi, M.; Couteau, E.; Seo, J. W.; Forro, L. *Langmuir* **2003**, *19*, 7026.
(387) Balani, K.; Agarwal, A. *Nanotechnology* **2008**, *19*, 165701.

(388) Park, C. D.; Jeon, H. J.; Wang, H. J.; Choa, Y. H.; Oh, S. T.; Kang, K. M.; Kang, S. G. Proceedings of the 3rd International Symposium on Designing, Processing and Properties of Advanced Engineering Materials, ISAEM-2003, Jeju Island, Korea, November 5−8, 2003. In *Materials Science Forum*; Kang, S.-G., Kobayashi, T., Eds.; Trans Tech Publications Inc.: Zurich, Switzerland, 2004; Vol. 449.
(389) Jiang, D. T.; Thomson, K.; Kuntz, J. D.; Ager, J. W.; Mukherjee, A. K. *Scr. Mater.* **2007**, *56*, 959.
(390) Jin, F.; Liu, Y.; Day, C. M.; Little, S. A. *J. Vac. Sci. Technol., B* **2007**, *25*, 1785.
(391) Zhang, D.; Pan, C.; Zhang, J.; Shi, L. *Mater. Lett.* **2008**, *62*, 3821.
(392) Shan, Y.; Gao, L. *Chem. Lett.* **2004**, *33*, 1560.
(393) Ma, L. L.; Yu, Y.; Huang, W. Y.; Zhu, L. P.; Li, J. L.; Zhuang, Y. Y.; Qi, X. H. *Acta Chim. Sinica* **2005**, *63*, 1641.
(394) Reddy, K. R.; Sin, B. C.; Yoo, C. H.; Park, W. J.; Ryu, K. S.; Lee, J. S.; Sohn, D. W.; Lee, Y. I. *Scr. Mater.* **2008**, *58*, 1010.
(395) Mahajan, S. V.; Hasan, S. A.; Cho, J.; Shaffer, M. S. P.; Boccaccini, A. R.; Dickerson, J. H. *Nanotechnology* **2008**, *19*, 195301.
(396) Jiang, L. Q.; Gao, L. *Chem. Mater.* **2003**, *15*, 2848.
(397) Peng, F.; Fu, X. B.; Yu, H.; Wang, H. J. *New Carbon Materials* **2007**, *22*, 213.
(398) Lee, W. T.; Im, S. J.; Han, J. G.; Yu, S.; Kim, H. Y.; Han, I. T.; Yoo, J. B.; Kim, K. Y.; Lee, J. W.; Kim, J. M.; Choi, E. H. *Jpn. J. Appl. Phys.* **2002**, *41*, 6550.
(399) Gong, K. P.; Yu, P.; Su, L.; Xiong, S. X.; Mao, L. Q. *J. Phys. Chem. C* **2007**, *111*, 1882.
(400) Fan, Z.; Chen, J.; Wang, M.; Cui, K.; Zhou, H.; Kuang, Y. *Diamond. Relat. Mater.* **2006**, *15*, 1478.
(401) Bottini, M.; Tautz, L.; Huynh, H.; Monosov, E.; Bottini, N.; Dawson, M. I.; Bellucci, S.; Mustelin, T. *Chem. Commun.* **2005**, 758.
(402) Fu, Q.; Lu, C.; Liu, J. *Nano Lett.* **2002**, *2*, 329.
(403) Seeger, T.; de la Fuente, G.; Maser, W. K.; Benito, A. M.; Callejas, M. A.; Martinez, M. T. *Nanotechnology* **2003**, *14*, 184.
(404) Fan, W. G.; Gao, L. *Chem. Lett.* **2005**, *34*, 954.
(405) Seeger, T.; Kohler, T.; Frauenheim, T.; Grobert, N.; Terrones, M.; Seifert, G.; Ruhle, M. *Z. Metallkd.* **2002**, *93*, 455.
(406) Fang, H. T.; Sun, X.; Qian, L. H.; Wang, D. W.; Li, F.; Chu, Y.; Wang, F. P.; Cheng, H. M. *J. Phys. Chem. C* **2008**, *112*, 5790.
(407) An, G. M.; Na, N.; Zhang, X. R.; Miao, Z. J.; Miao, S. D.; Ding, K. L.; Liu, Z. M. *Nanotechnology* **2007**, *18*, 435707.
(408) Wen, Z. H.; Wang, Q.; Zhang, Q.; Li, J. H. *Adv. Funct. Mater.* **2007**, *17*, 2772.
(409) Fan, W. G.; Gao, L.; Sun, J. *J. Am. Ceram. Soc.* **2006**, *89*, 2671.
(410) Wu, N.; Wang, S.; Rusakova, I. A. *Science* **1999**, *285*, 1375.
(411) Zhao, L.; Choi, M.; Kim, H. S.; Hong, S. H. *Nanotechnology* **2007**, *18*, 445501.
(412) Liu, Y. L.; Yang, H. F.; Yang, Y.; Liu, Z. M.; Shen, G. L.; Yu, R. Q. *Thin Solid Films* **2006**, *497*, 355.
(413) Lu, J.; Ma, A.; Yang, S. H.; Ng, K. M. *J. Nanosci. Nanotechnol.* **2007**, *7*, 1589.
(414) Han, Z. H.; Yang, B.; Kim, S. H.; Zachariah, M. R. *Nanotechnology* **2007**, *18*, 105701.
(415) Reddy, A. L. M.; Ramaprabhu, S. *J. Phys. Chem. C* **2007**, *111*, 7727.
(416) Yang, Y.; Qu, L.; Dai, L.; Kang, T.-S.; Durstock, M. *Adv. Mater.* **2007**, *19*, 1239.
(417) Oh, W. C.; Chen, M. L. *Bull. Korean Chem. Soc.* **2008**, *29*, 159.
(418) Huang, Q.; Gao, L. *J. Mater. Chem.* **2003**, *13*, 1517.
(419) Liu, B.; Zeng, H. C. *Chem. Mater.* **2008**, *20*, 2711.
(420) Fan, W.; Gao, L.; Sun, J. *J. Am. Ceram. Soc.* **2006**, *89*, 731.
(421) Wang, G.-J.; Lee, M.-W.; Chen, Y.-H. *Photochem. Photobiol.* **2008**, *20*.
(422) Xia, X.-H.; Jia, Z.-J.; Yu, Y.; Liang, Y.; Wang, Z.; Ma, L.-L. *Carbon* **2007**, *45*, 717.
(423) Jung, K. H.; Jang, S. R.; Vittal, R.; Kim, V. D.; Kim, K. J. *Bull. Korean Chem. Soc.* **2003**, *24*, 1501.
(424) He, D.; Yang, L.; S. Kuang, Q. C. *Electrochem. Commun.* **2007**, *9*, 2467.
(425) Kalbac, M.; Frank, O.; Kavan, L.; Zukalova, M.; Prochazka, J.; Klementova, M.; Dunsch, L. *J. Electrochem. Soc.* **2007**, *154*, K19.
(426) Kim, I.-H.; Kim, J.-H.; Cho, B.-W.; Kim, K.-B. *J. Electrochem. Soc.* **2006**, *153*, A1451.
(427) Bittencourt, C.; Felten, A.; Espinosa, E. H.; Ionescu, R.; Moreau, N.; Heszler, P.; Granqvist, C. G.; Pireaux, J.-J.; Llobet, E. *Smart Mater. Struct.* **2006**, *15*, 1555.
(428) Zhang, R.; Fan, L.; Fang, Y.; Yang, S. *J. Mater. Chem.* **2008**, *18*, 4964.
(429) Chen, C. S.; Chen, X. H.; Yi, B.; Liu, T. G.; Li, W. H.; Xu, L. S.; Yang, Z.; Zhang, H.; Wang, Y. G. *Acta Mater.* **2006**, *54*, 5401.
(430) Guo, G.; Guo, J.; Tao, D.; Choy, W. C. H.; Zhao, L.; Qian, W.; Wang, Z. *Appl. Phys.−Mater. Sci. Proc.* **2007**, *89*, 525.
(431) Lupo, F.; Kamalakaran, R.; Scheu, C.; Grobert, N.; Ruhle, M. *Carbon* **2004**, *42*, 1995.
(432) Shan, Y.; Gao, L. *Nanotechnology* **2005**, *16*, 625.
(433) Ci, L.; Ryu, Z.; Jin-Phillipp, N. Y.; Rühle, M. *Diamond. Relat. Mater.* **2007**, *16*, 531.
(434) Pang, L. X.; Sun, K. N.; Ren, S.; Sun, C.; Bi, J. Q. *J. Comp. Mater.* **2007**, *41*, 2025.
(435) Correa-Duarte, M. A.; Liz-Marzan, L. M. *J. Mater. Chem.* **2006**, *15*, 22.
(436) Engtrakul, C.; Kim, Y. H.; Nedeljkovic, J. M.; Ahrenkiel, S. P.; Gilbert, K. E. H.; Alleman, J. L.; Zhang, S. B.; Micic, O. I.; Nozik, A. J.; Heben, M. J. *J. Phys. Chem. B* **2006**, *110*, 25153.
(437) Fang, W.-C.; Chen, K.-H.; Chen, L.-C. *Nanotechnology* **2007**, *18*, 485716.

CR800433K